Regenerative performance and immunogenicity of engineered extracellular matrices.

Prithiviraj, Sujeethkumar

2025

Document Version:
Publisher's PDF, also known as Version of record

Regenerative performance and immunogenicity of engineered extracellular matrices

Sujeethkumar Prithiviraj

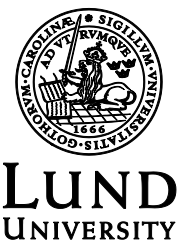

LUND
UNIVERSITY

DOCTORAL DISSERTATION

Doctoral dissertation for the degree of Doctor of Philosophy (PhD) at the Faculty of Medicine at Lund University to be publicly defended on the date of October 20th at 13:00 in Grunn Salen, BMC Lund.

Faculty opponent
Dr. Ioannis Papantoniou
Associate professor at KU Leuven, Belgium

Organization	Document name
LUND UNIVERSITY	DOCTORAL DISSERTATION
Cell Tissue and Organ Engineering	**Date of issue** 20th October, 2025
Author(s) Sujeethkumar Prithiviraj	Sponsoring organization

Title and subtitle: Regenerative Performance and Immunogenicity of Engineered Extracellular Matrices

Abstract

Critical-sized bone defects remain a significant unmet clinical need, with > 500,000 reconstructive procedures performed annually in the United States and Europe and associated costs exceeding US$3 billion. Autologous bone grafting—the current gold standard—suffers from limited harvest volume and donor-site morbidity, whereas allografts show variable integration and carry immunological and infection risks. Recombinant therapies using growth factors partly address these issues but require supraphysiological doses that provoke ectopic ossification and inflammation. Tissue engineering (TE) offers a conceptual solution by combining cells, bioactive cues, and scaffolds to fabricate living grafts; however, cell-laden constructs that rely on the in vitro expansion and differentiation of primary cells face considerable challenges, including variability between donors, extended production times, reduced viability upon implantation, and limited scalability. Engineered extracellular matrices (ECMs), acellular scaffolds deposited by cells and subsequently devitalized, offer a way to overcome these barriers by preserving intrinsic biological cues, thereby addressing the logistical and safety challenges associated with cell-based therapies. This thesis explores how eECMs can be optimized for bone regeneration by addressing four critical translational barriers: growth factor dependency, cell donor variability, programmable matrix function, and immune compatibility.

First, we show that a collagen–hydroxyapatite scaffold loaded with heterodimeric Bone morphogenetic protein (BMP) 2/7 significantly improves osteoinduction at lower doses than BMP-2 alone, enhancing osteogenic progenitor recruitment and matrix deposition (Paper 1). We then demonstrate the development of an off-the-shelf eECM generated from a standardized human mesenchymal stem/stromal cell line (MSOD-B), which, upon devitalization, supports robust endochondral ossification in a cell-free manner (Paper 2). We applied CRISPR/Cas9 editing to customize the composition and function of eECMs by targeting key regulators of endochondral ossification. Vascular endothelial growth factor (VEGF) knockout in MSOD-B cells yielded cartilage matrices that, despite delayed vascularization, retained full capacity to prime endochondral ossification in ectopic models, indicating that VEGF is dispensable for initiating this program. In contrast, Runt-related transcription factor 2 (RUNX2) knockout prevented cartilage hypertrophy and significantly reduced ossification, yet enhanced cartilage repair in a rat osteochondral defect model. These findings demonstrate that transcriptional engineering of ECM-producing cells enables the precise modulation of regenerative outcomes, allowing for programmable shifts between osteogenic and chondrogenic pathways (Paper 3). Finally, we characterized the immune response to ECMs from cartilage (Paper 4) and 3D-printed lung tissues (Paper 5) in various animal models, highlighting the correlation between early M2 macrophage recruitment and tissue regeneration, and noting the variability in the predictive outcomes of tissue regeneration based on early immune recruitment patterns.

In summary, we demonstrated the performance of ECMs in instructing tissue repair using standardized cell lines, of which genetic customization leads to tailored graft properties. We determined the immunogenicity of ECMs and revealed early immune response patterns in engineered and 3D-printed ECMs associated with successful tissue regeneration. Our research contributes to the development of effective repair strategies beyond the skeletal framework, facilitating the advancement of next-generation, personalized grafts.

Keywords: Tissue engineering, Engineered Extracellular Matrices, CRISPR/Cas9, Customisable matices, Cell-free, Off-the shelf,

Classification system and/or index terms (if any)

Supplementary bibliographical information	**Language** English
ISSN and key title: 1652-8220	**ISBN:** 978-91-8021-760-6
Recipient's notes / **Number of pages** 98	
Security classification	

Signature  Date 2025-07-31

Regenerative performance and immunogenicity of engineered extracellular matrices

Sujeethkumar Prithiviraj

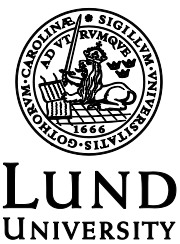

LUND
UNIVERSITY

DOCTORAL DISSERTATION

Doctoral dissertation for the degree of Doctor of Philosophy (PhD) at the Faculty of Medicine at Lund University to be publicly defended on the date of October 20th at 13:00 in Grunn Salen, BMC Lund.

Faculty opponent
Dr. Ioannis Papantoniou
Associate professor at KU Leuven, Belgium

Cover photo - Image generated using ChatGPT-4 by OpenAI, May 22, 2024

Faculty of Medicine
Department of Clinical Sciences, Lund

ISSN 1652-8220
ISBN 978-91-8021-760-6
Lund University, Faculty of Medicine Doctoral Dissertation Series 2025:10

Printed in Sweden by Media-Tryck, Lund University
Lund 2025

“The aim of science is not to open the door to infinite wisdom, but to set a limit to infinite error.”

— Bertolt Brecht, Life of Galileo

This thesis has in part been produced with the assistance of generative AI tools, specifically OpenAI's ChatGPT. I (along with my PI) independently developed the concept, research narrative, and scientific content. I used the AI model primarily to improve grammar, enhance sentence structure, and refine the overall clarity of the text. All suggestions from the tool were critically reviewed, edited, and incorporated by me, and I take full responsibility for the final content. A more detailed description of how and when the AI tools were used is provided in the methodology section.

Table of Contents

Abbreviations 9

Popular Summary 11

Swedish 12

German 13

Tamil 15

List of publications included in this thesis. 17

List of publications not included in this thesis. 18

Abstract 19

Introduction 21

Architecture and composition of bones 21

Intramembranous ossification 22

Endochondral ossification 23

Clinical need for bone regeneration 25

Tissue engineering: Concepts and components 27

Extracellular Matrix: 28

Cellular grafts: 30

Acellular Matrices: 31

Native Extracellular Matrices (nECMs) 32

Synthetic Extracellular Matrices (sECMs) 32

Engineered Extracellular Matrices (eECMs) 33

Immunogenicity in Tissue Repair and Scaffold Design 35

Challenges in Clinical Translation 37

Aims 39

Key Results 40

Paper I: Sustained delivery of a heterodimer bone morphogenetic protein-2/7 via a collagen hydroxyapatite scaffold accelerates and improves critical femoral defect healing 40

Paper II: Manufacturing of Human Tissues as Off-the-shelf Grafts Programmed to Induce Regeneration 42

Paper III: Compositional editing of extracellular matrices by CRISPR/Cas9 engineering of human mesenchymal stem cell lines 45

Paper IV: Engineered human cartilage matrix exhibits potent immunoregulatory properties while promoting complete femoral restoration in pre-clinical models 51

Paper V: Extracellular-Matrix-Reinforced Bioinks for 3D Bioprinting Human Tissue 56

Discussions and Future Perspectives 58

Paper I 58

Paper II 59

Paper III 61
Paper IV 63
Paper V 64
Methodology **66**
Cells: Expansion, Transfection and Differentiation 66
CRISPR/Cas9-Based Transfection of MSOD-B Cells 66
Cell Expansion 66
Chondrogenic Differentiation 66
Osteogenic Differentiation 66
Scaffold/graft processing and storage 67
Lyophilization 67
Animal models and implantation methods 67
Ectopic Implantation (Paper I-V) 67
Osteochondral defect model (Paper III) 68
Critical-sized femoral defect model 68
In vivo and ex vivo Angiogenesis assays 68
Cam Assay 68
Vascular density quantification 69
Molecular and cellular assays 69
Flow cytometry 69
Western blot 70
qPCR 70
GAG analysis 70
Histology and Image Analysis 71
Chemical staining 71
Histological Grading Method 72
Cartilage Quantification method 72
Trabecular Thickness (Tb.Th) and Trabecular Separation (Tb.Sp) 73
Immunofluorescence 73
In vivo Micro-CT scanning 73
In vitro Micro-CT scanning 73
Immune cell isolation and polarization methods 73
PBMCs preparation 74
Monocyte isolation and in vitro polarisation 74
Macrophage polarisation analysis 74
Acknowledgements **76**
References **79**

Abbreviations

BMP	Bone Morphogenetic Protein
BMP-2	Bone Morphogenetic Protein 2
BMP-7	Bone Morphogenetic Protein 7
CRISPR	Clustered Regularly Interspaced Short Palindromic Repeats
DBM	Demineralized Bone Matrix
ECM	Extracellular Matrix
eECM	Engineered Extracellular Matrix
FGF	Fibroblast Growth Factor
GelMA	Gelatin Methacrylate
HAp	Hydroxyapatite
Ihh	Indian Hedgehog
IL-1β	Interleukin-1 beta
IL-10	Interleukin-10
MMP	Matrix Metalloproteinase
MSC	Mesenchymal Stem/Stromal Cell
MSOD-B	Mesenchymal Stem/Stromal Cell Line B
nECM	Native Extracellular Matrix
PGA	Polyglycolic Acid
PEG	Polyethylene Glycol
PLA	Polylactic Acid
PLGA	Polylactic-co-Glycolic Acid
PTHrP	Parathyroid Hormone-related Protein
RGD	Arginylglycylaspartic Acid
RNP	Ribonucleoprotein
RUNX2	Runt-related Transcription Factor 2
sECM	Synthetic Extracellular Matrix
TAZ	Transcriptional Coactivator with PDZ-binding Motif
TE	Tissue Engineering

TGF-β	Transforming Growth Factor Beta
TNF-α	Tumor Necrosis Factor Alpha
VEGF	Vascular Endothelial Growth Factor
YAP	Yes-associated Protein

Popular Summary

Our body is like a thriving city, always busy, with some construction constantly going on—building, maintaining, or removing. The primary workers responsible for maintaining functionality and handling maintenance are our immune cells. However, there are times when things inevitably go out of control, accidents happen, and further assistance is required for repair and recovery.

We typically import construction materials, which we refer to as biomaterials, to address these issues. One important thing to emphasize is how sensitive it may be to anything it is not familiar with. Naturally, it does not like construction materials not made in its own land (our body). Traditionally, these imported construction materials (biomaterials) are used as replacements for damaged parts of the city (injured tissue).

In our lab, we have developed specialized materials (Engineered ECMs) that are akin to AI-integrated machines. They not only replace the damaged part of the city (tissue replacement) but also actively assist our maintenance workers (the immune system) in their natural repair processes and help construct the damaged part using their own materials (tissue regeneration). We have also developed an update (decellularization) to these special materials to remove any errors and improve their user-friendliness (integration) with the maintenance team.

The focus of this thesis is to study the performance of these special materials (Engineered ECMs). I test them in different locations (animal models) to see how they can assist the local maintenance team (immune system) in rebuilding damaged regions. Another important factor I worked on is user feedback (immune response). As you know, like any product, user satisfaction is an essential factor for the success of the product. It is of utmost importance to keep the users—in this case, the maintenance team (immune system)—happy. I conduct various interviews (experiments) to gather as much feedback as I can to improve the special material's design and make it more user-friendly (biocompatible).

In addition, I used cutting-edge technology (CRISPR/Cas9 gene editing) to upgrade our special materials (Engineered ECMs), making them more personalized according to the specific needs of different cities (different parts of the body). With this, we can customize the AI previously absent.

Hopefully, with this advanced material (Engineered ECMs) and all these upgrades (Decellularization and CRISPR/Cas9 modification), we aim to generate personalized, readily available materials to meet any city's needs (Personalized therapies for tissue regeneration).

Swedish

Vår kropp är som en blomstrande stad, alltid upptagen, med vissa konstruktioner som ständigt pågår - att bygga, underhålla eller ta bort. De huvudsakliga arbetarna som är ansvariga för att hålla saker och ting funktionella och sköta underhållet är våra immunceller. Men det finns tillfällen då saker oundvikligen går utom kontroll, olyckor inträffar och ytterligare hjälp krävs för reparation och återhämtning.

Vi importerar vanligtvis byggmaterial, som vi kallar biomaterial, för att åtgärda dessa problem. En viktig sak att betona är hur strikt vårt immunförsvar är – det kan vara väldigt känsligt och kan reagera på allt de inte känner till. Naturligtvis gillar den inte byggmaterial som inte är tillverkade i sitt eget land (vår kropp). Traditionellt används dessa importerade byggmaterial (biomaterial) som ersättning för skadade delar av staden (skadad vävnad).

I vårt labb har vi utvecklat specialmaterial (Engineered ECMs) som mer liknar AI-integrerade maskiner. De ersätter inte bara den skadade delen av staden (vävnadsersättning) utan hjälper aktivt våra underhållsarbetare (immunsystemet) i deras naturliga reparationsprocesser och hjälper till att konstruera den skadade delen med hjälp av deras egna material (vävnadsregenerering). Vi har också utvecklat en uppdatering (decellularisering) av dessa specialmaterial för att ta bort eventuella fel och förbättra deras användarvänlighet (integration) med underhållsteamet.

Fokus för denna avhandling är att studera prestandan hos dessa speciella material (Engineered ECMs). Jag testar dem på olika platser (djurmodeller) för att se hur de kan hjälpa det lokala underhållsteamet (immunsystemet) med att återuppbygga skadade regioner. En annan viktig faktor jag arbetat med är användarfeedback (immunrespons). Som du vet, precis som alla produkter, är användarnas tillfredsställelse en viktig faktor för produktens framgång. Det är av yttersta vikt att hålla användarna – i det här fallet underhållsteamet (immunsystemet) – nöjda. Jag genomför olika intervjuer (experiment) för att samla in så mycket feedback jag kan för att förbättra specialmaterialets design och göra det mer användarvänligt (biokompatibelt).

Dessutom använde jag banbrytande teknologi (CRISPR/Cas9 genredigering) för att uppgradera våra specialmaterial (Engineered ECMs), vilket gjorde dem mer personliga efter de specifika behoven i olika städer (olika delar av kroppen). Med detta kan vi anpassa AI:n i specialmaterialet för att hjälpa till att bygga de önskade förbättringarna som inte fanns tidigare.

Förhoppningsvis, med detta avancerade material (Engineered ECMs) och alla dessa uppgraderingar (Decellularization och CRISPR/Cas9 modifiering), siktar vi på att generera personligt anpassat, lättillgängligt material för alla städers behov (Personaliserade terapier för vävnadsregenerering).

German

Unser Körper ist wie eine florierende und stets aktive Stadt, in der ständig etwas gebaut, instandgehalten oder abgerissen wird. Die für die Funktionsfähigkeit und Wartung verantwortlichen Hauptarbeiter sind unsere Immunzellen. Aber manchmal geraten Dinge unvermeidlich außer Kontrolle, Unfälle passieren, und zusätzliche Hilfe für Reparatur und Genesung wird erforderlich.

Um diese Probleme zu beheben, importieren wir normalerweise Baumaterialien, die wir Biomaterialien nennen. Dabei ist es wichtig zu betonen, dass unser Immunsystem extrem streng ist – es ist sehr empfindlich und kann auf alles reagieren, was ihm unbekannt ist. Natürlich mag es keine Baumaterialien, die nicht in seinem eigenen Land (unserem Körper) hergestellt wurden. Traditionell werden diese importierten Baumaterialien (Biomaterialien) als Ersatz für beschädigte Bereiche in der Stadt (verletztes Gewebe) verwendet.

In unserem Labor haben wir spezielle Materialien (Engineered ECMs) entwickelt, die eher Maschinen mit künstlicher Intelligenz ähneln. Sie ersetzen nicht nur den beschädigten Teil der Stadt (Gewebeersatz), sondern unterstützen unsere Wartungsarbeiter (das Immunsystem) aktiv bei ihren natürlichen Reparaturprozessen und helfen beim Wiederaufbau des beschädigten Teils mit ihren eigenen Materialien (Geweberegeneration). Wir haben auch ein Update (Dezellularisierung) für diese Spezialmaterialien entwickelt, um Fehler zu beseitigen und ihre Benutzerfreundlichkeit (Integration) für das Wartungsteam zu verbessern.

Der Schwerpunkt dieser Forschungsarbeit liegt auf der Untersuchung der Leistung dieser Spezialmaterialien (Engineered ECMs). Ich teste sie an verschiedenen Orten (Tiermodellen), um zu sehen, wie sie das lokale Wartungsteam (Immunsystem) beim Wiederaufbau beschädigter Bereiche unterstützen können. Ein weiterer wichtiger Faktor, an dem ich gearbeitet habe, ist das Benutzerfeedback (Immunreaktion). Wie Sie wissen, ist die Benutzerzufriedenheit wie bei jedem Produkt ein wesentlicher Faktor für den Produkterfolg. Es ist von größter Bedeutung, die Benutzer – in diesem Fall das Wartungsteam (Immunsystem) – zufrieden zu stellen. Ich führe verschiedene Interviews (Experimente), um so viel Feedback wie möglich zu sammeln, das Design des Spezialmaterials zu verbessern und es benutzerfreundlicher (biokompatibel) zu machen.

Darüber hinaus habe ich modernste Technologie (CRISPR/Cas9-Genbearbeitung) verwendet, um unsere Spezialmaterialien (Engineered ECMs) zu verbessern und sie entsprechend den spezifischen Anforderungen verschiedener Stadtteile (verschiedener Körperteile) individueller zu gestalten. Damit können wir die künstliche Intelligenz im Spezialmaterial anpassen, um die gewünschten Verbesserungen zu erzielen, die es vorher nicht gab.

Hoffentlich können wir mit diesem fortschrittlichen Material (konstruierte ECMs) und all diesen Upgrades (Dezellularisierung und CRISPR/Cas9-Modifizierung) personalisierte, leicht verfügbare Materialien für die Bedürfnisse jeder Stadt erzeugen (personalisierte Therapien zur Geweberegeneration).

Tamil

நம் உடலானது செழித்து வளர்ந்து வரும் நகரத்தைப் போன்றது. எப்பொழுதும் தொடர்ச்சியாக ஓய்வின்றி , சில கட்டுமானங்கள், சீரமைப்பு அல்லது அகற்றும் பணிகள் நடைபெற்றுக் கொண்டிருக்கும். இவை இயங்குவதற்கும் பராமரிப்பைக் கையாளுவதற்கும் நமது நோயெதிர்ப்பு செல்கள் முக்கியமானவை. எனினும், சில தவிர்க்க இயலாத நேரங்களில் கட்டுப்பாட்டினை மீறி விபத்துகள் போன்றவை நிகழ்கையில், மேலும் பழுது மற்றும் மீட்புக்கு கூடுதல் உதவி தேவை. இந்த சிக்கலை சரிசெய்ய நாங்கள் வழக்கமாக இறக்குமதி செய்யும் கட்டுமான பொருட்களை , உயிர் பொருட்கள்(Biomaterials) என்று அழைக்கிறோம். வலியுறுத்த வேண்டிய ஒரு முக்கியமான விசயம் என்னவென்றால், நமது நோயெதிர்ப்பு அமைப்பு எவ்வளவு கண்டிப்பானது என்பது. அவை மிகவும் உணர்திறன் கொண்டவை, தனக்குத் தெரியாத அனைத்திற்கும் எதிர்வினையாற்றும். இயற்கையாகவே, அதன் சொந்த மண்ணில் (நம் உடல்) தயாரிக்கப்படாத எந்த ஒரு கட்டுமானப் பொருட்களையும் அவை விரும்புவதில்லை. பொதுவாக, இந்த இறக்குமதி செய்யப்பட்ட கட்டுமானப் பொருட்கள் (உயிர் பொருட்கள்) நகரத்தின் சேதமடைந்த பகுதிகளை (காயமடைந்த திசு) மாற்றுவதற்குப் பயன்படுத்தப்படுகின்றன.

எங்கள் ஆய்வகத்தில், செயற்கை நுண்ணறிவு - ஒருங்கிணைக்கப்பட்ட இயந்திரங்களைப் போன்ற சிறப்புப் பொருட்களை (பொறியியல் ECMகள்) உருவாக்கியுள்ளோம். அவை நகரின் சேதமடைந்த பகுதியை (திசு மாற்றுதல்) மாற்றுவது மட்டுமல்லாமல், எங்கள் பராமரிப்புப் பணியாளர்களுக்கு (நோய் எதிர்ப்பு அமைப்பு) அவர்களின் இயற்கையான பழுது பார்க்கும் செயல்முறைகளில் தீவிரமாக உதவுகின்றன மற்றும் சேதமடைந்த பகுதியை தங்கள் சொந்த பொருட்களைப் பயன்படுத்தி (திசு மீளுருவாக்கம்) மீண்டும் உருவாக்க உதவுகின்றன. ஏதேனும் பிழைகள் இருந்தால் அவற்றை நீக்கி, பராமரிப்புக் குழுவுடன் ஆன ஒருங்கிணைப்பை மேம்படுத்த, இந்த சிறப்புப் பொருட்களுக்கான புதுப்பிப்பை (செல்லுலரைசேஷன்) உருவாக்கியுள்ளோம்.

இந்த ஆய்வறிக்கையின் நோக்கம், இந்த சிறப்புப் பொருட்களின் (பொறியியல் ECMகள்) செயல்திறனைப் அறிவதாகும். சேதமடைந்த பகுதிகளை மீண்டும் உருவாக்க உள்ளூர் பராமரிப்புக் குழுவுக்கு (நோய் எதிர்ப்பு அமைப்பு) எவ்வாறு உதவ முடியும் என்பதைப் பார்க்க, அவற்றை வெவ்வேறு இடங்களில் (விலங்கு மாதிரிகள்) சோதித்தேன். நான் பணிபுரிய மற்றொரு முக்கியமான காரணம் பயனர்களுடைய மீள்கருத்து (நோய் எதிர்ப்பு வினை). உங்களுக்குத் தெரியும், எந்தவொரு தயாரிப்பையும் போலவே, தயாரிப்பின் வெற்றிக்கு பயனர் திருப்தி ஒரு முக்கிய காரணியாகும். பயனர்களை-இந்த விஷயத்தில், பராமரிப்பு குழு (நோய் எதிர்ப்பு அமைப்பு)-மகிழ்ச்சியாக வைத்திருப்பது மிகவும் முக்கியம். சிறப்புப் பொருளின் வடிவமைப்பை மேம்படுத்தவும், பயனர்களுக்கு ஏற்றதாக (உயிர் இணக்கத்தன்மை) உருவாக்கவும் என்னால் முடிந்த அளவு கருத்துக்களைச் சேகரிக்க பல்வேறு நேர்காணல்களை (சோதனைகள்) நடத்துகிறேன்.

மேலும், வெவ்வேறு நகரங்களின் (உடலின் வெவ்வேறு பாகங்கள்) குறிப்பிட்ட தேவைகளுக்கு எங்கள் சிறப்புப் பொருட்களை (பொறியியல் ECMகள்) பயனர்களுக்கு ஏற்றவாறு அதிநவீன தொழில்நுட்பத்தை (CRISPR/Cas9 மரபணு திருத்தம்) பயன்படுத்தினேன். இதன்மூலமாக, சிறப்புப் பொருட்களில் முன்னர் கிடைக்காத மேம்பாடுகளுடன் உருவாக்க உதவும் செயற்கை நுண்ணறிவை பயனர்களுக்கு தகுந்தவாறு அனுமதிக்கிறது. இந்த மேம்பட்ட பொருள் (பொறியியல் ECMகள்) மற்றும் இந்த மேம்பாடுகள் (Decellularization மற்றும் CRISPR/Cas9 மாற்றம்) மூலம், எந்தவொரு நகரத்தின் தேவைகளுக்கும் (திசு மீளுருவாக்கம் தனிப்பயனாக்கப்பட்ட சிகிச்சைகள்) பயனர்களுக்கு ஏற்ப, எளிதில் கிடைக்கக் கூடிய பொருட்களை உருவாக்குவதையே எங்கள் நோக்கமாகக் கொண்டுள்ளோம்.

List of publications included in this thesis.

1) Liu Y, Puthia M, Sheehy EJ, Ambite I, Petrlova J, **Prithviraj S**, Oxborg MW, Sebastian S, Vater C, Zwingenberger S, Struglics A, Bourgine PE, O'Brien FJ, Raina DB.

   Sustained delivery of a heterodimer bone morphogenetic protein-2/7 via a collagen hydroxyapatite scaffold accelerates and improves critical femoral defect healing. Acta Biomater. 2023 May;162:164-181. doi: 10.1016/j.actbio.2023.03.028. Epub 2023 Mar 24. PMID: 36967054.

2) S. Pigeot, T. Klein, F. Gullotta, S. J. Dupard, A. GarciaGarcia, A. García-García, **S. Prithiviraj**, P. Lorenzo, M. Filippi, C. Jaquiery, L. Kouba, M. A. Asnaghi, D. B. Raina, B. Dasen, H. Isaksson, P. Önnerfjord, M. Tägil, A. Bondanza, I. Martin, P. E. Bourgine

   Manufacturing of Human Tissues as off-the-shelf Grafts Programmed to Induce Regeneration. Adv. Mater. 33, (2021), 2103737

3) **Prithiviraj Sujeethkumar**, Garcia Alejandro Garcia, Linderfalk Karin, Yiguang Bai, Ferveur Sonia, Falck Ludvig Nilsén, Subramaniam Agatheeswaran, Mohlin Sofie, Hidalgo David, Dupard Steven J, Raina Deepak Bushan, Bourgine Paul E

   Compositional editing of extracellular matrices by CRISPR/Cas9 engineering of human mesenchymal stem cell lines eLife 13 (2024) :RP96941

4) Alejandro Garcia Garcia*, **Sujeethkumar Prithiviraj***, Deepak B. Raina, Tobias Schmidt, Aurelie Baudet-Quintino, Sara Gonzalez Anton, Laura Rabanal Cajal, David Hidalgo Gil, Robin Kahn, Magnus Tägil, Paul Bourgine

   Engineered human cartilage matrix exhibits potent immunoregulatory properties while promoting complete femoral restoration in pre-clinical models (In review)

5) De Santis MM, Alsafadi HN, Tas S, Bölükbas DA, **Prithiviraj S**, Da Silva IAN, Mittendorfer M, Ota C, Stegmayr J, Daoud F, Königshoff M, Swärd K, Wood JA, Tassieri M, Bourgine PE, Lindstedt S, Mohlin S, Wagner DE.

   Extracellular-Matrix-Reinforced Bioinks for 3D Bioprinting Human Tissue. Adv Mater. 2021 Jan;33(3):e2005476.

* These authors contributed equally and share co-first authorship

List of publications not included in this thesis.

1) Ani Grigoryan, Dimitra Zacharaki, Alexander Balhuizen, Christophe Rm Côme, Alejandro Garcia Garcia, David Hidalgo Gil, Anne-Katrine Frank, Kristina Aaltonen, Adriana Mañas, Javanshir Esfandyari, Pontus Kjellman, Emelie Englund, Carmen Rodriguez, Wondossen Sime, Ramin Massoumi, Nasim Kalantari, Sujeethkumar Prithiviraj, Yuan Li, Steven J Dupard, Hanna Isaksson, Chris D Madsen, Bo T Porse, Daniel Bexell, Paul E Bourgine

   Engineering human mini-bones for the standardized modeling of healthy hematopoiesis, leukemia, and solid tumor metastasis. Sci Transl Med . 2022 Oct 12;14(666):eabm6391

Abstract

Critical-sized bone defects remain a significant unmet clinical need, with > 500,000 reconstructive procedures performed annually in the United States and Europe and associated costs exceeding US$3 billion. Autologous bone grafting—the current gold standard—suffers from limited harvest volume and donor-site morbidity, whereas allografts show variable integration and carry immunological and infection risks. Recombinant therapies using growth factors partly address these issues but require supraphysiological doses that provoke ectopic ossification and inflammation. Tissue engineering (TE) offers a conceptual solution by combining cells, bioactive cues and scaffolds to fabricate living grafts; however, cell-laden constructs that rely on the in vitro expansion and differentiation of primary cells face considerable challenges, including variability between donors, extended production times, reduced viability upon implantation, and limited scalability. Engineered extracellular matrices (ECMs)—acellular scaffolds deposited by cells and subsequently devitalized—offer a way to overcome these barriers by preserving intrinsic biological cues, thereby addressing the logistical and safety challenges associated with cell-based therapies. This thesis explores how eECMs can be optimized for bone regeneration by addressing four critical translational barriers: growth factor dependency, cell donor variability, programmable matrix function, and immune compatibility.

First, we show that a collagen–hydroxyapatite scaffold loaded with heterodimeric Bone morphogenetic protein (BMP) 2/7 significantly improves osteoinduction at lower doses than BMP-2 alone, enhancing osteogenic progenitor recruitment and matrix deposition (Paper 1). We then demonstrate the development of an off-the-shelf eECM generated from a standardized human mesenchymal stem/stromal cell line (MSOD-B), which, upon devitalization, supports robust endochondral ossification in a cell-free manner (Paper 2). We applied CRISPR/Cas9 editing to customize the composition and function of eECMs by targeting key regulators of endochondral ossification. Vascular endothelial growth factor (VEGF) knockout in MSOD-B cells yielded cartilage matrices that, despite delayed vascularization, retained full capacity to prime endochondral ossification in ectopic models, indicating that VEGF is dispensable for initiating this program. In contrast, Runt-related transcription factor 2 (RUNX2) knockout prevented cartilage hypertrophy and significantly reduced ossification, yet enhanced cartilage repair in a rat osteochondral defect model. These findings demonstrate that transcriptional engineering of ECM-producing cells enables the precise modulation of regenerative outcomes, allowing for programmable shifts between osteogenic and chondrogenic pathways (Paper 3). Finally, we characterized the immune response to ECMs from cartilage (Paper 4) and 3D-printed lung tissues (Paper 5) in various animal models, highlighting the correlation between early M2 macrophage recruitment and tissue

regeneration, and noting the variability in the predictive outcomes of tissue regeneration based on early immune recruitment patterns.

In summary, we demonstrated the performance of ECMs in instructing tissue repair using standardized cell lines, of which genetic customization leads to tailored graft properties. We determined the immunogenicity of ECMs and revealed early immune response patterns in engineered and 3D-printed ECMs associated with successful tissue regeneration. Our research contributes to the development of effective repair strategies beyond the skeletal framework, facilitating the advancement of next-generation, personalized grafts.

Introduction

Architecture and composition of bones

Bones are complex organs that serve numerous physiological functions beyond merely providing structural support. They act as vital reservoirs of calcium and phosphate, which are critical for maintaining systemic mineral homeostasis.[1] This mineral reservoir facilitates various metabolic processes and helps regulate the body's mineral balance. Additionally, bones house the bone marrow, the primary site for hematopoiesis, underscoring its dual role in mineral regulation and blood cell production.[2] It is essential to recognize that bones function as a metabolically active tissue, playing a significant part in mineral homeostasis and hematopoiesis, thereby contributing to overall physical health.[3].

From a structural perspective, bones exhibit a hierarchical organization characterized by multiple length scales that confer exceptional mechanical resilience and regenerative capacity. At the nanoscale, bones primarily comprise type I collagen fibrils extensively mineralized with hydroxyapatite (HAp) crystals. These needle-like crystallites bond to form platelets, which stack into larger mineralized collagen units.[1]. The collagen fibrils arrange themselves into concentric layers known as lamellae, culminating in the formation of osteons—Haversian systems centered around vascular canals in cortical bones. This sophisticated multi-scale architecture provides cortical bones with enhanced mechanical properties such as stiffness and toughness, which are crucial for load-bearing roles.[4]

Conversely, trabecular bones comprise a porous network with interconnecting struts and plates. This architecture increases the surface area and vascularity, facilitating efficient metabolic exchange and supporting rapid calcium turnover.[5] Integrating a compact cortical shell with a metabolically active trabecular core allows bones to maintain a lightweight yet robust structure capable of dissipating stress and adapting to mechanical demands per Wolff's law.[6] Consequently, bone regeneration is fundamentally distinctive, differing from the disorganized fibrotic healing observed in soft tissues. Bone regeneration is an organized process unfolding through well-regulated phases of inflammation, repair, and remodeling, ultimately restoring the bone's form and function.[7–9] The effectiveness of this regenerative process is closely tied to the intricate hierarchical design of bones, from the organization of mineralized collagen at the nanoscale to the macro-level arrangements of the cortical and trabecular components.[10]

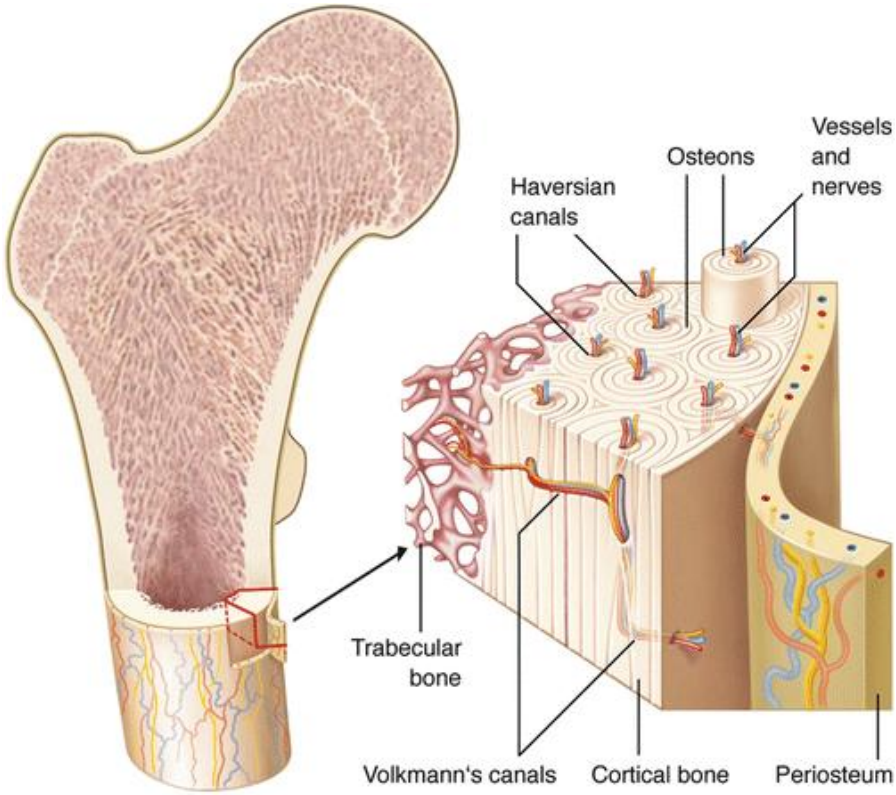

Structural organization of bone. *Cortical bone is composed of osteons arranged around Haversian canals, interconnected by Volkmann's canals that transmit vessels and nerves. The trabecular bone forms a porous lattice that enhances vascularity and metabolic exchange, while the periosteum provides an external covering that supports vascular supply and progenitor cell activity*[11].

Intramembranous ossification

Bone formation occurs through two primary developmental pathways: intramembranous and endochondral ossification. Intramembranous ossification is a direct mechanism where mesenchymal stem/stromal cells (MSCs) differentiate into osteoblasts without forming a cartilage intermediate. This pathway is crucial for forming the flat bones of the skull and clavicle and is regulated by a complex interplay of mechanical cues and molecular signals.[12] In this process, MSCs undergo condensation and begin to express the pivotal osteogenic transcription factor RUNX2, initiating the expression of essential bone matrix proteins, such as type I collagen and osteocalcin.[13]

Bone morphogenetic proteins (BMPs) serve as significant regulatory cues, promoting RUNX2 expression and osteoblast maturation, which are fundamental for bone formation. BMP2, in particular, activates cellular signaling pathways that

lead to the transcription of various osteogenic genes, including RUNX2 and Osterix, thereby driving the differentiation of MSCs[14,15]. Concurrently, the Wnt/β-catenin signaling pathway is supportive; it synergizes with BMP signaling to enhance osteogenic differentiation while inhibiting adipogenesis in MSCs.[13] Evidence shows that active Wnt signaling encourages a shift from fat lineage differentiation towards a bone-forming phenotype, reinforcing the commitment of MSCs to the osteogenic pathway.[16] Additionally, fibroblast growth factors (FGFs) significantly contribute to this process by stimulating the proliferation of osteoprogenitor cells and promoting their later differentiation into osteoblasts.[17,18] Disruption in FGF signaling has been correlated with impaired intramembranous bone formation, particularly evident in conditions such as craniosynostosis.[19]

The intricate relationship between osteoblasts and vascularization is critical during intramembranous ossification. As osteoblasts lay down the osteoid, angiogenic factors such as vascular endothelial growth factor (VEGF) are secreted, promoting blood vessel infiltration into the developing bone. This vascularization is essential, as it supplies the necessary oxygen and nutrients to support the high metabolic activity associated with bone formation.[20,21] Furthermore, growth factors like TGF-β1 have been observed to enhance intramembranous bone healing, with exogenous TGF-β1 accelerating regeneration in models of calvarial defects, thereby highlighting the compound's role in facilitating normal intramembranous pathways.[22]

Endochondral ossification

Endochondral ossification is a complex process that involves the formation of a cartilage template that is subsequently replaced by bone. This pathway is crucial for developing long bones and facilitating the natural healing of fractures, as it reflects various aspects of embryonic bone development that persist throughout adulthood. The process begins with the condensation of MSCs, which differentiate into chondrocytes under the influence of the transcription factor SOX9, a key regulator of chondrogenesis.[23,24]

During the progression of endochondral ossification, chondrocytes undergo proliferation and secrete a cartilage matrix. As the cartilage template matures, these chondrocytes undergo hypertrophy, characterized by increased cell size, and begin expressing osteogenic markers such as RUNX2 and Osterix (Sp7), which signify a transition to an osteogenic program.[25,26] Hypertrophic chondrocytes produce alkaline phosphatase, which contributes to the calcification of the cartilage matrix in preparation for the subsequent transition to bone formation.[27]. The apoptosis of these hypertrophic chondrocytes, or their transdifferentiation into osteoblast-like cells, is essential for depositing mineralized bone and indicates the dynamic nature of this growth process.[28,29]

The cartilage-to-bone transition is regulated through a sophisticated network of signaling pathways. BMPs are essential in promoting the maturation of chondrocytes and elevating RUNX2 expression, thereby driving hypertrophic chondrocyte differentiation and the ultimate formation of osteoblasts.[30,31] Concurrently, Wnt/β-catenin signaling regulates the differentiation pace; active Wnt signaling promotes the terminal differentiation of hypertrophic chondrocytes, while the loss of Wnt signaling results in the cessation of differentiation.[25,27] Conversely, FGFs, specifically through FGFR3, act as a negative regulator of endochondral growth by limiting chondrocyte proliferation and hypertrophy, a mechanism particularly observed in disorders such as achondroplasia.[32,33] This intricate coordination across various signaling pathways is vital to ensure a systematic progression from chondrocyte proliferation at the periphery to central hypertrophic changes, followed by timely bone replacement.[33,34]

A significant regulatory feature in endochondral ossification is the Indian hedgehog (Ihh)/parathyroid hormone-related protein (PTHrP) feedback loop. Hypertrophic chondrocytes produce Ihh, which diffuses to resting chondrocytes and stimulates the secretion of PTHrP. PTHrP ensures the continued proliferation of chondrocytes and delays their hypertrophy, allowing for the orderly growth of the cartilage template.[33,35] As the template elongates, a gradient of PTHrP helps maintain a reservoir of proliferating chondrocytes near the ends, while allowing older chondrocytes in the center to undergo hypertrophy. Genetic disruptions to the Ihh signaling have been associated with aberrant ossification, as seen in Ihh-deficient mice, which present with truncated long bones and failed normal bone collar formation.[26,29]

Following hypertrophy and programmed cell death of the chondrocytes, the cartilage matrix must be degraded to permit the encroachment of bone. Matrix metalloproteinases (MMPs), especially MMP-13, are secreted by the invading cells and hypertrophic chondrocytes, facilitating this degradation and allowing blood vessels to infiltrate the tissue. Research has demonstrated that MMP-9 is essential for vascular invasion of hypertrophic cartilage, as it helps release sequestered VEGF from the matrix, promoting angiogenesis within the growth plate.[36,37]. These newly formed blood vessels deliver osteoprogenitor cells and osteoclast precursors, leading to the resorption of calcified cartilage by osteoclasts and the deposition of new bone by osteoblasts onto the remaining cartilage matrix, resulting in the formation of primary spongiosa.[38,39] Ultimately, the woven bone formed through this process will mature into organized lamellar bone upon further remodeling.[40,41]

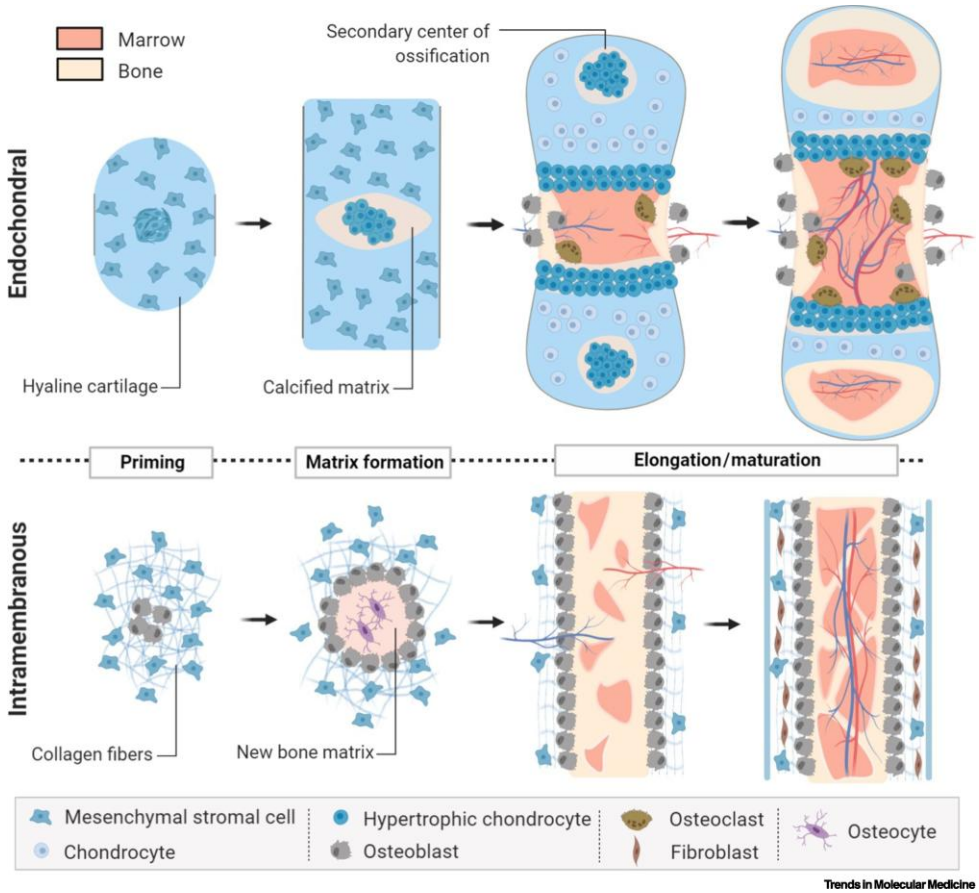

Pathways of bone formation. *In intramembranous ossification, mesenchymal stromal cells condense and differentiate directly into osteoblasts under the influence of osteogenic cues such as RUNX2, BMPs, and Wnt/β-catenin signaling. Osteoblasts secrete collagen-rich matrix that mineralizes, accompanied by vascular invasion and maturation into organized bone. In endochondral ossification, mesenchymal stromal cells first differentiate into chondrocytes to form a hyaline cartilage template. Chondrocytes proliferate and undergo hypertrophy, express RUNX2 and Osterix, and initiate matrix calcification. Subsequent vascular invasion, osteoclast-mediated resorption, and osteoblast deposition replace the cartilage scaffold with bone, establishing the mature structure of long bones*[42].

Clinical need for bone regeneration

Despite the remarkable regenerative capacity of bones, critical-sized bone defects arising from various causes, including trauma, infection, tumor resection, or congenital anomalies, present significant clinical challenges. Such defects do not heal spontaneously and necessitate medical intervention. The incidence of fractures and bone defects requiring surgical repair is substantial, with over half a million patients undergoing surgical reconstructions in the United States and Europe each

year, collectively incurring healthcare costs exceeding $3 billion.[43] The burden of these conditions extends beyond mere financial implications, as they lead to long-term disability, impaired limb function, and a diminished quality of life for affected individuals.[44]

The traditional approach to managing critical bone loss has been autologous bone grafting, where a segment of bone is harvested, usually from the iliac crest, and transplanted to the defect site. Autografts are prized for providing osteogenic cells, osteoinductive growth factors, and a suitable osteoconductive scaffold.[45] However, this approach is not without downsides; there are limitations related to the supply of autograft material and complications associated with harvesting bone, which can include chronic pain or even fracture at the donor site, reported in some studies to occur in a significant number of patients.[46] Moreover, the finite nature of autograft materials presents significant challenges when confronted with extensive defects, where there may be insufficient grafts to achieve complete reconstruction.[47]

Allogeneic bone grafts, obtained from cadaveric donors, are employed as viable substitutes to circumvent the limitations of autografts. These allografts provide structural support but typically lack viable cells, leading to variable osteoinductive potential and presenting risks of immune rejection and infection.[48] Even when allografts are processed to eliminate living cells, immune responses can still be incited due to residual materials[49] Furthermore, allografts have been associated with slower incorporation into the host bone compared to autografts, which complicates their clinical utility.[50]

In addition to grafting strategies, clinicians have explored the use of bioactive molecules to boost bone healing. Specifically, recombinant human BMP-2 and BMP-7 have received approval for specific indications related to bone repair. These growth factors have shown effectiveness in stimulating bone regeneration in challenging fracture cases or spinal fusions; however, administering supraphysiological doses of BMPs can lead to adverse effects, including ectopic bone formation, inflammation, and potentially increased cancer risk.[51,52] Clinical cases, particularly with BMP-2 in cervical spine fusions, have dealt with reported rates of unintended bone growth in surrounding tissues, leading to complications such as nerve compression.[53] Thus, while BMPs can catalyze osteogenesis, their associated risks necessitate careful management and consideration regarding their clinical application.

The significant drawbacks associated with autografts (such as donor site morbidity), allografts (like immunogenicity and variable quality), and growth factor therapies (cost and potential adverse effects) underscore a compelling need for innovative bone regenerative strategies. An ideal bone graft substitute would be readily available in ample quantities, biocompatible, immunologically tolerated, and inherently osteogenic/osteoconductive without necessitating high-risk doses of exogenous growth factors. Such a substitute would promote the infiltration and

mobilization of the patient's cells while facilitating adequate vascularization and new bone formation in an organized manner, thus enhancing the body's natural healing processes.[54,55]

Tissue engineering: Concepts and components

Given the challenges associated with traditional methods of bone repair, tissue engineering (TE) has emerged as a promising paradigm for regenerating bone and other tissues. Tissue engineering is "an interdisciplinary field that applies the principles of engineering and life sciences toward the development of biological substitutes that restore, maintain, or improve tissue function."[56] . Essentially, TE seeks to fabricate living, functional tissues in a laboratory setting that can be implanted to replace or support damaged tissues. The classical TE strategy involves three critical components: (1) cells—often stem cells or progenitors that will produce the tissue matrix; (2) bioactive signals—such as growth factors and cytokines to direct cell behavior and differentiation; and (3) scaffolds—3D structural matrices (natural or synthetic) that provide a template for tissue formation and guide the organization of cells and the extracellular matrix.[57,58]

In the realm of bone engineering, the selection of the cell source is paramount. MSCs are frequently utilized due to their multipotent nature (capable of differentiating into bone, cartilage, fat, etc.) and ease of harvesting from locations such as bone marrow or adipose tissue. MSCs can be the architects of new bone if provided with the appropriate signals.[59] Internal genetic programs regulate their differentiation into osteoblasts, notably the transcription factor RUNX2, which is often referred to as a master switch for osteogenesis. Additionally, external cues from the microenvironment—including growth factors and the mechanical properties of the scaffold—are critical influencers of MSC behavior.[60] To promote osteogenic differentiation, osteogenic growth factors such as BMP-2 are commonly incorporated, as BMPs stimulate the expression of RUNX2 and other genes essential for bone development.[61,62] Furthermore, FGF can be added to encourage MSC proliferation and delay premature differentiation. In contrast, VEGF plays a key role in vascular ingrowth, is crucial for nourishment, and is synergized with BMPs to enhance bone formation.[63,64]

The scaffold functions as an artificial extracellular matrix, essential for supporting and guiding cell behavior. An ideal scaffold for bone should exhibit biocompatibility, biodegradability (to allow gradual replacement with new bone), and a porous architecture that facilitates cell migration and vascular infiltration. Typical scaffold materials include ceramics such as hydroxyapatite or tricalcium phosphate, which closely mimic the mineral component of bone, alongside natural polymers like collagen and fibrin, and synthetic polymers like Polylactic-Co-Glycolic Acid (PLGA) and polyethylene glycol.[57,58] The scaffold's microstructure,

including pore size, interconnectivity, and mechanical properties, significantly influences cellular behavior. Pore sizes around several hundred microns are generally favored for optimal vascularized bone ingrowth, while a stiffness comparable to native bone provides the necessary mechanical cues to MSCs. Studies indicate that substrate elasticity can steer stem cell lineage commitment, with stiffer substrates promoting osteogenesis while softer substrates may lead to adipogenesis or chondrogenesis.[59,60]

Modern tissue engineering approaches exploit advanced bioreactor systems to culture cell-scaffold constructs under dynamic conditions. These systems enable continuous media flow perfusion, enhancing nutrient and oxygen delivery to cells within 3D scaffolds, thus preventing necrotic areas. Furthermore, these bioreactors can apply mechanical stimuli, like cyclic compression or fluid shear, to simulate physiological environments, which often results in more robust and mature tissue formation.[65–67] In bone engineering, mechanical loading has been shown to foster osteogenic gene expression and promote matrix deposition, reflecting the mechanoresponsive capabilities of bone cells.[66]

Extracellular Matrix:

The extracellular matrix (ECM) is the non-cellular component of tissues that provides structural support and biochemical signals to cells. In bone and other tissues, the ECM is more than a passive scaffold; it is a dynamic, bioactive environment that regulates cell behavior and modulates healing. Generally, the ECM consists of a 3D network composed of fibrillar proteins (mainly collagens), elastin, glycoproteins (like fibronectin and laminin), and proteoglycans (which contain protein cores with glycosaminoglycan side chains such as heparan sulfate and chondroitin sulfate).[68] The ECM also incorporates the mineral hydroxyapatite deposited within the collagen matrix in bones. This construction gives the bones´ ECM an intricate hierarchical structure that spans from the nanoscale collagen/mineral arrangement to the microscale osteon organization to the macroscale whole-bone geometry. This multiscale architecture imparts unique mechanical properties to the bone matrix; aligned collagen fibers resist tensile forces, while the embedded mineral phase bears compressive loads, producing anisotropic strength in the bone.[69]

Beyond mechanical support, the ECM serves as a reservoir of signaling molecules. Many growth factors and cytokines are sequestered by ECM components and released and controlled during tissue remodeling. For instance, heparan sulfate proteoglycans in the ECM bind factors such as FGF 2, transforming growth factor beta (TGF-β), BMPs, and VEGF, sequestering them within the local environment. This sequestration protects the growth factors from degradation and establishes localized gradients that guide cell migration and differentiation.[70] During bone

remodeling or injury repair, proteases such as matrix metalloproteinases (MMPs) degrade the matrix to create physical space and release growth factors from the ECM, amplifying regenerative signals as necessary. Thus, the ECM governs the spatiotemporal presentation of growth factors to cells, a principle that engineered scaffolds aim to replicate, often by designing materials with heparin-like domains that bind and gradually release BMP-2.[71]

Cells engage with the ECM through specialized receptors, chiefly the integrin family. Integrins are transmembrane proteins that physically link the ECM (via binding motifs like Arginylglycylaspartic acid **(**RGD) sequences found in fibronectin or collagen) to the cell's cytoskeleton. Upon clustering and binding ECM ligands, integrins trigger the formation of focal adhesions—complexes of structural and signaling proteins (such as talin, vinculin, and FAK)—which activate intracellular signaling cascades.[69]. A critical outcome of this signaling is the activation of focal adhesion kinase (FAK) and downstream pathways such as Rho GTPases, which regulate cytoskeletal tension. Mechanotransduction pathways converge on transcriptional regulators, including the transcriptional co-activators Yes-associated protein (YAP) and the transcriptional co-activator with PDZ-binding motif (TAZ), as well as RUNX2, which translocate to the nucleus in response to matrix stiffness or adhesion signals, thereby altering gene expression. A stiffer ECM that provides strong integrin engagement activates YAP/TAZ and RUNX2 in mesenchymal stem cells, driving osteogenic differentiation. At the same time, a soft matrix, which does not generate such tension, retains YAP in the cytoplasm and may favor other lineages.[72] YAP/TAZ functions as a mechanosensor, integrating signals from integrins and the cytoskeleton to modulate cell fate. The ECM can dictate stem cell behavior through mechanical means (such as elasticity and viscoelasticity) and biochemical means (such as bound growth factors).

Significantly, cells continuously remodel the ECM. Enzymes such as matrix metalloproteinases (MMPs) facilitate the degradation of ECM components, while enzymes like lysyl oxidase (LOX) crosslink collagen fibers, subsequently stiffening the matrix. Osteoclasts (which resorb matrix) and osteoblasts (which deposit new matrix) constantly turn over the bone ECM, enabling continual adaptation to mechanical loads. Furthermore, the ECM demonstrates viscoelastic behavior, allowing it to dissipate stress over time, a property important for accommodating physiological demands.[73] Recent studies indicate that matrix viscoelasticity—the stress relaxation rate under constant strain—can influence stem cell differentiation. Matrices that allow tension to relax over a timeframe similar to that of cell contraction can paradoxically promote osteogenesis, even when their initial stiffness is low, because cells find it easier to remodel viscoelastic matrices, leading to the formation of their pericellular matrix and the buildup of tension. Conversely, a purely elastic matrix might "lock in" tension, inhibiting adaptive responses. By permitting time-dependent deformation, viscoelastic ECMs provide mechanical

cues that closely mimic natural tissue characteristics and can enhance regenerative outcomes.[74–76]

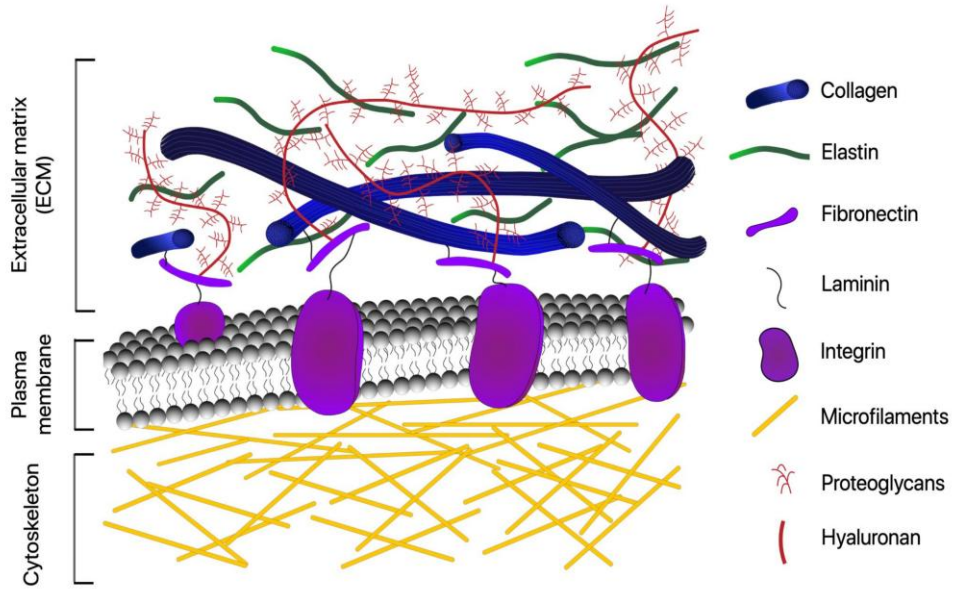

The extracellular matrix (ECM) and cell interactions. *The ECM is a 3D network of collagens, elastin, fibronectin, laminin, proteoglycans, and glycosaminoglycans that provides both structural integrity and biochemical cues. Integrins connect ECM ligands to the cytoskeleton, forming focal adhesions that activate mechanotransduction pathways (FAK, Rho GTPases, YAP/TAZ, RUNX2) to regulate cell fate. Continuous ECM remodeling and viscoelastic properties enable adaptation to mechanical demands and support tissue regeneration.*[77]

Cellular grafts:

One general approach in tissue engineering is to implant living cells with a matrix, effectively delivering a cellularized graft that can actively participate in regeneration. These cellular matrices typically consist of a scaffold in which cells are embedded or grown, enabling them to secrete their ECM in situ. The presence of living cells imparts dynamic, responsive properties to these matrices, which purely acellular materials lack. For instance, cells within the graft can remodel the matrix over time; they produce enzymes to reorganize or degrade the scaffold and synthesize new matrix components, adapting the material's properties to the host environment. [78,79] Cells also secrete various cytokines and growth factors that can stimulate host tissue repair. An MSC-laden scaffold, for example, might release VEGF to enhance blood vessel formation or BMPs to recruit host osteoprogenitors. Cellular grafts function as "mini-bioreactors" that modulate the local biological environment to favor healing.

One illustrative strategy involves utilizing principles from developmental engineering—guiding cells through lineage stages in vitro to prepare tissue primed for regeneration. Researchers have differentiated MSCs on 3D scaffolds into hypertrophic cartilage tissue, mimicking the embryonic precursor of bone. These engineered cartilage grafts can undergo endochondral ossification subcutaneously, forming new bone through a process similar to natural healing.[80,81] Studies have demonstrated that such hypertrophic cartilage templates encourage host blood vessel invasion and facilitate the formation of bone marrow elements, effectively catalyzing bone regeneration.[82] In one study, human MSC-derived cartilage rods implanted in a bone defect induced robust vascularized bone, leveraging the body's inherent ability to remodel cartilage into bone—a strategy termed endochondral bone tissue engineering. Likewise, co-culture systems have been developed to replicate the bone marrow niche, where stromal cells and early osteoblasts are grown together under dynamic flow conditions, producing a living matrix that retains hematopoietic stem cells and supports blood formation.

However, despite their conceptual strengths, cellular grafts pose several practical challenges. Culturing functional bone-like tissue in vitro requires considerable time, often weeks, during which cells must deposit a sufficient matrix. Extended culture durations in bioreactors result in high manufacturing costs and increased complexity. Moreover, maintaining cell viability in large 3D constructs is challenging due to diffusion constraints; cells in the interior may not receive adequate oxygen or nutrients if the constructs are excessively thick. Even with perfusion bioreactors, gradients can still develop, resulting in zones that may become hypoxic or accumulate waste, which can lead to inconsistent tissue quality.[83] Large-scale cell-based production also faces challenges related to batch-to-batch variability, as cells from different donors may exhibit inconsistent behavior, which can affect outcomes. Safety is a critical concern; the graft's cells may be immunogenic (potentially provoking a host immune response if they are allogeneic) or carry a tumorigenic risk if they proliferate uncontrollably. Furthermore, the cryopreservation of living grafts presents complications, as freezing and thawing can compromise cell viability and function, significantly limiting shelf life. Achieving truly off-the-shelf use would necessitate banking living constructs in ways that preserve their viability, a challenge that remains unresolved.[84]

Acellular Matrices:

To circumvent the difficulties associated with live-cell grafts, scientists have developed acellular matrices that can induce regeneration by leveraging the architecture and composition of the ECM alone. The idea is to provide the right scaffold, with all the structural and biochemical cues of native ECM, and allow the patient's cells to repopulate and remodel it. Acellular approaches eliminate concerns

about graft-versus-host immune reactions linked to living cells, and they are generally easier to sterilize, package, and store.

There are three main categories of acellular biomaterial scaffolds: (1) **native ECMs**, which retain their biological properties; (2) **synthetic ECMs**, engineered to mimic the properties of natural ECMs; and (3) **engineered ECMs**, which involve the use of ECMs produced by cultured cells.

Native Extracellular Matrices (nECMs) are derived through the decellularization of animal or human tissues, a process designed to remove immunogenic cellular components while preserving native ECM architecture and bioactivity. This is typically achieved using combinations of detergents, enzymes, and physical disruption methods.[85] The resulting scaffold retains the original tissue's three-dimensional structural and compositional features; for instance, decellularized bone preserves its mineralized collagen matrix, while cartilage and vascular tissues retain their type II collagen and elastin-rich architectures, respectively.

Notably, many bioactive signaling molecules—such as TGF-β, BMPs, and VEGF—remain embedded within the matrix, often bound to collagen or heparan sulfate-rich domains. This retained bioactivity enables nECMs to promote cell adhesion, migration, and differentiation.[86,87] While materials like demineralized bone matrix (DBM) are clinically employed for their osteoinductive potential, basement membrane extracts such as Matrigel are commonly used in preclinical studies to promote angiogenesis and tissue development.[86,88]

Despite their therapeutic promise, nECMs face several limitations. Donor-to-donor variability introduces significant inconsistencies in biochemical composition, mechanical properties, and growth factor content, which can negatively impact reproducibility and clinical performance. Moreover, harsh decellularization protocols may damage ECM ultrastructure, disrupt collagen integrity, or lead to the loss of essential components such as glycosaminoglycans.[85] Incomplete removal of cellular remnants may also provoke immune responses, necessitating further sterilization steps that can compromise matrix quality. Thus, ensuring the balance between immunological safety and preservation of native biofunctionality remains a central challenge in developing reliable nECM-based scaffolds. [87,89]

Synthetic Extracellular Matrices (sECMs) offer a modular and tunable alternative to native scaffolds, enabling precise control over biochemical and biophysical properties. These matrices are primarily composed of biocompatible polymers such as poly(ethylene glycol) (PEG), poly(lactic acid) (PLA), poly(glycolic acid) (PGA), and their copolymers (e.g., PLGA), as well as functionalized natural polymers like gelatin methacrylate (GelMA).[90] Unlike native ECMs, sECMs are synthesized de novo, allowing batch-to-batch consistency and the ability to systematically modulate variables such as stiffness, porosity, degradation kinetics, and ligand presentation.[91]

Crosslinked polymer networks, often fabricated via photopolymerization, can be engineered with mesh sizes on the order of tens to hundreds of nanometers and elastic moduli ranging from soft (~100 Pa) to stiff (~10 kPa), closely matching target tissue mechanics.[92] Degradation profiles are similarly customizable, with hydrolytically or enzymatically cleavable linkers enabling scaffold lifespans from days to months.[93]

Beyond mechanical tunability, sECMs can be biofunctionalized to present specific biochemical cues. Short peptide ligands, such as RGD (derived from fibronectin) or IKVAV (Ile-Lys-Val-ala-Val) (from laminin), are commonly grafted to enhance cell adhesion. At the same time, incorporating heparin-mimetic molecules allows sequestration and controlled release of growth factors.[94] For instance, BMP-2 can be embedded in sECM hydrogels at therapeutic doses, achieving sustained release with a defined half-life—this approach mitigates burst release and enhances localized efficacy.[95]

These features make sECMs valuable platforms for regenerative applications and mechanistic studies of cell-matrix interactions. Their compositional precision enables the isolation of individual parameters, such as stiffness or ligand density, thereby facilitating studies on cell behavior in highly controlled environments. [96]

Nevertheless, sECMs face inherent limitations. Despite their modularity, they lack the biochemical complexity of native ECMs. While individual ligands such as RGD can be presented, synthetic matrices do not replicate the full repertoire of bone-specific components such as osteopontin, bone sialoprotein, or tenascin-C. Moreover, ligand distribution is typically homogeneous, unlike the nanoscale clustering observed in native matrices, which critically influences integrin binding and downstream signaling.[97] Additionally, many synthetic polymers are not inherently degradable by cell-secreted enzymes unless specifically designed with protease-cleavable sequences, which can hinder matrix remodeling and cell migration.[98]

As the field progresses, strategies to bridge this biofunctionality gap, such as incorporating hierarchical ligand patterning and dynamic, cell-responsive degradation, are expected to enhance the fidelity of sECMs in mimicking the native extracellular environment.[90,91]

Engineered Extracellular Matrices (eECMs) represent an integrative approach that combines the biological fidelity of native ECMs with the tunability and reproducibility of synthetic scaffolds. These matrices are generated by culturing cells, typically stromal or progenitor cells, in vitro under defined conditions to deposit tissue-specific ECMs. Once a sufficient matrix is formed, the cells are removed through controlled devitalization, yielding an acellular scaffold that retains the spatial organization and biochemical complexity conferred by cellular assembly.[99] This strategy addresses several limitations inherent in both native and synthetic ECMs. Unlike decellularized native tissues, suffering donor variability

and potential immunogenic remnants, eECMs can be fabricated in standardized bioreactor settings using well-characterized cell sources, improving reproducibility and safety.[100,101]

Because the eECM is cell-derived, it captures a richer array of matrix components—including collagens, glycoproteins, proteoglycans, and matrix-bound signaling molecules—compared to most synthetic systems, which typically present only a limited variety of ligands or structural motifs. Significantly, eECMs benefit from the natural process of matrix organization executed by living cells, resulting in a physiologically relevant composition and microarchitecture. This includes fibrillar collagen alignment, hierarchical porosity, and the spatial patterning of adhesion cues—all of which are challenging to replicate using synthetic approaches.[102] These attributes are critical for guiding host cell behavior, promoting vascularization, and facilitating tissue-specific remodeling upon implantation.

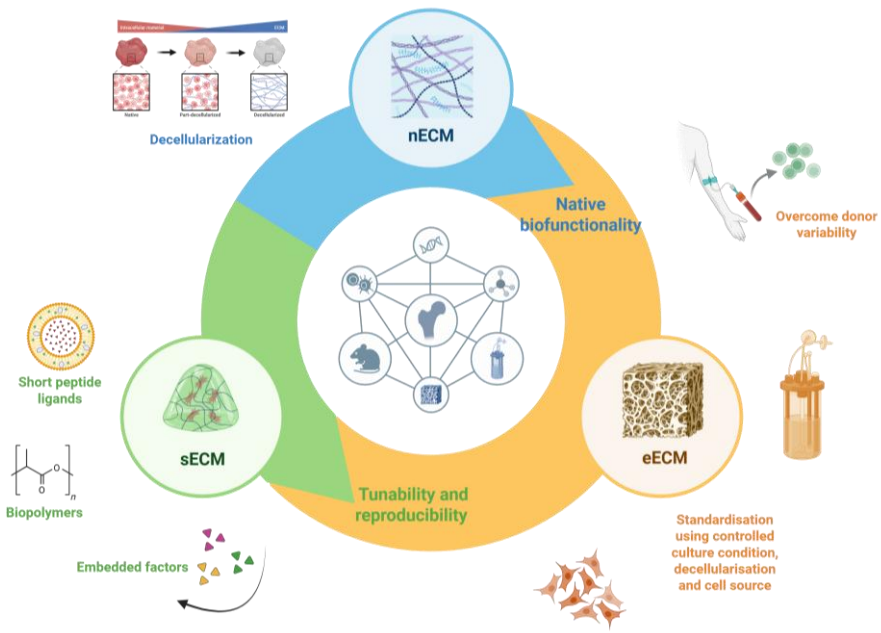

Acellular matrix classifications. *Acellular scaffolds are categorized as* ***native ECMs (nECM)****, derived from decellularized tissues that retain natural biofunctionality;* ***synthetic ECMs (sECM)****, polymer-based matrices with tunable mechanical and biochemical properties; and* ***engineered ECMs (eECM)****, cell-derived constructs offering physiological complexity with greater reproducibility. Each approach balances advantages and limitations, reflecting a trade-off between bioactivity and standardization in regenerative applications. Illustrated with BioRender.*

Moreover, the decellularization step can be finely tuned to preserve matrix integrity while minimizing immunogenic residues, thereby offering a middle ground between the complexity of native ECMs and the control inherent in synthetic scaffolds. The resulting constructs are shelf-stable, cell-free, and inherently instructive, making them attractive for off-the-shelf applications in regenerative medicine. By leveraging cellular machinery to build a complex matrix ex vivo and then removing the cells to ensure safety and scalability, engineered ECMs present a compelling solution to the challenges faced by first-generation biomaterials. Their ability to bridge biological relevance with design control positions them as a next-generation scaffold platform for tissue repair and regeneration. [103,104]

Immunogenicity in Tissue Repair and Scaffold Design

Once implanted, any biomaterial or graft will interface with the host's immune system. The immunogenicity of tissue-engineered constructs—the extent to which they provoke immune reactions—can significantly determine the success or failure of the regeneration effort.[103,104] An ideal scaffold elicits a constructive, transient immune response that leads to healing, rather than chronic inflammation or rejection. Early events at the implant site, such as protein adsorption and immune cell recruitment, lay the groundwork for downstream outcomes, including vascularization and new tissue formation. Modern biomaterials development emphasizes immunomodulation, designing scaffolds not only for mechanical support but also to guide the host immune response toward an actively pro-regenerative phenotype.

The initial responders to any implant are cells of the innate immune system, particularly macrophages. These versatile cells range from pro-inflammatory "M1" phenotypes to pro-healing "M2" phenotypes. Upon implantation, blood-derived monocytes infiltrate and differentiate into macrophages on the scaffold surface. The presence of detrimental signals or residual debris, such as cell membrane fragments, DNA, or cytotoxic components, can induce macrophage polarization toward a pro-inflammatory M1 phenotype, characterized by the secretion of cytokines such as tumor necrosis factor-alpha (TNF-α) and interleukin-1 beta (IL-1β).[105] M1 macrophages are effective at pathogen defense and debris clearance, but if they persist too long, they can damage surrounding tissue and scaffolds, inhibiting regenerative processes. In contrast, M2 macrophages secrete anti-inflammatory cytokines (including IL-10 and TGF-β) and growth factors that promote tissue repair, angiogenesis, and matrix deposition. Successful healing often necessitates an initial M1 response (to clear inflammatory debris or infectious agents) that transitions promptly to an M2-dominated response of regeneration. Studies have indicated that the ratio of M2 to M1 macrophages within the first 1–2 weeks after implantation correlates with positive remodeling outcomes: a high M2:M1 ratio often predicts constructive remodeling of a scaffold and new tissue with organized

structure, whereas a high presence of M1 macrophages typically indicates a predisposition toward fibrotic encapsulation or chronic inflammation.[106]

Well-prepared ECM-based biomaterials often promote a switch to M2 macrophages within 7–14 days post-implantation, while materials with harsh chemistry or residual antigens may lead to prolonged M1 activation. Various strategies are employed to tune the macrophage response. For example, properly decellularized ECM scaffolds can contain signaling molecules that promote macrophages toward an M2 phenotype when thoroughly cleansed of cell remnants.[107] Researchers have incorporated specific immunomodulatory molecules into scaffolds, such as IL-4-releasing microspheres or coatings with CD47 (an immune "do not eat me" signal), to bias macrophages toward a healing mode. The goal is to create a scenario where the material triggers a brief inflammatory response for cleanup, followed by a prompt transition into a regenerative environment. Macrophages play a central role in this process, as they orchestrate the involvement of other immune cells and progenitors.

The adaptive immune system, particularly T cells, can influence scaffold outcomes. The host may mount a specific immune response if the scaffold carries foreign proteins (e.g., xenogeneic proteins in a decellularized matrix that have not been completely removed). Cytotoxic T cells can directly attack any residual living donor cells or secrete factors that exacerbate inflammation and potentially lead to implant rejection. Helper T cells come in subsets: Th1 cells support cell-mediated immune responses and can contribute to chronic inflammation, while Th2 cells assist B cells and are often linked with humoral immunity and fibrosis. An imbalance, such as a predominantly strong Th1 response, may perpetuate inflammation and impair healing. Conversely, regulatory T cells (Tregs) function as peacekeepers by dampening excessive immune reactions. They can suppress effector T cells and macrophages, facilitating immune tolerance of the implanted material. A healthy regenerative response often involves Tregs to temper the immune attack and promote constructive remodeling. Some studies have shown that depletion of Tregs results in poorer outcomes with biomaterial implants, while enhancing Tregs can improve integration by preventing overactive immune responses.

To leverage this knowledge, scaffold designers are experimenting with methods to make materials more "immune-instructive." This may entail surface modifications that reduce unwanted protein adsorption (thus minimizing immune cell activation) or incorporating ligands that engage immune cell receptors to steer them toward pro-healing phenotypes. Examples include grafting peptides that bind macrophage mannose receptors (which tend to induce an M2 response) or releasing IL-10 or other anti-inflammatory cytokines from a scaffold to mitigate inflammation locally. Another approach is to control the physical properties of the scaffold (such as pore size and fiber alignment), as studies have shown that larger pore scaffolds can facilitate greater M2 polarization compared to denser, small-pore scaffolds.[108,109] This effect is likely due to the influence of porosity on the foreign body reaction; if

cells can infiltrate without excessive isolation from the scaffold, the immune response is typically more favorable.

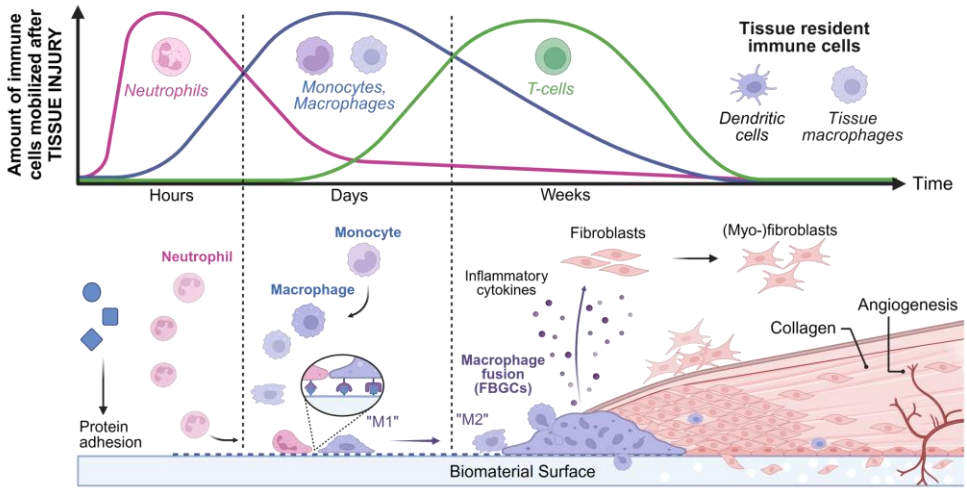

Significance of immune cells during scaffold integration and tissue repair. *Immune cells drive tissue regeneration following scaffold implantation, with neutrophils initiating debris clearance and monocytes differentiating into macrophages. The M1-to-M2 macrophage transition promotes ECM remodeling and angiogenesis, while T cells regulate immune responses and support scaffold integration. Illustrated with BioRender.*

Challenges in Clinical Translation

While eECMs have emerged as a promising class of biomaterials for regenerative medicine, their clinical translation remains hindered by several unresolved challenges that span biological, technical, and regulatory domains. These challenges highlight the complexity of fabricating functional tissue surrogates and the opportunity to redefine how we design and deploy bioinstructive scaffolds.

One of the most pressing obstacles is the scalable and reproducible production of eECMs. Current efforts often succeed on a laboratory scale but translating this success into manufacturing workflows that can reliably produce grafts of varying sizes—ranging from small dental plugs to long segmental bone substitutes—while holding collagen-to-Glycosaminoglycans ratios, mineral content, mechanical strength, sterility, and shelf-life within tight, regulator-defined tolerances across every batch is a significant engineering hurdle. Eliminating donor-to-donor variability, ensuring uniform nutrient delivery in centimeter-thick tissues, and preserving matrix integrity through devitalization, drying, and sterilization remain formidable challenges.[92] Overcoming these obstacles would permit eECMs to be

realized as truly off-the-shelf, lot-consistent devices—unlocking standardized logistics, reducing costs, and enhancing patient access to advanced therapies.

Another frontier is the achievement of programmable intrinsic bioactivity within these engineered matrices. Current grafts often rely on bolus delivery of exogenous growth factors such as recombinant BMP-2—a strategy that risks supraphysiological dosing, ectopic bone formation, and unpredictable pharmacokinetics. The vision is to create an engineered matrix that autonomously generates and retains bioactive cues during matrix deposition—scaffolds that release signaling molecules physiologically relevant, spatially controlled, and temporally sustained. Realizing such intrinsic functionality would eliminate the need for post-fabrication factor loading, simplifying clinical implementation and closely emulating native healing environments.[110]

Building on this, the prospect of exquisitely tailoring matrix composition using genetic manipulation of the matrix-producing cells offers a paradigm shift in scaffold design. If the biological properties of an ECM could be programmed at the cellular level—by modulating the expression of key structural or signaling proteins—the result would be a new class of "custom-designed" matrices created for specific applications. The integration of genome editing tools, such as CRISPR/Cas9, with advanced biofabrication platforms like 3D bioprinting holds the potential to engineer matrices that are both compositionally and spatially optimized.[111]

However, the ability to predictably design and manufacture such engineered matrices remains largely aspirational and technically demanding. Furthermore, a major translational bottleneck lies in the unpredictability of host immune responses to implanted matrices. Even acellular scaffolds can provoke divergent outcomes depending on patient age, comorbidities, and subtle compositional differences.[112] A persistent challenge is understanding—and ultimately anticipating—how an eECM's molecular signature shapes macrophage polarization, vascular ingrowth, and bone remodeling. Developing robust in vitro or silico indices that forecast in vivo performance would transform quality control and clinical trial design, thereby mitigating late-stage failures and tailoring therapies to patient-specific immune profiles.[113]

Aims

The primary goal of this thesis is to explore the transformative potential of engineered extracellular matrices (ECMs) and advanced tissue engineering strategies for regenerative medicine. The study examines how material properties, bioactive cues, and immune responses can be leveraged to optimize scaffold-based tissue regeneration, with a focus on clinical translation. The specific objectives are:

1. ***To explore the incorporation of bioactive factors into scaffold-based systems to enhance regenerative outcomes***
   This work examines how bioactive molecules, such as BMP-2/7, synergize with scaffold materials like collagen-hydroxyapatite composites to improve tissue healing and bone regeneration, addressing challenges in dosage optimization and therapeutic safety. **(Paper I)**
2. ***To standardize the design and production of scalable, non-cellular grafts for predictable and reproducible tissue regeneration***
   By engineering human hypertrophic cartilage as a devitalized scaffold material, this study aims to create grafts that serve as robust, off-the-shelf solutions, addressing challenges in variability, scalability, and clinical readiness in tissue engineering. **(Paper II)**
3. ***To advance the precision engineering of extracellular matrices through molecular modulation***
   Utilizing CRISPR/Cas9 technology, this objective focuses on tailoring the molecular composition of ECMs to enhance their bioactivity, elucidate key factors driving endogenous repair, and ensure the stability and safety of such modifications in pre-clinical contexts. **(Paper III)**
4. ***To optimize scaffold immunogenicity and assess immune interactions in diverse transplantation environments***
   This study investigates the impact of decellularization on ECM integrity and immunogenicity, exploring how decellularized grafts perform in immunodeficient and immunocompetent models. It highlights the role of immune regulation in tissue regeneration. **(Paper IV)**
5. ***To evaluate the regenerative and immunological potential of biomaterials derived from different organs and their integration into advanced fabrication technologies***
   This objective examines early immune recruitment patterns and their correlation with regenerative outcomes across biomaterials derived from different organs. **(Paper V)**

Key Results

Paper I: Sustained delivery of a heterodimer bone morphogenetic protein-2/7 via a collagen hydroxyapatite scaffold accelerates and improves critical femoral defect healing

This study shows that a heterodimeric bone morphogenetic protein-2/7 (BMP-2/7), encapsulated in a collagen hydroxyapatite (CHA) scaffold, significantly increases bone regeneration at lower doses than BMP-2 alone. This study aimed to investigate whether the combination of BMP-2/7 could enhance osteoinductivity while reducing the dose of the treatment and side effects. CHA scaffold was used because it can hold proteins and release them at the implantation site at a controlled rate.

To detail the cellular processes involved in bone formation by BMP-2/7, CHA scaffolds loaded with BMP-2/7 were examined for their ability to attract progenitor cells as an early sign of cellular response. Progenitor cell populations that could differentiate into three lineages were identified by established markers (PDGFR-α+, SCA-1+, CD-31−, and CD-45−), and an intermediate BMP-2/7 dose of 0.5 μg was chosen based on dose optimization experiments. Flow cytometry showed that loading with BMP-2/7 significantly increased the number of progenitor cells at the implantation site at day 10 compared with BMP-2. Histological analyses (Safranin O/Fast Green and hematoxylin and eosin staining) revealed that scaffolds loaded with BMP-2/7 supported the formation of more cartilage and bone at 10 days postimplantation, with higher GAG and hydroxyproline content also characterized in the formed tissue. However, there was no difference in the density of these ECM components.

Gene expression analysis of the transcriptomes of BMP-2/7-loaded CHA scaffolds extended previous findings that suggested that the expression of several genes involved in bone formation was increased, consistent with the histological data. In addition, release kinetics experiments showed that both BMP-2/7 and BMP-2 were released from the CHA scaffold sustainably, which further supports the use of this scaffold for growth factor delivery.

These findings are significant for the development of BMP-2/7 in bone tissue engineering, allowing for the creation of new growth factor-based therapies with reduced systemic side effects for critical bone defects. The results also conclude that the early recruitment of specific cell populations to the implantation site, although not an absolute predictor, is a valuable indicator of the final regenerative outcome (**Paper IV**). This insight highlights the broader potential of early cellular events to provide meaningful predictions in various regenerative contexts.

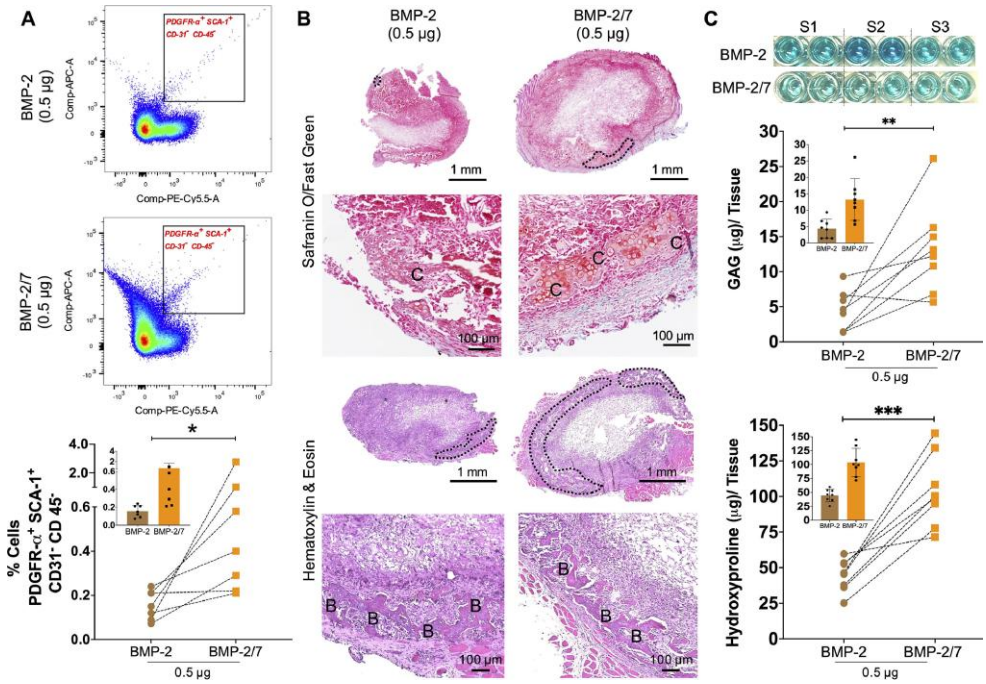

Cellular, histological, and biochemical characterization of the neo-tissue formed after 10 days of BMP-2 (0.5 µg) or BMP-2/7 (0.5 µg) treated CHA scaffold implantation in the abdominal muscle pouch of rats was performed in a biologically paired experimental setup. *(A) Flow cytometry-based characterization of progenitor cell homing in the BMP-2 (top) and BMP-2/7 (middle) treated CHA scaffolds (n=7). The representative scatter plots and the gating indicate PDGFR-α$^+$, SCA-1$^+$, CD-31$^-$, and CD-45$^-$ progenitor cell homing in the respective growth factor-treated scaffold. The bottom panel in A indicates a pairwise comparison of the % of progenitor cells (out of total cells analyzed) homed in BMP-2 vs. BMP-2/7 treated CHA scaffolds. Inset in A, the bottom represents the mean ± SD of the same data. (B) Histological characterization of the neo-tissue formed after implanting CHA+BMP-2 or CHA+-BMP-2/7 treated scaffolds using Safranin O/Fast green (top) and hematoxylin and eosin (bottom) (n=2). In the histology images, C indicates tissue regions with chondrocytes; B indicates regions with bone matrix; dashed black indicates regions with prominent cartilage (top) and bone (bottom) tissue. (C) Biochemical characterization of the neo-tissue matrix using Alcian blue assay for colorimetric glycosaminoglycan (GAG) quantification: top indicates three representative samples from each group; middle: total GAG/tissue (n=8); bottom: hydroxyproline assay for collagen quantification (n=8)*

Paper II: Manufacturing of Human Tissues as Off-the-shelf Grafts Programmed to Induce Regeneration

This study addresses the limitations of current bone grafting methods, including the variability of autologous grafts and the safety concerns associated with supraphysiological BMP-2 delivery, by developing a scalable, off-the-shelf osteoinductive graft that mimics endochondral ossification. The strategy centers on a genetically engineered, immortalized human mesenchymal stromal cell line (MSOD-B), which constitutively expresses bone morphogenetic protein-2 (BMP-2), enabling the formation of robust hypertrophic cartilage (HyC) enriched in osteoinductive extracellular matrix (ECM) cues.

Initially, MSOD cells were created by transducing primary hBM-MSCs with hTERT and an inducible caspase-9 (iCasp9) suicide gene. These cells were then further modified to express BMP-2, resulting in the MSOD-B line. This line retained the mesenchymal phenotype ($CD29^+$, $CD90^+$, $CD146^+$, $CD73^+$, $CD34^-$, $CD45^-$), exhibited improved osteogenic and chondrogenic differentiation potential, and secreted physiologically relevant levels of BMP-2. Under 3D culture conditions, MSOD-B cells generated cartilage with hypertrophic features, including type II and X collagen and glycosaminoglycans, although with slightly lower Bern scores than primary MSCs, but with markedly higher BMP-2 content (~40 ng per construct).

Upon ectopic implantation, MSOD-B-derived HyC remodeled efficiently into bone and marrow tissue, surpassing living HyC derived from highly chondrogenic hBM-MSCs in speed and ossicle maturity. Importantly, BMP-Smad1/5/9 signaling was found essential for MSOD-B chondrogenesis; inhibition of this pathway abrogated cartilage formation, despite unaltered BMP-2 secretion and active TGFβ-Smad2/3 signaling.

To create a devitalized, cell-free ECM, apoptosis was induced using iCasp9 activation. The resulting tissues retained their structure and composition, undergoing complete endochondral ossification in vivo. Devitalized MSOD-B HyC outperformed both devitalized MSOD HyC and BMP-2-loaded synthetic materials (PEG or Infuse) even when the latter contained 10- to 100-fold higher BMP-2 doses. Bone formation was shown to correlate with cartilage maturity (Bern score and GAG content), but not BMP-2 concentration, emphasizing the instructive role of ECM composition rather than BMP-2 dose.

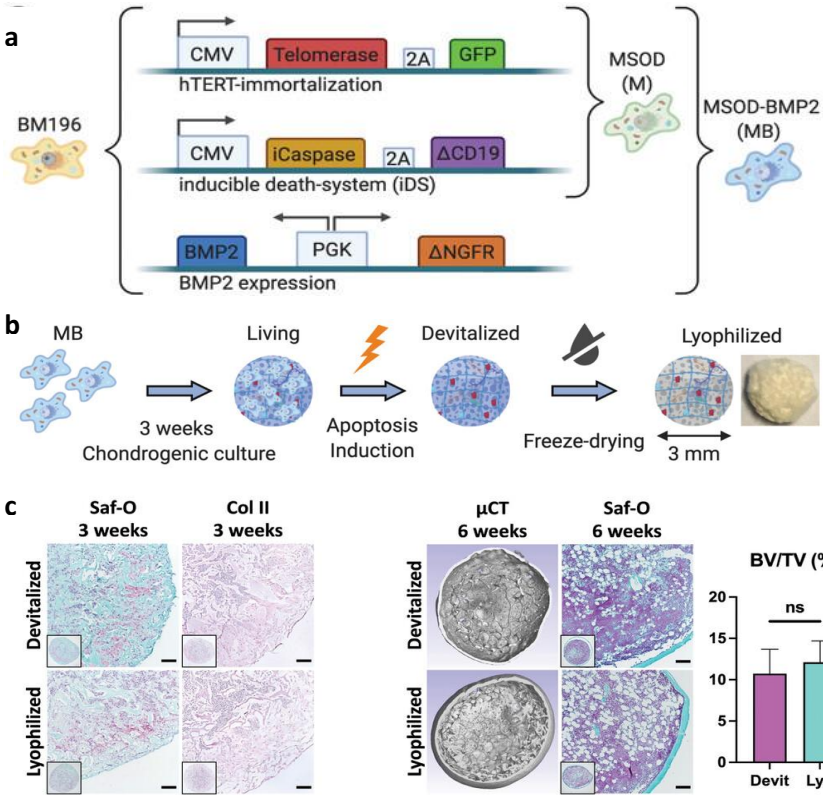

Devitalization and lyophilization of MSOD-B cartilage result in an off-the-shelf graft material with preserved composition and bone formation capacity. *(A). Generation of mesenchymal cell lines by genetic engineering of primary human bone marrow-derived mesenchymal stromal cells (hBM-MSCs) from a single donor (BM196). Immortalization and death-inducibility were conferred by human telomerase reverse transcriptase (hTERT) and inducible caspase 9 (iCaspase) expression, respectively, leading to the MSOD (M) line. The MSOD-B (MB) cell line resulted from the subsequent implementation of constitutive bone morphogenetic protein-2 (BMP-2) expression. (B) Cartilage tissues were engineered by the chondrogenic culture of MSOD-B (MB) (Living group), subsequently devitalized by apoptosis induction (Devitalized), and further lyophilized (Lyophilized) through a freeze-drying process. The impact of the devitalization and lyophilization processes was analyzed using mass spectrometry and functional in vivo implantation. (C) The devitalization and lyophilization did not affect the bone formation capacity of MB cartilage tissues, as assessed by histological (Saf-O, Collagen type II) and µCT analysis of in vitro and subcutaneously implanted grafts. Scale bars = 100 µm. Bone volume (BV) as a percentage of total volume (TV) (n = 6) and ossicle maturity scoring (n = 6) were analyzed from in vivo implanted tissues. The graphs represent mean + SD—statistical analysis based on two-tailed unpaired t-tests.*

For long-term storage and off-the-shelf use, the devitalized HyC was lyophilized. Proteomic analysis confirmed the preservation of key ECM proteins post-devitalization and lyophilization, including type II collagen, aggrecan, COMP, BMP-2, and TGFBI. Over 77% of identified proteins were common across living, devitalized, and lyophilized groups. Lyophilized tissues retained their osteoinductive potential after >3 months of storage at 4°C and successfully remodeled into mature bone and marrow upon implantation.

To enable scalable manufacturing, a custom perfusion bioreactor was employed to generate cartilage discs (25 mm diameter) with a 20-fold increase in volume compared to static cultures. These bioreactor-engineered grafts exhibited equivalent ECM quality (histology, Bern score) and maintained osteoinductive performance when implanted subcutaneously in mice.

The therapeutic potential of the engineered HyC was validated in a critical-sized rat mandibular defect model. When used in combination with SmartBone, a clinically approved scaffold, the lyophilized HyC enhanced new bone formation and osteointegration within the defect site. Notably, SmartBone alone failed to induce comparable levels of bone formation or integration, demonstrating the synergistic effect of the ECM component.

Paper III: Compositional editing of extracellular matrices by CRISPR/Cas9 engineering of human mesenchymal stem cell lines

This study aims to investigate the use of CRISPR/Cas9 in modifying ECM produced by human MSCs by focusing on VEGF and RUNX2 genes to understand their function in cartilage and bone formation. These findings demonstrate how these genetic modifications affect angiogenesis, cartilage repair, and bone remodeling, highlighting how our approach can be harnessed to identify the essential eECM factors driving endogenous repair.

The first set of outcomes centered on VEGF, a positive regulator of angiogenesis and endochondral ossification. CRISPR/Cas9 was used to introduce frameshift mutations in exon 1 of VEGFA in MSOD-B, yielding two VEGFA-knockout clones (MSOD-BΔV1 and MSOD-BΔV2). Knockout was confirmed by sequencing and by ELISA on pellet-culture supernatants, which revealed near-zero VEGFA secretion. After in vitro differentiation, safranin-O staining and Blyscan assays showed that VEGFA-knockout constructs accumulated glycosaminoglycans (GAGs) equivalent to unedited controls, showing that the VEGF editing did not affect the cartilage-forming capacity. Immunofluorescence for collagen II (COL2A1) and collagen X (COL10A1) confirmed that hypertrophic maturation proceeded normally in the absence of VEGFA.

To assess angiogenic potential, devitalized, lyophilized cartilage pellets were implanted on the chick chorioallantoic membrane (CAM) for 4 days. Quantification of $CD31^+$ vessel density via Q-VAT image analysis showed a ~60 % reduction in vessel ingrowth around VEGFA-knockout tissues compared to controls. In parallel, 2-week subcutaneous implants in immunodeficient mice were sectioned, stained for CD31, and quantified by isosurface reconstructions in Imaris; VEGFA-knockout grafts displayed significantly fewer vessels per tissue volume (0.23 μm^3 vs. 0.52 μm^3 in controls).

Despite reduced early vascularization, 6-week subcutaneous implants underwent complete endochondral remodeling. MicroCT (μCT) quantification of bone volume over tissue volume (BV/TV) revealed no statistical difference (17 % vs. 16 %). Histology (Masson's trichrome, Safranin-O) confirmed mature cortical and trabecular bone with marrow compartments in both VEGFA-knockout and unedited constructs. These data demonstrate that VEGFA, while enhancing early angiogenesis, is dispensable for complete endochondral ossification.

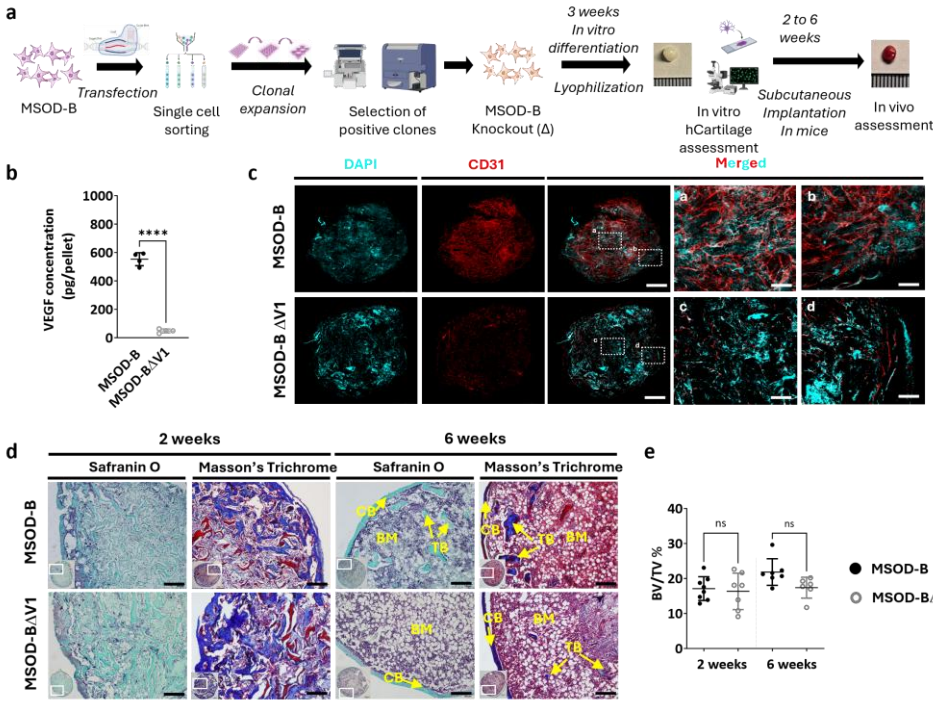

CRISPR/Cas9 edited VEGF knockout cartilage tissues retain cartilage forming and bone remodeling capacity despite reduced early-stage vascularization. *A) Experimental scheme depicting the generation of CRISPR/Cas9-edited MSOD-B lines, and the subsequent in vitro and in vivo tissue formation assessment. B) ELISA-based quantitative assessment of VEGF protein in in vitro differentiated constructs, post-lyophilization. Unpaired t-test, n = 3-4 biological replicates, ****p < 0.0001. C) Immunofluorescence images of MSOD-B and MSOD-BΔV1 tissues two weeks post-in vivo implantation. Displayed images consist of 3D stacks from 80-100 µm thick sections, vessels stained with mouse CD31 (red), and nuclei with DAPI (cyan) (Scale bars at 500 µm except for magnified white inserts at 80 µm). Box "a" and "c" display the periphery, whereas Box "b" and "d" show the central region of MSOD-B and MSOD-BV1 constructs, respectively. A reduction in tissue vascularization is observed in MSOD-BΔV1 samples. D) Histological analysis of in vivo tissues using Safranin O and Masson's trichrome stains at two (2W) and six weeks (6W) post-implantation. Both sample types underwent complete remodeling into a bone organ after 6 weeks, with bone structures and a bone marrow compartment (Scale bars = 200 µm). CB – cortical bone; BM – bone marrow. TB – trabecular bone e)Microtomography-based quantification of the sample's bone/ mineralized volume over their total volume (ratio). No significant differences between MSOD-B and MSOD-BΔV1 could be observed. (BV: Bone Volume, TV: Total Volume). Ordinary One-way ANOVA, n=8 biological replicates, n.s. = not significant).*

The second set of results looked at the function of RUNX2, a transcription factor required for chondrocyte hypertrophy and osteogenesis. CRISPR/Cas9 targeting of RUNX2 exon 6 produced two knockout clones (MSOD-BΔR1 and MSOD-BΔR2). The genetic modification was verified by Sanger sequencing. Intracellular flow cytometry showed reduced RUNX2 expression, and western blot analysis confirmed successful editing by detecting a truncated RUNX2 protein. After 3 weeks of in vitro chondrogenic differentiation, GAG quantification (Blyscan) was comparable to MSOD-B, and COL2 immunostaining was uniform across all groups. However, COLX levels—assessed by immunofluorescence and quantified in Imaris—were reduced by ~70 % in RUNX2-knockout pellets, indicating failure of hypertrophic maturation and mineralization. Quantitative RT-PCR showed downregulation of COL10A1 and alkaline phosphatase (ALPL) transcripts in MSOD-BΔR clones. At the same time, COL1A1 (collagen I) expression was upregulated, indicating arrested hypertrophic maturation and a shift toward a more cartilage-like matrix.

For in vivo remodeling, devitalized, lyophilized RUNX2-knockout and control constructs were implanted subcutaneously into immunodeficient mice. After 6 weeks, µCT scans revealed a marked decrease in BV/TV in RUNX2-knockout implants (4.3 % vs. 20.0 %). Histology (Masson's trichrome, Safranin-O) showed immature bone islands and extensive fibrotic tissue in RUNX2-knockout grafts, whereas unedited constructs displayed well-organized cortical and trabecular bone with marrow. These results suggest that while cartilage formation proceeds in the absence of RUNX2, its presence is essential for hypertrophic progression and the eventual transition to bone.

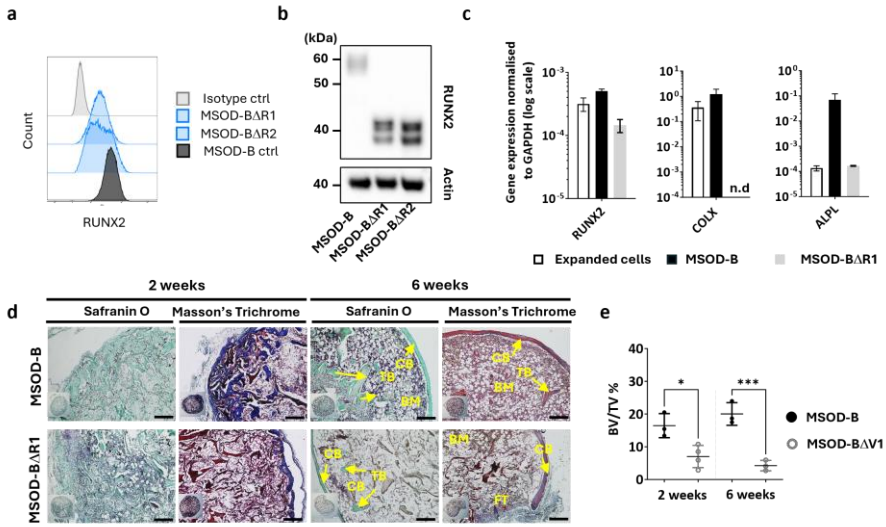

RUNX2 knockout in cartilage tissues retains cartilage forming capacity but disrupts hypertrophy and effective ectopic bone formation. *A) Intracellular flow cytometry for RUNX2 detection in MSOD-B and RUNX2-edited clones. An apparent protein reduction could be observed in the 6.1_1 and 6.1_23 clones. b) Western blot analysis of RUNX2 in cultured MSOD-B and RUNX2-edited cells. The detection of the truncated proteins confirms the genetic editing of RUNX2. Actin is used as a control to normalize the protein content. c) Quantitative PCR analysis displaying the relative expression levels of osteogenesis-related genes: RUNX2, COL1, and ALPL. The expression is normalized to GAPDH as a housekeeping gene. n.d= not detected. d) Histological analysis of in vivo constructs using Safranin O and Masson's trichrome stains. After two weeks (2W), a higher bone formation is already evident in the MSOD-B control group. The MSOD-BΔR1 samples explanted after 6 weeks (6W) displayed the presence of cortical and trabecular bone and a significant amount of fibrous tissue, indicating an incomplete remodeling. (Scale bars = 200 μm). e) Microtomography-based quantification of the sample's bone/mineralized volume over their total volume (ratio). (BV: Bone Volume, TV: Total Volume). A marked difference is observed as early as two weeks, with lower mineral content in MSOD-BΔR1 samples. Ordinary one-way ANOVA, n=3 biological replicates, *p < 0.05, ***p < 0.001.*

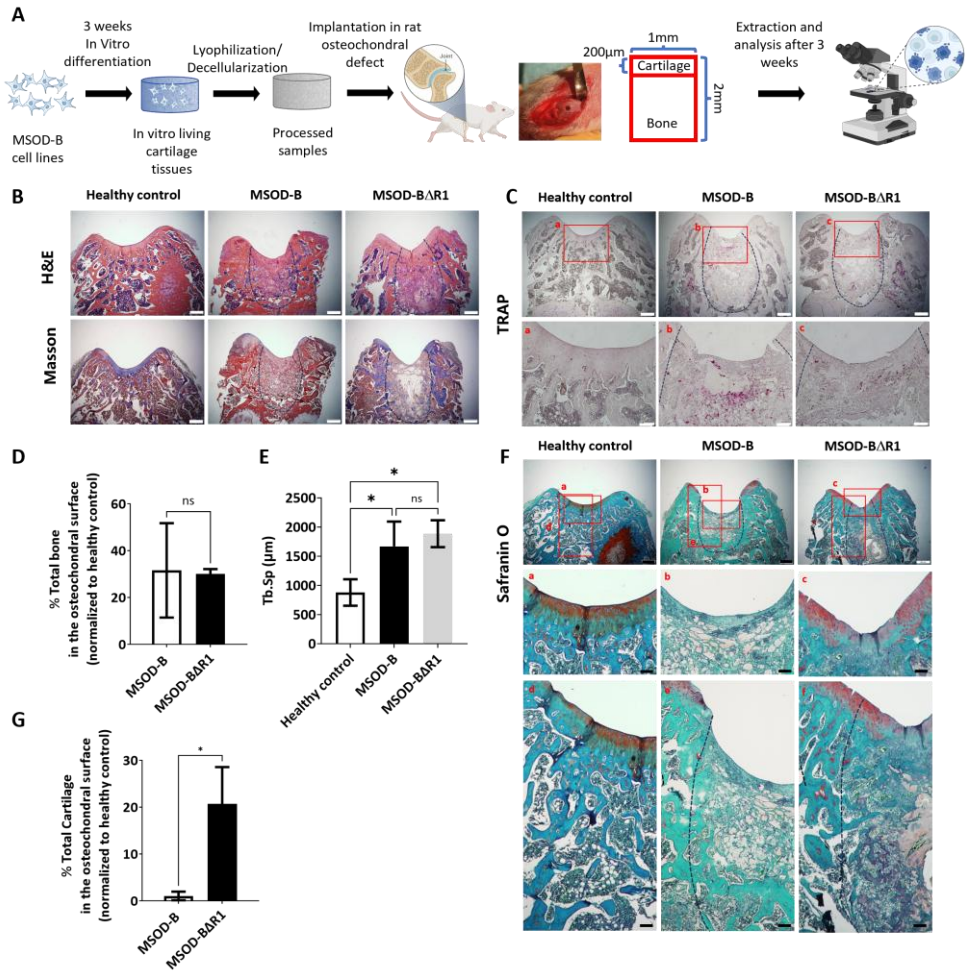

RUNX2 knockout in cartilage tissues leads to better cartilage regeneration and maintenance in osteochondral defects in rats. *A) Experimental scheme for the regenerative potential assessment of MSOD-B & MSOD-BΔR1 cartilage tissues in a rat osteochondral defect. B) Histological analysis of the osteochondral defects for each group using H&E and Masson's trichrome stains at three weeks post-implantation. The dashed line marks the defective area. (Scale bars = 500 µm) C) Histological analysis of the osteochondral defects using TRAP staining, reporting osteoclastic activity at three weeks post-implantation. The dashed line marks the defective area. (Scale bars = 500 µm and 100 µm for magnified areas) D) Microtomography-based quantification of the sample's total bone/mineralized volume normalized to the healthy control in percentage. Unpaired t-test, n=3 biological replicates, n.s. = not significant. = not significant. E) Image J-based quantification of Trabecular separation (Tb.Sp). One-way ANOVA test, n=3 biological replicates, *p < 0.05 F). Histological analysis of the osteochondral defects using Safranin O staining. After three weeks, a higher regeneration of the*

*surface cartilage is evident in the MSOD-BΔR1 group (a,b,c) (Scale bars = 500 μm and 100 μm for magnified areas). The magnified regions of the subchondral area (d,e,f) show higher cartilage remnants and integration in the MSOD-BΔR1 group. G) Quantitative analysis of cartilage regeneration in the osteochondral surface compared to the healthy control (100%). Unpaired t-test, n=3 biological replicates, *p < 0.05.*

To evaluate the regenerative capacity of the eECMs in an orthotopic setting, MSOD-B and RUNX2-knockout MSOD-BΔR1 constructs were implanted into osteochondral defects in the femoral condyle of immunodeficient rats. Histological analyses (H&E and Masson's trichrome) and micro-CT imaging performed at the study endpoint revealed de novo bone formation in both groups. However, incomplete remodeling was indicated by persistent fibrotic tissue and reduced marrow compartment. Tartrate-resistant acid phosphatase (TRAP) staining revealed elevated osteoclastic activity in MSOD-B implants relative to MSOD-BΔR1, suggesting reduced bone turnover in the knockout group. Micro-CT quantification showed comparable bone repair in both groups, covering approximately 30% of the defect area. Trabecular separation was elevated in both groups, consistent with ongoing remodeling, while trabecular thickness remained statistically unchanged. Despite similar bone outcomes, cartilage regeneration was markedly different. Safranin O staining revealed minimal chondral repair in MSOD-B grafts, whereas MSOD-BΔR1 constructs promoted robust cartilage regeneration, accounting for 20.67% of the condyle surface, compared to only 1.05% in MSOD-B implants. Enhanced glycosaminoglycan retention and better tissue integration were observed in MSOD-BΔR1 sections. A semiquantitative histological scoring system was applied to assess tissue morphology, matrix quality, integration, and surface regularity. MSOD-BΔR1 outperformed MSOD-B across all parameters, with higher scores in cellular morphology (66% vs. 33%), matrix staining (50% vs. 16%), cartilage thickness (33.3% vs. 8.3%), subchondral bone formation (25% vs. 16.6%), surface regularity (41% vs. 50%), and integration with host tissue (50% vs. 33%).

These findings demonstrate that deleting RUNX2 shifts the regenerative outcome from bone formation toward cartilage preservation within an osteochondral lesion.

Paper IV: Engineered human cartilage matrix exhibits potent immunoregulatory properties while promoting complete femoral restoration in pre-clinical models

This study investigates the development and therapeutic potential of decellularized hypertrophic cartilage (D-HyC) grafts derived from engineered human mesenchymal stromal cells as standardized, off-the-shelf biomaterials for bone repair. An optimized decellularization protocol was established to preserve the structural and bioactive features of the engineered tissue. The osteoinductive capacity and immunogenic profile of D-HyC were systematically evaluated using ectopic implantation in both immunodeficient and immunocompetent mouse models, as well as in vitro co-culture assays with allogeneic human antigen-presenting cells. Finally, D-HyC grafts were tested as a callus substitute in a critical-sized femoral defect model. The results demonstrate that D-HyC retains potent osteoinductive properties, elicits minimal immune activation, and supports robust bone regeneration, underscoring its promise for clinical translation as a safe and effective acellular bone graft.

To generate decellularized grafts, Multiple decellularization protocols were assessed for their ability to efficiently remove DNA while preserving the ECM. Among them, one protocol emerged as optimal, achieving greater than 99.7% DNA removal, with residual DNA levels reduced to 0.039 µg/mg dry weight, compared to 13.4 µg/mg in non-decellularized controls (L-HyC). Decellularized samples displayed increased surface porosity and exposure of fibrillar matrix structures, as confirmed by scanning electron microscopy, while histological analyses revealed partial preservation of ECM components, including glycosaminoglycans (GAGs), collagen type II, and collagen type X. Quantitative assays indicated a 12% loss in GAG content but complete retention of BMP-2 and collagen levels, demonstrating minimal impact on the matrix's functional composition.

The osteoinductive capacity of D-HyC was evaluated in immunodeficient (ID) mice via ectopic implantation. By 6 and 12 weeks, histological and micro-CT analyses revealed that L-HyC and D-HyC constructs remodeled into mature bone tissue, including cortical and marrow compartments. Early remodeling stages showed dense cellular colonization and matrix deposition, confirmed by Safranin-O and Masson’s trichrome staining. Quantitative micro-CT analysis revealed comparable bone volume (BV) and bone volume relative to tissue volume (BV/TV) between L-HyC and D-HyC grafts, with D-HyC exhibiting a thicker cortical bone layer at earlier times. These findings demonstrate that decellularization does not impair the graft’s capacity to support robust endochondral ossification in ID models.

In contrast, immunocompetent (IC) mice exhibited limited L-HyC and D-HyC graft remodeling. While D-HyC constructs showed increased vascularization and reduced

degradation compared to L-HyC, neither group achieved significant mineralization or complete bone formation. TRAP staining confirmed the absence of osteoclastic activity, and histological analyses indicated that L-HyC grafts were primarily surrounded by fibrotic tissue with minimal vascularization. Small areas of mineralization were detected in D-HyC samples, though these were insufficient for complete bone remodeling. These findings suggest that the immunocompetent environment imposes barriers to the full osteoinductive potential of engineered cartilage grafts.

Immune profiling revealed differences in immune recruitment between graft types and animal models. In ID mice, total immune cell infiltration (CD45+ cells) was lower in D-HyC than L-HyC by day 7, though macrophages dominated the response in both groups. By day 10, macrophage polarization shifted from an initial pro-inflammatory (M1) profile to a pro-regenerative (M2) phenotype in both L-HyC and D-HyC grafts, correlating with successful bone formation. In IC mice, macrophages dominated immune infiltration but remained predominantly unpolarized (M0) at later stages, with declining M1 and M2 activity. This lack of polarization likely contributed to the failure of bone formation in IC animals.

In vitro assays were conducted using human macrophages, peripheral blood mononuclear cells (PBMCs), and dendritic cells (DCs) to further investigate immunogenicity. L-HyC and D-HyC grafts elicited minimal macrophage activation, with reduced M1 and M2 marker expression in D-HyC-treated macrophages. Co-culture with PBMCs revealed low T-cell activation and proliferation, while DC maturation assays showed no significant immune stimulation. These findings confirm the low immunogenicity of decellularized cartilage grafts, underscoring their potential as immune-privileged materials for clinical use.

The regenerative potential of D-HyC was validated in an orthotopic rat critical-sized femoral defect model. D-HyC grafts supported robust bone regeneration, achieving complete defect bridging by 12 weeks, as confirmed by micro-CT and histological analysis. Bone volume in the defect region was significantly higher in D-HyC-treated rats than in empty controls, and regenerated bone exhibited organized cortical and trabecular structures. Biomechanical testing demonstrated that D-HyC-treated defects achieved functional restoration with comparable stiffness to healthy controls. These results highlight the capacity of D-HyC to support structural and functional bone regeneration in clinically relevant scenarios.

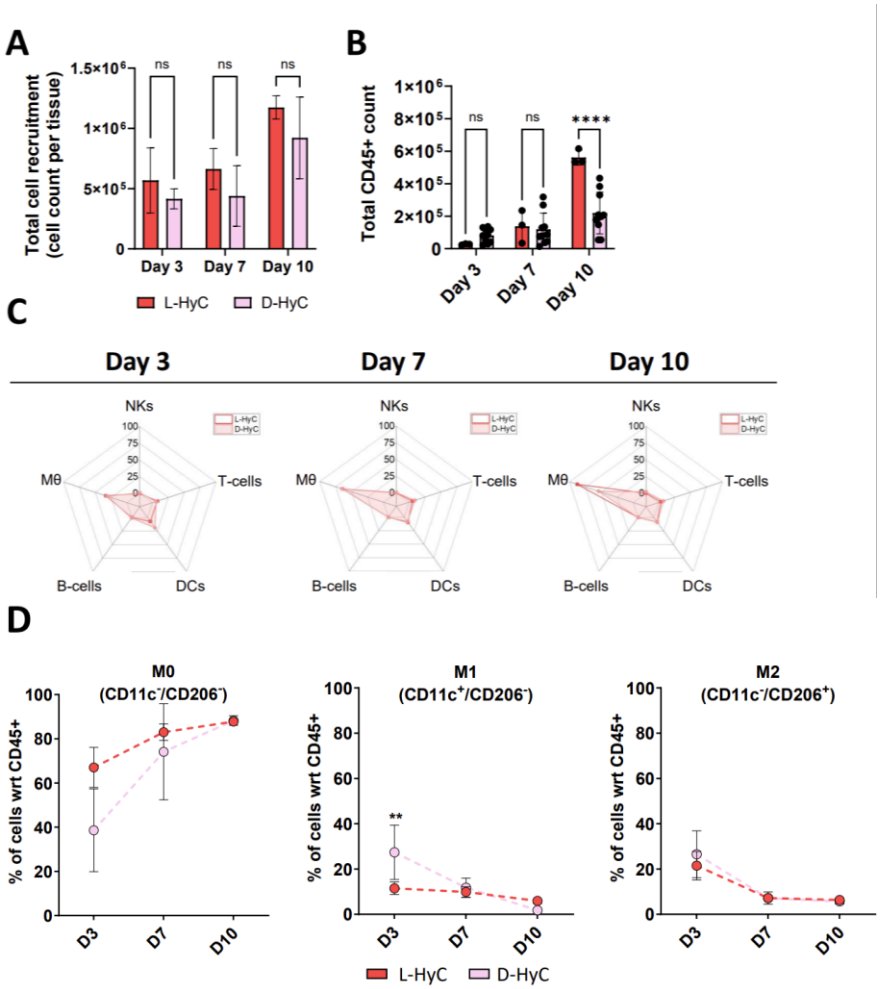

Decellularized human cartilage grafts display lower immunogenicity but fail at inducing macrophage polarization in immunocompetent animals. A) Total cell number captured in explanted tissues after -3, 7-, and -10 days post-implantation. The graphs represent mean + standard deviation (SD), ns $p > 0.1$, determined by Two-way ANOVA. B) Total CD45+ cells captured by flow cytometry in explanted tissues after 3-, 7-, and 10-day periods, and 10-day post-implantation. C) From right to left, representative radar plots representing percentages of early time recruitment of B-cells, T-cells, Dendritic cells, Natural Killers, and Macrophages captured in explanted tissues after -3, -7, and -10 days, respectively. D) Percentage of CD11b + and F4-80 + macrophage subtypes in L-HyC and D-HyC grafts explanted at 3-, 7-, and 10-days post-implantation, analyzed by flow cytometry. The graphs represent mean + standard deviation (SD), $**p \leq 0.01$, determined by Two-way ANOVA.

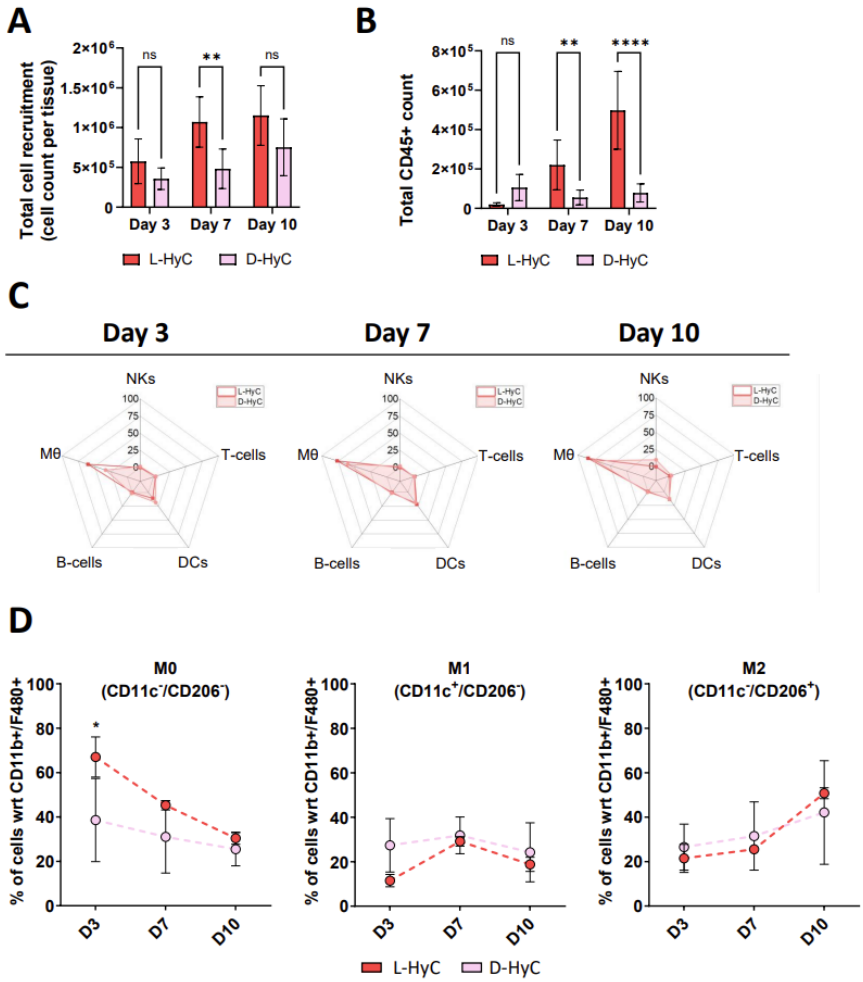

Decellularized human cartilage grafts exhibit lower immune recruitment but preserved pro-regenerative macrophage polarization capacity. A) Total cell number captured in explanted tissues after -3, 77 7, -7 7, and -10 10 days post-implantation. The graphs represent mean + standard deviation (SD), **p ≤ 0.01, determined by Two-way ANOVA. B) Total CD45+ cells captured by flow cytometry in explanted tissues after 3-, 7-, and 10-day, and 10-day post-implantation. C) From right to left, representative radar plots representing percentages of early time recruitment of B-cells, T-cells, Dendritic cells, Natural Killers, and Macrophages captured in explanted tissues after -3, -7, -7, -7, and -10 days, respectively. D Percentage of CD11b + and F4-80 + macrophage subtypes in L-HyC and D-HyC grafts explanted at 3-, 7-, and 10-days post-implantation, analyzed by flow cytometry. Error bars: The graphs represent mean + standard deviation (SD), *p ≤ 0.1, determined by a two-tailed unpaired t-test.

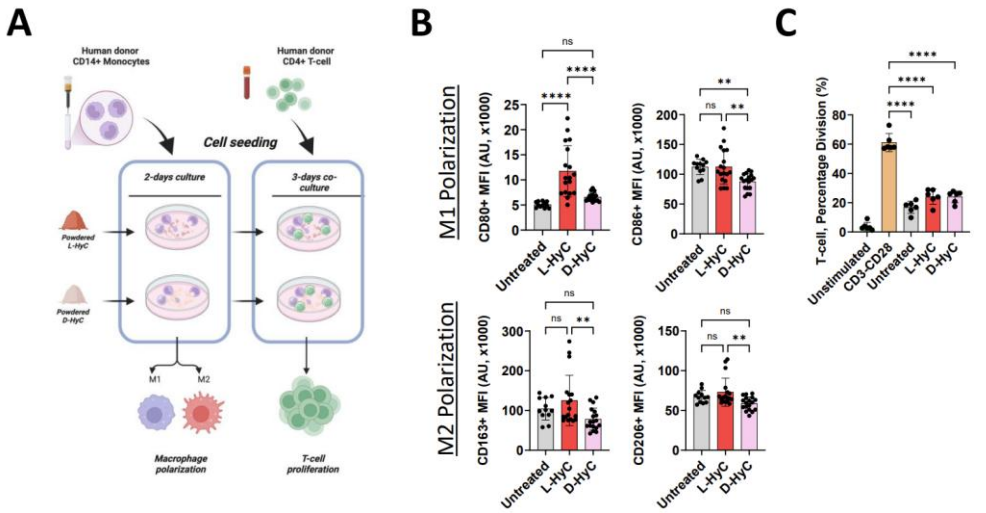

Decellularized engineered cartilage grafts promote distinct macrophage polarization with minimal M1 activation. *A) Experimental scheme of the direct effect of powdered L-HyC and D-HyC on macrophage polarization and indirect T-cell activation potential. B) From top to bottom, total CD80+ and CD86+ MFI indicate M1 polarization, and total CD163+ and CD206+ MFI indicate M2 polarization after 5 days of co-culture with either L-HyC or D-HyC powdered cartilages. The graphs represent mean + standard deviation (SD), *p ≤ 0.1, **p ≤ 0.01, *** p ≤ 0.001, ****p ≤ 0.0001, determined by Ordinary one-way ANOVA,, **p ≤ 0.01, *** p ≤ 0.001, ****p ≤ 0.0001, determined by Ordinary one-way ANOVA. CD3+ FACS assessed percentage division after co-culture of 5 × 10^45 × 10^4 CD3+ cells with 2.5 × 10^3 macrophages co-cultured with either L-HyC or D-HyC powdered cartilages. The graphs represent mean + standard deviation (SD), ****p ≤ 0.0001, determined by Ordinary one-way ANOVA*

Paper V: Extracellular-Matrix-Reinforced Bioinks for 3D Bioprinting Human Tissue

This study evaluated the immune and regenerative responses of hybrid bio-inks composed of alginate reinforced with decellularized lung ECM. These materials aim to address the limitations of conventional bioinks, such as poor gelation and limited biological activity, by combining the structural stability of alginate with the bioactivity of tissue-specific ECM components. Various results were analyzed in a broader investigation, including material properties, cellular responses, vascularization, immune interactions, and tissue remodeling.

Subcutaneous implantation of 3D-printed ECM hydrogels in FoxN1 KO mice (Figure 2D) demonstrated superior tissue integration after 28 days, with no inflammation or foreign body response, unlike alginate hydrogels, which showed encapsulation and inflammatory debris. Histological and light sheet microscopy revealed robust neovascularization in rECM hydrogels, with blood vessels containing red blood cells throughout the graft, highlighting their capacity to support vascularized remodeling and host integration.

A critical component of this immune response involved macrophages, which were analyzed in terms of their polarization states. The study revealed distinct macrophage behaviors in response to the implanted materials. At seven days post-implantation, rECM hydrogels supported a higher proportion of anti-inflammatory M2 macrophages compared to alginate hydrogels, which exhibited increased pro-inflammatory M1 macrophages. M2 macrophages, associated with constructive remodeling, likely contributed to the favorable integration and vascularization observed in rECM constructs. Moreover, the overall inflammatory profile of rECM hydrogels was significantly lower, correlating with reduced fibrosis and enhanced tissue remodeling outcomes.

Other aspects of the study highlighted the broader potential of rECM bioinks, such as their ability to support cellular survival and differentiation. Constructs printed with rECM bio-inks exhibited higher metabolic activity and proliferation of embedded cells, as well as pro-angiogenic properties demonstrated in a chick chorioallantoic membrane (CAM) assay. Additionally, ECM bio-inks provided the structural and biological cues to differentiate primary human lung cells into airway-like tissues.

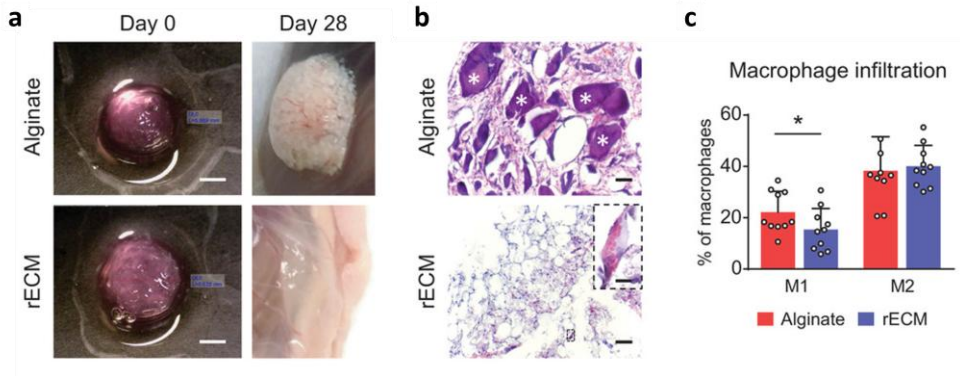

Biocompatibility and angiogenic potential of rECM hydrogels: *a) 3D printed alginate and rECM hydrogels in disk shape before subcutaneous implantation and when explanted on day 28. Scale bars: 2 mm. b) H&E staining of subcutaneously implanted alginate and rECM hydrogels after 28 days. White asterisks * indicate large, non-proteinaceous debris. Inset showing red blood cells in the inner lumen of a blood vessel. Scale bars: 50 and 10 µm (inner panel). c) Macrophage infiltration (defined by CD45$^+$, CD11b$^+$, and F4/80$^+$) in implanted alginate and rECM hydrogels on day 7 (n = 10 animals per group).*

Discussions and Future Perspectives

Paper I

Effective bone regeneration necessitates orchestrating cellular recruitment, bioactive signaling, and scaffold integration. Bone morphogenetic proteins (BMPs), particularly BMP-2 and BMP-7, have been pivotal in these processes, yet their clinical use remains limited by high therapeutic doses, rapid clearance, and off-target effects.[114,115]. This study demonstrates how the BMP-2/7 heterodimer delivered via collagen-hydroxyapatite (CHA) scaffolds can overcome these barriers, offering a clinically translatable solution for bone repair.

Progenitor cell recruitment is a cornerstone of bone healing, as these cells provide the building blocks for bone formation. Osteoprogenitors marked by PDGFR-α and SCA-1 are essential for endochondral ossification in the muscle interstitium and periosteum.[116,117]. BMP-2/7 significantly enhanced osteoprogenitor homing to CHA scaffolds, as evidenced by increased expression of osteogenic markers such as *Dlx5*, *Mmp13*, and *Dmp1*, critical regulators of matrix remodeling and osteoblast differentiation[118,119]. These findings align with studies highlighting the heterodimer's superior receptor-binding affinity and resistance to antagonists, such as Noggin.[120,121].

The robust osteoprogenitor recruitment observed here underscores BMP-2/7's potential to drive early-stage regeneration, a phase often characterized by cartilage formation and matrix deposition.[122]. Glycosaminoglycans and collagen—key ECM components—were significantly elevated in BMP-2/7-treated scaffolds, further validating their role in promoting endochondral ossification.[123].

Bioactive molecules such as BMPs orchestrate cellular behavior during tissue repair. However, achieving sustained delivery and localized action remains a challenge. Traditional delivery systems, such as absorbable collagen sponges (ACS), are prone to rapid protein release, necessitating supraphysiological doses that increase Absorbable collagen sponges (ACS), are prone to rapid protein release, necessitating supraphysiological doses that increase the risk of inflammation and ectopic bone formation. [114,124]. This study employed CHA scaffolds, which the electrostatic binding properties of hydroxyapatite to achieve a controlled and prolonged release of BMP-2/7 for up to three weeks. [125,126]. The resulting sustained availability ensures continuous activation of osteogenic pathways, aligning with findings from studies that emphasize the importance of release kinetics in bone repair. [127,128].

The heterodimeric BMP-2/7 outperformed BMP-2 at equivalent doses in promoting osteogenesis, confirming its superior bioactivity. Studies suggest that BMP-2/7's enhanced efficacy arises from its ability to activate Smad-dependent and non-canonical ERK pathways and its reduced susceptibility to antagonistic

inhibitors.[120,129]. These properties make BMP-2/7 suitable for clinical applications requiring low-dose, high-potency solutions.

In a critical-sized rat femur defect model, BMP-2/7 delivered via CHA scaffolds achieved radiographic union in 12 of 13 specimens within four weeks, outperforming BMP-2 at matched doses and equaling the performance of a 20-fold higher BMP-2 dose. Histological analysis revealed cortical bridging and intramedullary space formation, consistent with effective endochondral ossification. Importantly, no ectopic bone formation was observed, a common side effect associated with high-dose BMP-2[115]. These findings are clinically significant, highlighting the potential of BMP-2/7 for reducing therapeutic doses while maintaining efficacy.

This study paves the way for integrating bioactive factors into advanced tissue engineering platforms. The demonstrated efficacy of BMP-2/7 in CHA scaffolds underscores its potential for creating off-the-shelf grafts for bone repair. Future studies should explore its application in large-animal models and evaluate mechanical properties over time to ensure translational readiness. Additionally, combining BMP-2/7 with emerging fabrication technologies, such as 3D bioprinting, could enable the creation of anatomically and biologically precise constructs tailored to individual patient needs[130,131].

Paper II

Cell-based scaffolds have revolutionized tissue engineering by providing dynamic systems that integrate biological signals, ECM remodeling, and immune modulation. These properties make cellular scaffolds particularly promising for complex clinical situations such as significant bone defects or cartilage degeneration, where acellular or synthetic constructs are insufficient. Identifying a reproducible, scalable, and osteoinductive cell source remains a critical challenge despite this potential.[132,133].

Primary hBM-MSCs and human nasal chondrocytes (hNCs) have been widely used in cartilage engineering due to their chondrogenic potential. However, these cells exhibit significant inter-donor variability, limiting their reproducibility in clinical [134,135]. Immortalization strategies, such as introducing the human telomerase catalytic subunit (hTERT), have been employed to mitigate donor variability but often compromise the cells' chondrogenic capacity[136]. In this study, we circumvent these limitations by engineering a human mesenchymal cell line (MSOD-B) with constitutive BMP-2 expression, enabling robust and reproducible chondrogenesis.

BMP-2, a key regulator of endochondral ossification, was integrated into the MSOD line using lentiviral transduction. The resulting MSOD-B line retained its mesenchymal phenotype and demonstrated enhanced chondrogenic and osteogenic

differentiation while maintaining adipogenic potential. This advancement addresses a significant barrier in tissue engineering by offering a consistent and scalable cell source capable of initiating cartilage formation and subsequent bone remodeling[114,116]. The role of bioactive factors such as BMP-2 in cartilage and bone regeneration is well-established. BMP-2 not only promotes chondrogenic differentiation but also drives hypertrophy and matrix remodeling, essential for endochondral ossification[137,138]. In this study, BMP-2 overexpression in MSOD-B cells enhanced the production of hypertrophic cartilage enriched in glycosaminoglycans, collagen types II and X, and BMP-2 itself. This matrix provided critical biochemical cues for subsequent osteoinduction, as confirmed by in vivo remodeling into bone and bone marrow tissues.

Notably, the osteoinductive capacity of the engineered cartilage was dependent on BMP-Smad 1/5/9 pathway activation, as evidenced by the inhibition of cartilage formation with the BMP receptor inhibitor LDN193189. This finding aligns with previous reports emphasizing the importance of BMP-Smad signaling in chondrogenesis and bone formation . [120,123]. A critical innovation of this study is the development of devitalized MSOD-B-derived HyC as an osteoinductive, cell-free material. Devitalization via an inducible apoptotic system preserved the ECM's biochemical and structural integrity while eliminating immunogenic cellular components. This devitalized HyC demonstrated superior osteoinductive performance compared to living cartilage generated from highly chondrogenic hBM-MSCs, achieving faster and more complete bone remodeling in vivo. The enhanced performance of devitalized HyC was attributed to its cartilaginous composition rather than BMP-2 content. Modulating cartilage maturity through controlled TGFβ3 exposure further emphasized the role of ECM composition in osteoinduction. These findings underscore the potential of engineering "beyond-natural" matrices with defined biological and mechanical properties to achieve predictable clinical outcomes.

Scalability and reproducibility are critical for the clinical translation of tissue-engineered products. By leveraging bioreactor systems, we achieved a 20-fold increase in graft volume while maintaining the quality and osteoinductive capacity of the engineered HyC. This streamlined approach reduces contamination risks and batch variability, addressing a significant barrier in current manufacturing processes[139]. Additionally, the integration of lyophilization enables long-term storage and off-the-shelf availability, enhancing the practicality of devitalized HyC for diverse clinical applications.

When combined with a mechanical scaffold, the devitalized HyC demonstrated efficacy in an orthotopic rat mandibular defect model, significantly enhancing new bone formation and implant integration. These results highlight the potential of combining devitalized ECM materials with synthetic scaffolds to meet site-specific mechanical and biological requirements. This approach aligns with emerging

regenerative medicine paradigms, prioritizing endogenous tissue regeneration through the use of bioactive scaffolds.[140–142].

Paper III

It has been established that multiple biological processes, including lineage-specific differentiation, angiogenesis, and especially ECM remodeling, which must be orchestrated in tandem for effective tissue regeneration, particularly in skeletal repair.[143–145]. It has also been acknowledged that these processes are intrinsically dependent on the molecular composition of the scaffold, notably the ECM, which influences cellular recruitment, fate decisions, and overall repair outcomes.[146,147]. Through the integration of CRISPR/Cas9-mediated modifications into an established human mesenchymal cell platform (MSOD-B), a foundation has been provided for eECMs that precisely target different aspects of healing and remodel themselves to align with the host's regenerative requirements.

A central focus of this work is the discovery that modifying key molecular mediators in cells can substantially alter the structure and function of the secreted ECM. Traditional scaffold-based strategies often rely on matrix components from decellularized tissues or synthetic analogs and have not fully captured the nuanced interplay among angiogenic, osteogenic, and immunomodulatory signals . [148,149]. However, this approach tailored the ECM composition directly at the cellular level. CRISPR/Cas9 technology was utilized to perform knockouts of vascular endothelial growth factor (VEGF) and runt-related transcription factor 2 (RUNX2), representing two complementary targets: removal of a pro-angiogenic factor (VEGF) to assess how vascularization kinetics affect endochondral ossification and inhibition of an essential transcription factor (RUNX2) that drives hypertrophy to explore cartilage stability and bone formation boundaries.

The depletion of VEGF proved especially revealing. Although angiogenesis is typically considered essential for robust bone formation[150,151]It was observed that early progenitor recruitment and osteoinduction were not impaired by VEGF deficiency. This observation differs from strategies that rely solely on intramembranous mechanisms, which have historically required exogenous VEGF to achieve sufficient vascularization[152,153]. In the engineered system described here, BMP-2 and other ECM-embedded factors likely compensated for the absence of VEGF, indicating a sophisticated interplay of signals shaping endochondral processes. Clinically, these findings suggest that growth factor optimization for bone repair may not always demand elevated levels of VEGF if other osteoinductive cues are adequately modulated.

Meanwhile, the silencing of RUNX2 inhibited cartilage hypertrophy and markedly delayed bone marrow formation, thereby maintaining a stable chondral phenotype. This outcome is particularly relevant for articular cartilage repair, where unwelcome

hypertrophy compromises long-term tissue stability.[154–156]. The RUNX2 knockout eECMs integrated more effectively into osteochondral defects by prolonging the chondral stage, yielding higher-quality cartilage regeneration at early intervals. Although the ultimate extent of in vivo cartilage was limited, these findings highlight a powerful strategy to regulate or impede the ossification cascade—a concept that could support personalized medicine. For instance, individuals who require protracted cartilage repair might benefit from RUNX2-suppressed eECMs, whereas those with extensive bone defects could employ unmodified or otherwise edited ECMs to expedite bone formation.

A broader implication of this work is that CRISPR/Cas9-engineered ECMs establish a robust platform to elucidate the molecular triggers of tissue regeneration systematically. By shifting the editing emphasis away from direct cell therapy and toward matrix-mediated repair[157,158]ECMs with a high degree of compositional specificity can be produced, while the genetically altered cells are removed before implantation. This strategy particular defect type, immunological status, or healing trajectory.[104,159]A future eECM might contain elevated pro-angiogenic factors for patients with reduced angiogenic potential; downregulation of RUNX2 could help preserve stable cartilage in patients prone to ossification.

Furthermore, this framework allows simultaneous or subsequent modifications, such as altering immunogenic proteins or adding inducible cell death switches, to advance safety and clinical efficacy further.[160,161]. The MSOD-B platform—a stable, immortalized cell source that expresses BMP-2—already mitigates donor variability, thus providing a reproducible cell line adapted to various regenerative needs.[162,163]. Lyophilization for off-the-shelf grafts extends these advantages to clinical settings by simplifying storage requirements and enabling timely use without undermining the bioactivity.[145,149].

In short, the synergy between CRISPR/Cas9-based compositional editing and cell-derived ECM technologies marks a pivotal shift in scaffold-based regeneration. Rather than universally enhancing or blocking selected molecules, the ECM blueprint can now be precisely adjusted to expedite or postpone distinct phases of healing according to patient-specific therapeutic goals.[142,164]. By examining the roles of targets such as VEGF or RUNX2, vital information emerges about the timing and interplay of key processes—angiogenesis, cartilage hypertrophy, matrix remodeling—and this knowledge steers the design of advanced eECMs that unite precision, consistency, and large-scale feasibility. As validations in large-animal models and clinical studies progress, this blueprint for personalized tissue repair appears poised to alter approaches to challenging bone and cartilage defects, balancing biological complexity and regulatory considerations to deliver the next generation of regenerative therapies.[165,166].

Paper IV

In light of the growing burden of skeletal injuries and the critical need for advanced biomaterials in musculoskeletal therapies[167,168]This study underscores how decellularized tissue-engineered grafts can address existing limitations in bone repair[169,170]. By generating D-HyC through an optimized decellularization process, a scaffold with immunoregulatory properties, potent osteoinductivity, and a clear potential for clinical translation was demonstrated, in agreement with observations that endochondral ossification can be harnessed for bone regeneration[171–173]. Notably, these findings expand on the utility of stable mesenchymal cell lines for tissue engineering.[162,174], bridging critical gaps in reproducibility, safety, and large-scale manufacturing for biomaterial-based regenerative therapies[175,176].

A major challenge in advancing such therapies lies in the immunogenicity of engineered grafts, particularly off-the-shelf constructs, since immune-mediated rejection can negate the scaffold's regenerative benefits.[144,177,178]. Decellularization of engineered cartilage effectively removes immunogenic cellular components while retaining key ECM elements critical for endochondral bone formation, thereby mitigating safety concerns associated with living implants. However, translating these acellular grafts from preclinical models to the clinic remains challenging, given that disparities in immune responses across species and the complexity of the human immune system may influence outcomes.[177,179]. In this context, efforts to scrutinize early immune recruitment events around the implanted scaffold have gained importance, as such interactions can determine whether the graft is integrated or ultimately rejected[180–182] .

D-HyC induced robust new bone formation in immunodeficient (ID) mice, correlating with early M2-dominated macrophage infiltration. This M2 phenotype has been implicated in pro-angiogenic and pro-regenerative processes, consistent with previous data linking macrophage polarization to scaffold integration[167,183–185]. In sharp contrast, the same constructs did not induce bone formation in immunocompetent (IC) mice, presumably due to the lack of beneficial immune polarization. Although decellularization lowered the DNA content below recommended thresholds[186] and reduced cell debris, large inter-species immunological differences still impeded successful remodeling at ectopic sites[180,187,188]. These findings imply that the scaffold's acceptance depends on its composition and the host's immune context.

In vitro co-culture assays with macrophages, T cells, dendritic cells, and peripheral blood mononuclear cells (PBMCs)[189–191] Were conducted to assess immunocompatibility in a more clinically relevant environment. The decellularized constructs, lacking living cells, still reduced T-cell activation and elicited minimal dendritic cell maturation, implying that the immune-privileged status often linked to cartilage may primarily reside in its ECM. These in vitro results echo the immunomodulatory potential observed in other cell-based approaches.[189,190]

However, it highlights how ECM alone can guide host immune cells at the earliest stages.

Despite the unsatisfactory ectopic bone formation in IC mice, D-HyC successfully facilitated bone repair in a weight-bearing rat femoral defect model—underscoring the importance of the orthotopic niche. Bone regeneration in a mechanically and vascularly relevant environment suggests that local cues can override the muted pro-regenerative immune polarization witnessed in ectopic settings. In these paralleling studies, biomechanical and environmental stimuli critically affected endochondral constructs.[171,173,181,192]. From a practical perspective, these data imply that matching graft design to the defect's local environment can prime the immune cells toward a reparative state.

On a translational level, these observations reinforce the promise of acellular ECM-based grafts as scalable, off-the-shelf options for tissue regeneration. D-HyC, which balances biochemical complexity with reduced immunogenicity, may be a compelling alternative to living constructs hindered by donor variability and regulatory complexities.[144,178]. The importance of analyzing early immune events to predict long-term outcomes is highlighted by pinpointing macrophage polarization as a determinant of bone regeneration. Future scaffold designs might, therefore, incorporate immunomodulatory strategies—such as specialized surface properties or growth factor delivery—to encourage M2-dominant responses.[184,193,194]. In addition, real-time monitoring of immune infiltration and polarization[184] Could yield predictive indicators of scaffold performance, paralleling the emerging focus on personalized regenerative interventions.

These findings illustrate that devitalized tissue-engineered cartilage can orchestrate notable bone formation while avoiding typical complications of cell-based approaches. By coupling decellularization with immune-aware assessment protocols, ECM-driven constructs can sustain the osteoinductive potential of hypertrophic cartilage and minimize immunological drawbacks. These insights align with an evolving perspective in tissue engineering: understanding and steering early immune-scaffold interactions can sharpen scaffold efficacy and longevity.[167,168,171]. Continuously refining scaffolds to favor reparative immune cell recruitment—via modulated macrophage polarization, T-cell regulation, or other biomolecular cues—may ultimately fulfill the promise of regenerative medicine for severe skeletal injuries.

Paper V

Recent advances in 3D bioprinting—where cells and biomaterials are deposited in tandem—have spurred efforts to engineer grafts that recapitulate native structure and function.[195–200]. However, it remains challenging to devise bio-inks that simultaneously maintain mechanical fidelity and provide biologically relevant

signals.[201–204]. A novel approach is presented here: decellularized ECM (ECM) is combined with alginate (rECM) to yield rapidly cross-linkable hydrogels containing organ-specific proteins and growth factors.[205–209]. This strategy allows for the interpenetration of ECM-derived molecules within an alginate scaffold.[210–214], effectively bridging the gap between print precision and cell-supportive biochemical cues.

A key observation involves the immunological dimension of scaffold function, particularly at early time points. Given the known linkage between scaffold remodeling, vascularization, and host compatibility, an immune assay investigated how host cells—such as macrophages—respond to ECM hydrogels.[215–219]. Constructs printed using rECM demonstrated an attenuated inflammatory profile, favoring an environment that may promote beneficial macrophage polarization and subsequent vascular ingrowth. These findings are consistent with other studies indicating that materials capable of eliciting an immunomodulatory effect—often marked by a reduced foreign body reaction—can facilitate engraftment and scaffold longevity.[220–225].

Crucially, the early recruitment of immune cells appeared to align with the eventual success of tissue remodeling at the graft–host interface. Such a pattern suggests that scaffold composition should be tuned for mechanical fidelity and immunocompatibility so that a pro-regenerative cascade can be initiated[226–228]. The inclusion of tissue-specific ECM—obtained, for instance, from the lung—underscores the broader utility of this approach, as these bioprinted constructs retained physiologic features pertinent to the source organ while mitigating inflammatory responses[229–232].

These observations suggest that hybrid ECM scaffolds can meet the intertwined requirements of 3D printing fidelity and biologically adaptive behavior. Such a strategy may be extended from alveolar to skeletal tissues to various organ-derived ECMs, offering a scaffold platform that supports cell viability, orchestrates beneficial immune infiltration, and fosters functional regeneration.[233,234].

Methodology

Cells: Expansion, Transfection and Differentiation

Across this work (**Papers II, III, and IV), MSOD-B cells and their modified derivatives were central to developing eECM** and evaluating tissue regeneration. MSOD-B cells were utilized consistently for chondrogenic differentiation, while CRISPR modifications and osteogenic differentiation were specifically applied in paper 3.

CRISPR/Cas9-Based Transfection of MSOD-B Cells

Transfections were performed on MSOD-B to generate CRISPR-modified MSOD-B cells (MSOD-BΔV and MSOD-BΔR). Cells were seeded at a density of 400,000 cells per well in 12-well plates, reaching 80% confluency the next day. DNA mixtures containing one µg plasmid, 2 µL P3000 reagent, and 50 µL OptiMEM were combined with a lipofectamine cocktail (24 µL lipofectamine 3000 in 400 µL OptiMEM) at a 1:1 ratio. After 48 hours, mCherry-positive cells were isolated via fluorescence-activated cell sorting (FACS) using ARIA (BD Biosciences) and single-cell sorted into 96-well plates. Successfully expanded clones were further characterized and used for subsequent experiments in paper 3.

Cell Expansion

MSOD-B cells and their CRISPR-modified derivatives were cultured in α-minimum essential medium (αMEM) supplemented with 10% fetal bovine serum, 1% HEPES, 1% sodium pyruvate, 1% penicillin-streptomycin-glutamine solution, and five ng/ml fibroblast growth factor-2. Cells were seeded at 3200 cells/cm² and passaged upon reaching 90% confluency. Media were replaced twice weekly to maintain cell viability and proliferation.

Chondrogenic Differentiation

MSOD-B cells were harvested using Trypsin-EDTA (0.25%) and seeded onto cylindrical collagen type I scaffolds (6 mm diameter, 3 mm thickness) at a density of 2×10^6 cells per scaffold. To prevent attachment, scaffolds were placed in 12-well plates coated with 1% agarose. Chondrogenic medium consisted of DMEM supplemented with 1% penicillin-streptomycin-glutamine, 1% HEPES, 1% sodium pyruvate, 1% ITS, 0.47 mg/ml linoleic acid, 0.12% bovine serum albumin, 0.1 mM ascorbic acid, 10^{-7} M dexamethasone, and 10 ng/ml TGF-β3. Tissue constructs were cultured for three weeks, with media replaced twice weekly.

Osteogenic Differentiation

MSOD-B cells and their CRISPR-modified progeny were seeded in 12-well plates at a density of 2×10^6 cells per well and cultured in an osteogenic medium. The medium consisted of αMEM supplemented with 10% fetal bovine serum, 1%

HEPES, 1% sodium pyruvate, 1% penicillin-streptomycin-glutamine solution, 0.01M β-dexamethasone, and 0.1M ascorbic acid. Constructs were maintained for three weeks, with media replaced twice weekly to support osteogenic differentiation and matrix mineralization.

Scaffold/graft processing and storage

Lyophilization was utilized for tissue constructs in both in vitro and in vivo studies across Papers II, III, and IV to facilitate long-term storage and preservation.

Lyophilization

Tissue constructs were rinsed twice with PBS (pH 7.2, without calcium and magnesium, Gibco) to remove residual media. Constructs were then snap-frozen in liquid nitrogen for five minutes to stabilize the matrix and subsequently lyophilized using a freeze dryer (Labconco) at −80 °C and 0.05 bar overnight. Once lyophilized, tissue constructs were stored at 4 °C to maintain their structural integrity and bioactivity for downstream applications.

Animal models and implantation methods

The choice of animal models and implantation techniques was tailored across the studies to evaluate the regenerative potential of engineered constructs under various physiological and immunological conditions. These models enabled comprehensive assessments of tissue remodeling, immune interactions, and functional regeneration. Ectopic implantation was consistently employed across all studies (**Papers I–V**) to evaluate graft performance and immune recruitment in non-load-bearing environments. In addition, specific defect models, including the osteochondral defect model (**Paper III**) and the critical-sized femoral defect model (**Paper IV**), were used to assess the regenerative capacity of engineered constructs in load-bearing and anatomically relevant scenarios.

Ectopic Implantation (Paper I-V)

Ectopic implantation was performed to evaluate immune recruitment, tissue remodeling, and the bone formation efficiency of engineered constructs.

Muscle Pouch Model in Immunocompetent Rats (Paper I):

Cylindrical CHA scaffolds (4 mm diameter, 5 mm height) were prepared and loaded with BMP-2/7 or BMP-2 at varying doses. Scaffolds were implanted into muscle pouches created surgically in immunocompetent **Sprague Dawley rats**. Grafts were analyzed after implantation to assess ectopic bone formation.

Subcutaneous Pouch in Mice (Papers II–V):

Engineered human cartilage grafts were implanted subcutaneously in 6–8-week-old **FoxN1 KO BALB/C nude mice** (Papers II–V) and **C57BL/6J immunocompetent mice** (Paper IV). Up to six implants were placed per animal, and samples were

explanted after 3, 5, and 7 days or 6 and 12 weeks for micro-CT, histological (Safranin-O staining), and FACS analyses.

Osteochondral defect model (Paper III)

An osteochondral defect model was established in rats to evaluate the regenerative capacity of CRISPR-modified MSOD-B cells and their engineered constructs. Ten- to 12-week-old male Sprague Dawley rats were anesthetized, and an articular cartilage defect (2 mm depth, 1 mm diameter) was created at the trochlear groove of the femur. Grafts were push-fitted into the defect without sutures, and the joint capsule, muscle tissue, and skin were closed with resorbable sutures. Animals began load-bearing immediately after surgery. After 3 weeks, femurs were harvested for micro-CT and histological characterization to assess the regenerative capacity of the constructs.

Critical-sized femoral defect model

A critical-sized femoral defect model was utilized in rats to assess the bone regeneration potential of decellularized constructs. Ten- to 12-week-old male Sprague Dawley rats underwent a surgical procedure to create a 5-mm mid-diaphyseal defect in the femur, stabilized with a custom internal fixation plate. The defect was filled with three decellularized grafts without sutures, and the wound was closed in a layered fashion. Animals began load-bearing immediately after surgery. Femurs were harvested after 6 and 12 weeks for micro-CT, mechanical testing, and histological analysis, including Safranin-O, Masson's trichrome, and hematoxylin and eosin staining.

In vivo and ex vivo Angiogenesis assays

Paper III primarily employed these methods to evaluate the angiogenic potential of MSOD-B VEGF knockout constructs. The CAM assay was selected for its sensitivity in detecting early vascularization. At the same time, vascular density quantification provided a robust metric for assessing vessel formation and distribution within graft regions, critical for understanding the impact of VEGF knockout on regenerative outcomes.

Cam Assay

The chick chorioallantoic membrane (CAM) assay evaluated the angiogenic potential of tissue-engineered grafts, explicitly focusing on constructs derived from MSOD-B and MSOD-BΔVEGF1 cells. Fertilized Lohmann Brown chicken eggs were incubated under controlled conditions (37.5 °C with constant humidity) for six days before the start of the experiment. On Day -3, a small window was aseptically created in the eggshell to provide access to the CAM, resealed with adhesive tape, and returned to incubation. On Day 0, lyophilized MSOD-B constructs, wild-type, and VEGF knockout were placed on the CAM. The eggs were resealed and returned to the incubator. Brightfield images were acquired on Day 4 using a LEICA S9i

microscope. These images were subsequently analyzed for vascular density to assess the angiogenic response of the grafts.

Vascular density quantification

The Quantitative Vascular Analysis Tool (Q-VAT) was used to quantify vascular density, allowing for a detailed analysis of CAM assay images. The digital microscope images were segmented into tiles, and binary vascular masks were generated to identify vascular structures within the tissue. Q-VAT's automated functionality enabled the differentiation of vessel measurements based on diameter, facilitating the quantification of both macro- and microvasculature. The vascular density, defined as the proportion of tissue area occupied by vessels, was calculated for each tile, and the mean vascular density was computed across all tiles for each sample. In addition, double- or triple-stained slides were analyzed using Q-VAT to determine the overlapping percentage of vessels, allowing for comparisons across various time points.

Molecular and cellular assays

Molecular and cellular analyses were employed throughout the study to qualitatively and quantitatively assess immune responses, protein expression, and biochemical composition. Flow cytometry was utilized across Papers I, III, IV, and V to investigate osteoprogenitor homing (Paper I), intracellular RUNX2 expression (Paper III), immune cell recruitment and distribution (Papers IV and V), and macrophage polarization (Papers IV and V). ELISA and Western blot analyses in Paper III were used to quantitatively and qualitatively verify the modifications of MSOD-B cells by measuring VEGF and RUNX2 protein expression. qPCR in Paper III further supported these findings by analyzing changes in gene expression. GAG analysis was performed in Papers II, III, and IV to ensure consistent glycosaminoglycan deposition following chondrogenic differentiation, serving as a quality control measure for the engineered constructs.

Flow cytometry

For **Paper I**, neo-tissue specimens were harvested and enzymatically digested to obtain single-cell suspensions. Cells were stained with primary antibodies for osteoprogenitor markers and analyzed using a BD LSRFortessa™ analyzer. For immune cell recruitment (**Papers IV and V**), subcutaneous implants were digested using a collagenase type II, P, and CaCl2 cocktail. The resulting cell suspensions were washed, stained with primary and secondary antibodies, and analyzed using a BD LSRFortessa™ cell analyzer. Intracellular staining (**Paper III**) involved fixing and permeabilizing cells with a Fixation/Permeabilization Kit, followed by RUNX2 staining using a rabbit anti-human primary antibody and a donkey anti-rabbit APC-labeled secondary antibody. Fluorescence compensation was set using UltraComp eBeads™, and all data were analyzed with FlowJo™ software.

Innate Immune Markers: APC Fire CD11b (Rat IgG2b, κ, Biolegend 101235), PE F4/80 (Rat IgG2a, κ, Biolegend 123110), PECy7 CD11c (Armenian Hamster IgG, Biolegend 117318), AF647 CD206 (Rat IgG2a, κ, Biolegend 141712), BV650 NK1.1: (Mouse IgG2b, κ, Biolegend 108736).

Adaptive Immune Markers: PerCPCy5.5 CD45 (Rat IgG2b, κ, Biolegend 147706), APC Fire 750 CD8 (Rat IgG2b, κ, Biolegend 344746), PE CD19 (Rat IgG2a, κ, Biolegend 152408), PECy7 CD3 (Armenian Hamster IgG, Biolegend 100220), AF647 CD4 (Rat IgG2b, κ, Biolegend 100424).

Intracellular Markers: RUNX2: (Rabbit anti-human, Thermo-Fischer PA5-82787) with secondary antibody Donkey anti-rabbit IgG DyLight™ 649 (Biolegend 406406).

Osteogenic Markers: CD31 PE (Mouse IgG1, κ, BD Biosciences 555027), CD45 Alexa Fluor® 488 (Mouse IgG1, κ, Abcam Ab256254), PDGFR-α AF647 (Rabbit IgG, Abcam Ab150075, secondary for Ab203491), SCA-1 Cy 5.5 (Goat IgG, Abcam Ab6951, secondary for R&D Systems AF1226).

Blocking Control: CD16/32 (Fc Block): (Rat IgG2a, λ, Biolegend 101302)

Western blot

Western blotting in **Paper III** evaluated RUNX2 protein expression in MSOD-B and MSOD-BΔRUNX2 cells. Cell lysates were prepared in RIPA buffer supplemented with protease and phosphatase inhibitors, separated by Bolt gels, and transferred to PVDF membranes. Primary antibodies included RunX2 (D1L7F, Cell Signaling Technology 12556) and Actin (Becton Dickinson 612656). HRP-conjugated secondary antibodies (Anti-Mouse GENA931, Sigma-Aldrich; Anti-Rabbit NA9340V, Thermo Fisher Scientific) were used for detection via chemiluminescence.

qPCR

qPCR was performed in **Paper III** to evaluate gene expression of RUNX2, ALP, and ColX in differentiated MSOD-B constructs. Total RNA was extracted using the Quick-RNA extraction kit (Zymo Research) and reverse-transcribed into cDNA using Invitrogen's cDNA synthesis kit. TaqMan assays were quantified, with GAPDH as the reference gene.

GAG analysis

Biochemical quantification of GAG content was conducted in **Papers II, III, and IV** to ensure consistent ECM production after chondrogenic differentiation. Lyophilized constructs were digested overnight in Proteinase K solution (1 mg/mL Proteinase K, 10 µg/ml pepstatin A, one mM EDTA, 100 mM Iodoacetamide, 50 mM Tris, pH 7.6, 56°C) and analyzed using the Glycosaminoglycan Assay Blyscan kit (Biocolor).

Histology and Image Analysis

Histological and imaging techniques were employed across the studies to qualitatively and quantitatively evaluate tissue morphology, matrix composition, and regenerative outcomes. Safranin O staining was applied in Papers II, III, and IV to assess glycosaminoglycan content in engineered cartilage. Masson's Trichrome staining in Papers III and IV enabled the visualization of collagen deposition and fibrosis. Hematoxylin and Eosin (H&E) staining in Paper III provided a comprehensive view of general tissue morphology. TRAP staining in Papers III and IV highlighted osteoclastic activity, which is crucial for understanding bone remodeling. Advanced methodologies such as histological grading, cartilage quantification, and trabecular parameter analysis were primarily utilized in Paper III to assess cartilage and bone repair in osteochondral defect models. In Papers III and IV, immunofluorescence was used to localize cell-specific markers and proteins within the constructs. Micro-CT imaging in Papers II, III, and IV quantified bone architecture, including trabecular thickness, separation, and vascular density, further elucidating the efficacy of the engineered constructs

Chemical staining

Both in vitro and in vivo samples are fixed in formaldehyde overnight. After fixation in formaldehyde, in vivo tissues were decalcified using 10% EDTA (Sigma Aldrich, USA) at pH 8.0 and maintained at 4°C for two weeks. Samples were then progressively dehydrated through a graded ethanol series (35%, 70%, 95%, and 99.5%; Solveco) with two 20-minute immersions at each concentration. Following dehydration, tissues were washed in a 1:1 solution of 99.5% ethanol and xylene (Fisher Scientific) for 10 minutes, then immersed in xylene alone for two 20-minute washes. Tissues were subsequently embedded in paraffin at 56°C overnight and sectioned into 7–10 μm slices using a microtome. The sections were dried overnight at 37°C. Deparaffinization was done by rinsing sections twice in xylene for 7 minutes each, followed by a 3-minute wash in a 1:1 ethanol/xylene (99.5%) mixture. Rehydration was performed using a graded ethanol series (99.5%, 95%, 70%, and 35%), each step lasting 7 minutes and repeated twice.

Safranin O staining

Safranin O staining was employed to qualitatively assess the cartilage formation in the differentiated tissues in Papers II, III, and IV. Paraffin-embedded sections were stained using Mayer's hematoxylin solution (Sigma-Aldrich) for 10 minutes and then rinsed in distilled water. Samples were then treated with 0.01% fast green solution (Fisher Scientific) for five minutes and rinsed briefly in 1% acetic acid solution. Staining with 0.1% Safranin O (Fisher Scientific) was performed for five minutes. Slides were dehydrated through a graded ethanol series and xylene and mounted with a PERTEX mounting medium (HistoLab). This protocol enabled precise visualization of cartilage-specific GAG content.

Masson's Trichrome staining

This staining was performed to complement Safranin O staining, allowing for better visualization of collagen deposition, particularly in Papers III and IV. Following paraffin embedding, sections were deparaffinized and treated with Bouin's solution at room temperature overnight to enhance staining. The slides were stained with Weigert's iron hematoxylin for nuclear detection, Biebrich Scarlet-Acid Fuchsin for cytoplasm, and aniline blue for collagen. After treatment with phosphotungstic acid, the sections were dehydrated and mounted. This staining enabled differentiation between fibrotic tissue and native cartilage or bone.

Haematoxylin and Eosin (H&E) staining.

H&E staining was used mainly in Paper III to examine general tissue morphology in both in vitro and in vivo samples. After deparaffinization, sections were stained with Mayer's hematoxylin solution for 10 minutes and rinsed in running water. Eosin Y solution (Sigma-Aldrich) was applied as a counterstain for one minute. After dehydration and clearing, sections were mounted with PERTEX medium. This method provided a detailed visualization of cellular organization and tissue structure.

TRAP (Tartrate Resistant Acid Phosphatase) staining

TRAP staining was employed in Papers III and IV to assess osteoclastic activity in decellularized and lyophilized constructs after in vivo implantation. The slides were treated with a sodium tartrate and Fast Red TR Salt staining solution at 37°C for two hours. After counterstaining with Mayer's hematoxylin, the sections were examined under a microscope. This method allowed quantification of osteoclast activity within the graft and surrounding host tissue.

Histological Grading Method

In Paper III, a semi-quantitative grading system based on a customized adaptation of the Wakitani scoring method was applied to evaluate cartilage repair in rat femoral condyles. The system included six parameters: cellular morphology, matrix staining, surface regularity, cartilage thickness, subchondral bone formation, and integration with neighboring cartilage. Each parameter was scored on a scale of 0–4, with a maximum possible score of 16 representing optimal repair. This grading provided a comprehensive evaluation of cartilage quality and integration.

Cartilage Quantification method

Cartilage regeneration was quantified in Paper III by defining a standardized Region of Interest (ROI) in the femoral condyle defects. ImageJ software calculated the percentage of cartilage-positive regions within the ROI relative to the total defect area. This method allowed a direct comparison of cartilage formation between

experimental and control samples, providing quantitative insight into the effectiveness of different treatment approaches.

Trabecular Thickness (Tb.Th) and Trabecular Separation (Tb.Sp)

In Paper III, bone microarchitecture was analyzed using trabecular thickness (Tb.Th) and trabecular separation (Tb.Sp) as key parameters. A rectangular interface region (2 × 1 mm) was defined as the ROI in the defect space. Trabecular parameters were calculated using the BoneJ plugin in ImageJ to evaluate bone quality and structural integrity. This analysis was instrumental in assessing the regeneration potential of engineered constructs in critical-sized defects.

Immunofluorescence

Immunofluorescence staining was applied to spatially localize proteins and cell-specific markers in engineered and native tissues. In Paper III, agarose-embedded sections were treated with Triton X-100 and donkey serum for blocking and permeabilization. Primary antibodies, including mouse anti-Collagen II (Invitrogen, MA137493), rabbit anti-Collagen X (abba, abx101469), and VEGF (Bioss Antibodies, bs-0279R), were applied overnight at 4°C. Secondary antibodies such as CF568 donkey anti-rabbit (Biotium, 20098) and CF633 donkey anti-mouse (Sigma-Aldrich, SAB4600131) were used. Sections were imaged using a Zeiss LSM780 confocal microscope. In Paper IV, additional antibodies, such as goat anti-mouse CD31 (R&D Systems, YZU0119121), were used to evaluate vascularization. Tissue sections were treated with a TrueView Autofluorescence Quenching Kit (Vector Laboratories) to enhance image quality.

In vivo Micro-CT scanning

In Papers II, III, and IV, in vivo micro-CT scanning was performed to evaluate bone regeneration and vascularization at 4–6 weeks post-implantation. Rats were anesthetized using isoflurane and positioned for scanning with a U-CT system (MILABS). Volumes were reconstructed at 30 μm isotropic voxel size, and bone parameters such as volume and density were quantified using Seg3D and Blender software.

In vitro Micro-CT scanning

Ex vivo scanning was performed on fixed samples to achieve higher resolution (10 μm isotropic voxel size). Subcutaneous implants in mice and orthotopic femoral samples in rats were analyzed for bone volume and architecture. This analysis provided detailed insights into the effectiveness of constructs in promoting bone regeneration and vascularization.

Immune cell isolation and polarization methods

These assays were conducted primarily in **Paper IV** and aimed to evaluate the immunogenicity and immune response of human cells toward the engineered

matrices before and after decellularization. These studies focused on the interactions between engineered cartilage constructs and immune cells, with an emphasis on monocyte-derived macrophages and their subsequent effects on T-cell behavior.

PBMCs preparation

Peripheral blood mononuclear cells (PBMCs) were isolated from heparinized blood via density gradient centrifugation using Lymphoprep (Axis-Shield) at 640g for 20 minutes with a low break. The cells were washed twice with PBS, counted, and prepared for downstream applications. When required, monocytes were further purified from the PBMC fraction using CD14+ magnetic bead separation (Miltenyi) following the manufacturer's instructions. Additionally, CD4+ T-cells were isolated using the EasySep™ CD4+ T-cell Isolation Kit (Stemcell Technologies) per the manufacturer's protocol and prepared for use in co-culture studies.

Monocyte isolation and in vitro polarisation

Monocytes were freshly isolated from PBMCs obtained from healthy donors (n=6; median age 43, 50% female) after informed consent. The monocytes were cultured for five days in 24-well plates (Falcon) at a density of 0.5 x 10^6 cells/mL in complete α-Minimum Essential Medium (α-MEM) supplemented with 10% heat-inactivated fetal bovine serum (FBS), 1% HEPES (1M), 1% sodium pyruvate (100mM), and 1% penicillin/streptomycin/glutamine solution, along with 40 ng/mL macrophage colony-stimulating factor (M-CSF). The media was then replaced with a fresh medium containing 200 µg/mL of powdered HyC (L-HyC or D-HyC) without M-CSF and cultured for an additional two days to induce polarization.

Macrophage polarisation analysis

After the two-day polarization, macrophages were detached using ice-cold PBS containing one mM EDTA and gentle pipetting, followed by washing with PBS and resuspension in RPMI-1640 supplemented with 10% heat-inactivated FBS and 1% penicillin/streptomycin solution. A portion of the polarized macrophages (2.5×10^3 cells) was reserved for a T-cell proliferation assay, while the remaining cells were stained for flow cytometry analysis. The cells were incubated with the following antibodies, all diluted 1:100, for 20 minutes at room temperature: **CD80 (BV650, BD), CD86 (BV650, BD)**, **CD163 (PE, BD)**, **CD206 (APC, BD)**. The stained cells were washed, counted, and analyzed using flow cytometry to evaluate polarization patterns. These analyses provided insights into the pro- or anti-inflammatory phenotypes adopted by macrophages in response to the engineered cartilage constructs. They set the stage for subsequent studies, involving co-culture of immune cells.

Use of Generative AI Tools

By guidelines from the Faculty of Medicine at Lund University, I disclose here my use of generative AI tools in the preparation of this thesis. OpenAI's ChatGPT

(GPT-4 model, accessed via ChatGPT) was used during the drafting of the introductory summary and select sections of the text. The primary purposes were: 1) rephrasing and refining my original text to enhance clarity, flow, and professional tone; 2) checking and improving grammar and syntax; and 3) reviewing transitions and paragraph structure for coherence. No content related to scientific data analysis, interpretation of results, or formulation of research questions was generated by AI. All substantive ideas, conceptual framing, and critical analysis were developed independently. AI-generated outputs were critically reviewed and manually revised before inclusion. I take full responsibility for the accuracy, integrity, and originality of the content presented.

Acknowledgements

Though I stand at the end of my doctoral journey, I did not get here by fortune, determination, or the occasional burst of competence alone. I was carried, mostly, by generous colleagues, stubborn cells, and unwilling martyrs (thank you, mice; your sacrifice will not be forgotten). This is my imperfect but heartfelt attempt to thank everyone and everything that shaped me: for the wisdom shared, the patience extended, and my foolishness tolerated.

Paul. The supervisor who took a chance with me after a Skype call and brought me to Sweden. You taught me more than science: how to set up a lab from scratch, how hard work is in its maintenance, and how painful but rewarding paper writing and rebuttals can be. I immensely appreciate your willingness to set appointments for meetings anytime I needed. You pushed me to research school, where I somehow won the best presentation in my first year. You made me climb up to the terrace to scream away my shyness, and I thoroughly enjoyed and cherished our time outside the lab as well, including hikes, dinners, an escape room, a Spa evening, paintball, and the mini adventure to find the log for our thesis nail. I am always grateful.

Filipe. My co-supervisor, with a different lens than Paul, always gives unique perspectives and wisdom, especially regarding immune response. You pushed me into collaborations with your students, who not only helped with experiments but also rescued me with molecular biology ingredients whenever I was stuck.

WCMM Research School. Anja Meisner, Joao Duarte, and Vinay Swaminathan, thank you for creating a friendly space to interact with fellow scientists. You taught me to take on new responsibilities as a student representative, provided me with the opportunity to practice with research grants (Isabella, thank you for collaborating), and helped me present my initial work, which ultimately won me the best presentation award in my very first year. I will never forget that. Thank you to the FACS facility, Anna Fossum, Zhi Ma, and Anna Hammarberg. Thank you to Pernilla for the MentLife organisation and to Alena Germanenko Hansen for providing clarity on industry expectations and for training me in CV preparation and job interviews.

Collaborators. I thank Ivan Martin, my academic grandparent, for the opportunity to contribute to my first collaborative paper as a member of the lab, and for the enriching knowledge transfer during our lab retreat. Darcy Wagner and Martina De Santis, our first direct collaboration, felt great to be treated as an “expert” in a particular experiment and to be trusted with an essential aspect of your work. Agatheesh, thank you for being a friend when I needed it, both in life advice and in experiments. Andrei Chagin and Robin Kahn, thank you for providing valuable halftime feedback and for the improvements you made for me. Tobias Schmidt,

thank you for your expertise, time, and kindness whenever I asked for help. Deepak Raina, thank you for your skills, guidance, and mentoring throughout my thesis work, from animal experimentation to histology. Sofia Mohlin, thank you for your hospitality and your help in the CAM assay.

My wonderful labmates. Soran Alatas and Marvin Grischke for helping me begin my life in Lund together, learning to set up the lab and do experiments while also exploring Lund. Pilar Lorenzo for assisting in ordering and administrative work. Sonia Ferveur, thank you for inviting me and showing me around your hometown during my lonely Christmas, and thank you for letting me continue your project, which became my first first-author paper. Tommi Glorioso, thank you for the fun times and your blunt medical advice. Melissa Langlois and Panajot Kristofori, thank you for helping me in the lab and for entertaining lab meetings. Ani Grigoryan, a special thank you for being a mentor, a friend, for philosophical discussions, and for guidance. Karin Linderfalk, thank you for working along with me and helping me improve my basis for the first-author paper, and thank you for the movie and book discussions. Joao Pinheiro, Ludovica Perotti, Yuan Li, Lucille Degos, Medea Gabriel, Alexandra-Lydia Chatzidaniil, and Patrizia Kühne, thank you for your support during my work and also for the fun time and discussions during the breaks.

Bai Yiguang, thank you for your wild travel stories, excellent surgical skills, and your contribution to my first-author paper. Laura Rabanal Cajal, Sara González Antón, and Camille Sauter, thank you for your warm friendship despite our time at the lab not coinciding. David Hidalgo Gil, thank you for your timeless support, the drama updates, and your willingness to help me anytime. Aurélie Baudet, thank you for your wisdom, mentoring, and ever-positive vibes. Steven Dupard, thank you for our shared PhD experience and being a cool friend. Alejandro Garcia-Garcia, one of the funniest people I know: ever honest, ever dependable, and an excellent office mate. Dimitra Zacharaki, thank you for being there whenever I needed anything, from scientific advice to life advice, for the ever-critical lab-meeting questions, but always with the best intentions, and for being ever reliable.

Gym and crew. Lotte , Mezie (special thanks for training me), and Lisa, thank you for being my gym buddies.

New home base. Sandra Lindstedt and Franziska Olm, thank you for trusting me and giving me an opportunity before even finishing my PhD. Nicholas Bèchet, Margareta Mittendorfer, Qi Wang, Runchuan Gu, Liselott Looström, Anna Niroomand, Embla Boden, Fanny Svereus, Gabriel Hirdman, and Jie Tang, thank you for making me feel welcome very early in the new lab. Candela Vázquez and Julia Zhou, thank you for being my new helping hands and helping me learn more about guiding.

People who made Sweden feel like home to me. Mridula , Albertas , Irem , Nadja , Jelte , Jurgen, and Nath, thank you for making my life in Sweden memorable and worthwhile, and for all the enjoyable moments I shared.

My parents. நான் இப்போ இங்க இருக்குறதுக்கு முக்கிய காரணம் நீங்க தான், அம்மா, அப்பா. நான் எப்ப என்ன வேணும்னு கேட்டாலும் வாங்கி தந்து, என்ன படிக்கப்போறேன்னு முழுசா புரியலனாலும் உங்க சக்திக்கு மேல என்ன கண்டம் தாண்டி படிக்க வச்சி, நம்ம குடும்பத்துல முதல் பட்டதாரி மட்டும் இல்லாம முதல்ல டாக்டர் பட்டம் வாங்கவச்சிருக்கறீங்க. நான் உங்களுக்கு எப்போதும் கடமைப்பட்டிருக்கிறேன்

And Vini, thank you for always being there for me, even from far away, and for making me feel close.

And finally, Valy. What would I do without you? You made me the best version of myself and upgraded almost every facet of my life, and I am forever grateful for you being you in my life, at present, my greatest present.

References

1. Osterhoff, G. *et al.* Bone Mechanical Properties and Changes With Osteoporosis. *Injury* (2016) doi:10.1016/s0020-1383(16)47003-8.
2. Mäkitie, R. E. *et al.* Defective WNT Signaling Associates With Bone Marrow Fibrosis—a Cross-Sectional Cohort Study in a Family With WNT1 Osteoporosis. *Osteoporosis International* (2017) doi:10.1007/s00198-017-4309-4.
3. Rankin, E. B. *et al.* The HIF Signaling Pathway in Osteoblasts Directly Modulates Erythropoiesis Through the Production of EPO. *Cell* (2012) doi:10.1016/j.cell.2012.01.051.
4. Chang, G. *et al.* In Vivo Estimation of Bone Stiffness at the Distal Femur and Proximal Tibia Using Ultra-High-Field 7-Tesla Magnetic Resonance Imaging and Micro-Finite Element Analysis. *J Bone Miner Metab* (2011) doi:10.1007/s00774-011-0333-1.
5. Enoki, S., Higashiura, M., Sato, M., Tanaka, K. & KATAYAMA, T. Evaluation on Mechanical Properties of a Single Trabecular in Bovine Femur. (2012) doi:10.2495/hpsm120061.
6. Iolascon, G. The Contribution of Cortical and Trabecular Tissues to Bone Strength: Insights From Denosumab Studies. *Clinical Cases in Mineral and Bone Metabolism* (2013) doi:10.11138/ccmbm/2013.10.1.047.
7. Chubb, R. *et al.* In Vivo Rescue of the Hematopoietic Niche by Pluripotent Stem Cell Complementation of Defective Osteoblast Compartments. *The International Journal of Cell Cloning* (2017) doi:10.1002/stem.2670.
8. Chiodo, C. P., Hahne, J., Wilson, M. G. & Glowacki, J. Histological Differences in Iliac and Tibial Bone Graft. *Foot Ankle Int* (2010) doi:10.3113/fai.2010.0418.
9. Hardouin, P., Rharass, T. & Lucas, S. Bone Marrow Adipose Tissue: To Be or Not to Be a Typical Adipose Tissue? *Front Endocrinol (Lausanne)* (2016) doi:10.3389/fendo.2016.00085.
10. Johnson, C. B., Zhang, J. & Lucas, D. The Role of the Bone Marrow Microenvironment in the Response to Infection. *Front Immunol* (2020) doi:10.3389/fimmu.2020.585402.
11. Bartl, R. & Bartl, C. Bone disorders: Biology, diagnosis, prevention, therapy. *Bone Disorders: Biology, Diagnosis, Prevention, Therapy* 1–602 (2017) doi:10.1007/978-3-319-29182-6.

12. Kar, S., Jasuja, H., Katti, D. R. & Katti, K. S. WNT/B-Catenin Signaling Pathway Regulates Osteogenesis for Breast Cancer Bone Metastasis: Experiments in an <i>In Vitro</I> Nanoclay Scaffold Cancer Testbed. *ACS Biomater Sci Eng* (2019) doi:10.1021/acsbiomaterials.9b00923.

13. Li, L., Li, A., Zhu, L., Gan, L. & Zuo, L. Roxadustat Promotes Osteoblast Differentiation and Prevents Estrogen Deficiency-Induced Bone Loss by Stabilizing HIF-1α and Activating the WNT/B-Catenin Signaling Pathway. *J Orthop Surg Res* (2022) doi:10.1186/s13018-022-03162-w.

14. Li, X. *et al.* Icariin Augments Bone Formation and Reverses the Phenotypes of Osteoprotegerin-Deficient Mice Through the Activation of WNT/<b><i>β</I></B>-Catenin-BMP Signaling. *Evidence-Based Complementary and Alternative Medicine* (2013) doi:10.1155/2013/652317.

15. Yang, Y. *et al.* Lgr4 Promotes Aerobic Glycolysis and Differentiation in Osteoblasts via the Canonical WNT/B-Catenin Pathway. *Journal of Bone and Mineral Research* (2020) doi:10.1002/jbmr.4321.

16. Zhang, R. *et al.* WNT/B-Catenin Signaling Activates Bone Morphogenetic Protein 2 Expression in Osteoblasts. *Bone* (2013) doi:10.1016/j.bone.2012.09.029.

17. Bruedigam, C. *et al.* A New Concept Underlying Stem Cell Lineage Skewing That Explains the Detrimental Effects of Thiazolidinediones on Bone. *Stem Cells* (2010) doi:10.1002/stem.405.

18. Hwang, J. *et al.* Euodia Sutchuenensis Dode Extract Stimulates Osteoblast Differentiation via WNT/B-Catenin Pathway Activation. *Exp Mol Med* (2015) doi:10.1038/emm.2014.115.

19. Lund, T. *et al.* First-line Treatment With Bortezomib Rapidly Stimulates Both Osteoblast Activity and Bone Matrix Deposition in Patients With Multiple Myeloma, and Stimulates Osteoblast Proliferation and Differentiation <i>in Vitro</I>. *Eur J Haematol* (2010) doi:10.1111/j.1600-0609.2010.01485.x.

20. Sollazzo, V., Palmieri, A., Girardi, A., Farinella, F. & Carinci, F. Early Effects of P-15 on Human Bone Marrow Stem Cells. *J Oral Maxillofac Res* (2010) doi:10.5037/jomr.2010.1104.

21. Griffin, M., Iqbal, S. A., Sebastian, A., Colthurst, J. & Bayat, A. Degenerate Wave and Capacitive Coupling Increase Human MSC Invasion and Proliferation While Reducing Cytotoxicity in an in Vitro Wound Healing Model. *PLoS One* (2011) doi:10.1371/journal.pone.0023404.

22. Makoto, F. *et al.* Derivation of Mesenchymal Stromal Cells From Pluripotent Stem Cells Through a Neural Crest Lineage Using Small Molecule Compounds With Defined Media. *PLoS One* (2014) doi:10.1371/journal.pone.0112291.

23. Ng, J. *et al.* Ectopic Implantation of Juvenile Osteochondral Tissues Recapitulates Endochondral Ossification. *J Tissue Eng Regen Med* (2017) doi:10.1002/term.2500.

24. Ghimire, S. *et al.* The Investigation of Bone Fracture Healing Under Intramembranous and Endochondral Ossification. *Bone Rep* (2021) doi:10.1016/j.bonr.2020.100740.

25. Ripmeester, E. G., Timur, U. T., Caron, M. M. & M. Welting, T. J. Recent Insights Into the Contribution of the Changing Hypertrophic Chondrocyte Phenotype in the Development and Progression of Osteoarthritis. *Front Bioeng Biotechnol* (2018) doi:10.3389/fbioe.2018.00018.

26. Nishimura, R. *et al.* Osterix Regulates Calcification and Degradation of Chondrogenic Matrices Through Matrix Metalloproteinase 13 (MMP13) Expression in Association With Transcription Factor Runx2 During Endochondral Ossification. *Journal of Biological Chemistry* (2012) doi:10.1074/jbc.m111.337063.

27. Li, J. *et al.* Ceria Nanoparticles Enhance Endochondral Ossification–based Critical-sized Bone Defect Regeneration by Promoting the Hypertrophic Differentiation of BMSCs <i>via</I> DHX15 Activation. *The Faseb Journal* (2019) doi:10.1096/fj.201802187r.

28. Nishimura, R. *et al.* Osterix Regulates Calcification and Degradation of Chondrogenic Matrices Through Matrix Metalloproteinase 13 (MMP13) Expression in Association With Transcription Factor Runx2 During Endochondral Ossification. *Journal of Biological Chemistry* (2012) doi:10.1074/jbc.m111.337063.

29. Lazarus, S. *et al.* Characterization of Normal Murine Carpal Bone Development Prompts Re-Evaluation of Pathologic Osteolysis as the Cause of Human Carpal-Tarsal Osteolysis Disorders. *American Journal of Pathology* (2017) doi:10.1016/j.ajpath.2017.05.007.

30. Tortelli, F., Tasso, R., Loiacono, F. & Cancedda, R. The Development of Tissue-Engineered Bone of Different Origin Through Endochondral and Intramembranous Ossification Following the Implantation of Mesenchymal Stem Cells and Osteoblasts in a Murine Model. *Biomaterials* (2010) doi:10.1016/j.biomaterials.2009.09.038.

31. Bernhard, J. *et al.* Effects of Endochondral and Intramembranous Ossification Pathways on Bone Tissue Formation and Vascularization in Human Tissue-Engineered Grafts. *Cells* (2022) doi:10.3390/cells11193070.

32. Notoh, H. *et al.* Basement Membrane Extract Potentiates the Endochondral Ossification Phenotype of Bone Marrow-Derived Mesenchymal Stem Cell-Based Cartilage Organoids. (2023) doi:10.1101/2023.12.11.571194.

33. Yu, S. *et al.* Circadian BMAL1 Regulates Mandibular Condyle Development by Hedgehog Pathway. *Cell Prolif* (2019) doi:10.1111/cpr.12727.

34. He, J. *et al.* Dissecting Human Embryonic Skeletal Stem Cell Ontogeny by Single-Cell Transcriptomic and Functional Analyses. *Cell Res* (2021) doi:10.1038/s41422-021-00467-z.

35. Kohn, A. *et al.* Notch Signaling Controls Chondrocyte Hypertrophy via Indirect Regulation of Sox9. *Bone Res* (2015) doi:10.1038/boneres.2015.21.

36. Xia, S. *et al.* <scp>miR</Scp>-335-5p Inhibits Endochondral Ossification by Directly Targeting <scp>SP1</Scp> in <scp>TMJ OA</scp>. *Oral Dis* (2023) doi:10.1111/odi.14736.

37. Che, X. *et al.* Hypoxia-inducible Factor 2α Is a Novel Inhibitor of Chondrocyte Maturation. *J Cell Physiol* (2021) doi:10.1002/jcp.30356.

38. Laurie, L. E., Kokubo, H., Nakamura, M., Saga, Y. & Funato, N. The Transcription Factor Hand1 Is Involved in Runx2-Ihh-Regulated Endochondral Ossification. *PLoS One* (2016) doi:10.1371/journal.pone.0150263.

39. Spiegelaere, W. De, Cornillie, P., Casteleyn, C., Burvenich, C. & Den Broeck, W. Van. Detection of Hypoxia Inducible Factors and Angiogenic Growth Factors During Foetal Endochondral and Intramembranous Ossification. *Anat Histol Embryol* (2010) doi:10.1111/j.1439-0264.2010.01005.x.

40. Scotti, C. Engineering of a functional bone organ through endochondral ossification. *Proc. Natl. Acad. Sci. U. S. A* **110**, 3997–4002.

41. McDermott, A. M. *et al.* Recapitulating Bone Development Through Engineered Mesenchymal Condensations and Mechanical Cues for Tissue Regeneration. *Sci Transl Med* (2019) doi:10.1126/scitranslmed.aav7756.

42. Dupard, S. J., Grigoryan, A., Farhat, S., Coutu, D. L. & Bourgine, P. E. Development of Humanized Ossicles: Bridging the Hematopoietic Gap. *Trends Mol Med* **26**, 552–569 (2020).

43. Kurien, T., Pearson, R. G. & Scammell, B. E. Bone Graft Substitutes Currently Available in Orthopaedic Practice. *Bone Joint J* (2013) doi:10.1302/0301-620x.95b5.30286.

44. Kim, J. Y., Lee, J. & Kim, S. Comparison Between Minimally Invasive Plate Osteosynthesis and the Deltopectoral Approach With Allogenous Fibular Bone Graft in Proximal Humeral Fractures. *Clin Shoulder Elb* (2020) doi:10.5397/cise.2020.00199.

45. Deepika-Penmetsa, S. L., Thomas, R., Baron, T. K., Shah, R. & Mehta, D. S. Cortical Lamina Technique: A Therapeutic Approach for Lateral Ridge Augmentation Using Guided Bone Regeneration. *J Clin Exp Dent* (2016) doi:10.4317/jced.53008.

46. Viscioni, A. *et al.* Effectiveness of Fresh Frozen and Cryopreserved Homologue Iliac Crest Grafts Used in Sinus Lifting: A Comparative Study. *Cell Tissue Bank* (2010) doi:10.1007/s10561-010-9192-6.

47. Wallace, S. C. & Gellin, R. G. Clinical Evaluation of Freeze-Dried Cancellous Block Allografts for Ridge Augmentation and Implant Placement in the Maxilla. *Implant Dent* (2010) doi:10.1097/id.0b013e3181e5d2a1.

48. Acıkan, İ. & Dündar, S. Biomechanical Examination of Osseointegration of Titanium Implants Placed Simultaneously With Allogeneic Bone Transfer. *Journal of Craniofacial Surgery* (2021) doi:10.1097/scs.0000000000007880.

49. Özcan, E. C. *et al.* Biomechanical Evaluation of the Osseointegration Levels of Implants Placed Simultaneously With Tibia, Femur, and Jaw Allogeneic Bone Grafts. *Journal of Craniofacial Surgery* (2024) doi:10.1097/scs.0000000000010517.

50. Danesh-Sani, S., Engebretson, S. P. & Janal, M. N. Histomorphometric Results of Different Grafting Materials and Effect of Healing Time on Bone Maturation After Sinus Floor Augmentation: A Systematic Review and Meta-analysis. *J Periodontal Res* (2016) doi:10.1111/jre.12402.

51. Li, D.-Q. *et al.* Improved Repair of Bone Defects With Prevascularized Tissue-Engineered Bones Constructed in a Perfusion Bioreactor. *Orthopedics* (2014) doi:10.3928/01477447-20140924-06.

52. Meza-Mauricio, J. *et al.* How Efficacious Is the Combination of Substitute Bone Graft With Autogenous Bone Graft in Comparison With Substitute Bone Graft Alone in the Horizontal Bone Gain? A Systematic Review and Meta-Analysis. *J Clin Exp Dent* (2022) doi:10.4317/jced.59087.

53. Tournier, P. *et al.* An Extrudable Partially Demineralized Allogeneic Bone Paste Exhibits a Similar Bone Healing Capacity as the “Gold Standard” Bone Graft. *Front Bioeng Biotechnol* (2021) doi:10.3389/fbioe.2021.658853.

54. Blume, O., Donkiewicz, P., Back, M. & Born, T. Bilateral Maxillary Augmentation Using CAD/CAM Manufactured Allogenic Bone Blocks for Restoration of Congenitally Missing Teeth: A Case Report. *Journal of Esthetic and Restorative Dentistry* (2019) doi:10.1111/jerd.12454.

55. Monje, A. *et al.* On the Feasibility of Utilizing Allogeneic Bone Blocks for Atrophic Maxillary Augmentation. *Biomed Res Int* (2014) doi:10.1155/2014/814578.

56. Dermenoudis, S. & Missirlis, Y. F. Bioreactors in Tissue Engineering. *Adv Eng Mater* (2010) doi:10.1002/adem.201080018.

57. Hutmacher, D. W., Schantz, J. -T., F. Lam, C. X., Tan, K. C. & Lim, T. C. State of the Art and Future Directions of Scaffold-Based Bone Engineering From a Biomaterials Perspective. *J Tissue Eng Regen Med* (2007) doi:10.1002/term.24.

58. Guarino, V., Gloria, A., Raucci, M. G., Santis, R. De & Ambrosio, L. Bio-Inspired Composite and Cell Instructive Platforms for Bone Regeneration. *International Materials Reviews* (2012) doi:10.1179/0950660812z.00000000021.

59. Kneser, U. *et al.* Tissue Engineering of Bone. *Minimally Invasive Therapy & Allied Technologies* (2002) doi:10.1080/136457002320174177.

60. Gao, C. *et al.* Preparation And<i>in Vitro</I>characterization of Electrospun PVA Scaffolds Coated With Bioactive Glass for Bone Regeneration. *J Biomed Mater Res A* (2012) doi:10.1002/jbm.a.34072.

61. Govoni, M., Muscari, C., Guarnieri, C. & Giordano, E. Mechanostimulation Protocols for Cardiac Tissue Engineering. *Biomed Res Int* (2013) doi:10.1155/2013/918640.

62. Oragui, E. The Role of Bioreactors in Tissue Engineering for Musculoskeletal Applications. *Open Orthop J* (2011) doi:10.2174/1874325001105010267.

63. Loh, Q. L. & Choong, C. Three-Dimensional Scaffolds for Tissue Engineering Applications: Role of Porosity and Pore Size. *Tissue Eng Part B Rev* (2013) doi:10.1089/ten.teb.2012.0437.

64. Chen, S., Zhou, X., Li, T. & He, C. Vascularization and Innervation for Bone Tissue Engineering. *Acc Mater Res* (2024) doi:10.1021/accountsmr.4c00165.

65. Kazimierczak, P. & Przekora, A. Bioengineered Living Bone Grafts—A Concise Review on Bioreactors and Production Techniques in Vitro. *Int J Mol Sci* (2022) doi:10.3390/ijms23031765.

66. Vyas, C. *et al.* Biological Perspectives and Current Biofabrication Strategies in Osteochondral Tissue Engineering. *Biomanufacturing Reviews* (2020) doi:10.1007/s40898-020-00008-y.

67. Dupard, S. J., Garcia, A. G. & Bourgine, P. E. Customizable 3D printed perfusion bioreactor for the engineering of stem cell microenvironments. *Front Bioeng Biotechnol* **10**, (2023).

68. Theocharis, A. D., Manou, D. & Karamanos, N. K. The Extracellular Matrix as a Multitasking Player in Disease. *Febs Journal* (2019) doi:10.1111/febs.14818.

69. Theocharis, A. D., Skandalis, S. S., Gialeli, C. & Karamanos, N. K. Extracellular matrix structure. *Advanced Drug Delivery Reviews* vol. 97 4–27 Preprint at https://doi.org/10.1016/j.addr.2015.11.001 (2016).

70. Zhang, X. *et al.* Decellularized Extracellular Matrix Scaffolds: Recent Trends and Emerging Strategies in Tissue Engineering. *Bioact Mater* (2022) doi:10.1016/j.bioactmat.2021.09.014.

71. Nicolas, J. *et al.* 3D Extracellular Matrix Mimics: Fundamental Concepts and Role of Materials Chemistry to Influence Stem Cell Fate. *Biomacromolecules* (2020) doi:10.1021/acs.biomac.0c00045.

72. Wu, H., Li, F., Shao, W., Gao, J. & Ling, D. Promoting Angiogenesis in Oxidative Diabetic Wound Microenvironment Using a Nanozyme-Reinforced Self-Protecting Hydrogel. *ACS Cent Sci* (2019) doi:10.1021/acscentsci.8b00850.

73. Porzionato, A. *et al.* Tissue-Engineered Grafts From Human Decellularized Extracellular Matrices: A Systematic Review and Future Perspectives. *Int J Mol Sci* (2018) doi:10.3390/ijms19124117.

74. Zhang, J. *et al.* Harnessing Mechanical Stress With Viscoelastic Biomaterials for Periodontal Ligament Regeneration. *Advanced Science* (2024) doi:10.1002/advs.202309562.

75. Nam, S., Stowers, R. S., Lou, J., Xia, Y. & Chaudhuri, O. Varying PEG Density to Control Stress Relaxation in Alginate-Peg Hydrogels for 3D Cell Culture Studies. *Biomaterials* (2019) doi:10.1016/j.biomaterials.2019.02.004.

76. Prouvé, É. *et al.* Evaluating Poly(Acrylamide-<i>co</I>-Acrylic Acid) Hydrogels Stress Relaxation to Direct the Osteogenic Differentiation of

Mesenchymal Stem Cells. *Macromol Biosci* (2021) doi:10.1002/mabi.202100069.

77. Poole, J. J. A. & Mostaço-Guidolin, L. B. Optical Microscopy and the Extracellular Matrix Structure: A Review. *Cells* **10**, 1760 (2021).

78. Turnbull, G. *et al.* 3D Bioactive Composite Scaffolds for Bone Tissue Engineering. *Bioact Mater* (2018) doi:10.1016/j.bioactmat.2017.10.001.

79. Leijten, J. *et al.* Cell based advanced therapeutic medicinal products for bone repair: Keep it simple? *Adv Drug Deliv Rev* **84**, 30–44 (2015).

80. Koons, G. L., Diba, M. & Mikos, A. G. Materials design for bone-tissue engineering. *Nature Reviews Materials* Preprint at https://doi.org/10.1038/s41578-020-0204-2 (2020).

81. Nilsson Hall, G. *et al.* Developmentally Engineered Callus Organoid Bioassemblies Exhibit Predictive In Vivo Long Bone Healing. *Advanced Science* **7**, (2020).

82. Himeles, J. R. & Ratner, D. Cartilage Tissue Engineering for Nasal Alar and Auricular Reconstruction: A Critical Review of the Literature and Implications for Practice in Dermatologic Surgery. *Dermatologic Surgery* (2023) doi:10.1097/dss.0000000000003826.

83. Liu, Y. *et al.* Double Network Hydrogels Encapsulating Genetically Modified Dedifferentiated Chondrocytes for Auricular Cartilage Regeneration. *J Mater Chem B* (2025) doi:10.1039/d4tb02352h.

84. Khatib, N., Parisi, C. & Nowlan, N. C. Differential Effect of Frequency and Duration of Mechanical Loading on Fetal Chick Cartilage and Bone Development. *eCM* (2021) doi:10.22203/ecm.v041a34.

85. Keane, T. J., Swinehart, I. T. & Badylak, S. F. Methods of Tissue Decellularization Used for Preparation of Biologic Scaffolds and in Vivo Relevance. *Methods* (2015) doi:10.1016/j.ymeth.2015.03.005.

86. Saldin, L. T., Cramer, M. C., Velankar, S., White, L. J. & Badylak, S. F. Extracellular Matrix Hydrogels From Decellularized Tissues: Structure and Function. *Acta Biomater* (2017) doi:10.1016/j.actbio.2016.11.068.

87. Fok, S. W. *et al.* Macromolecular Crowding and Decellularization Method Increase the Growth Factor Binding Potential of Cell-Secreted Extracellular Matrices. *Front Bioeng Biotechnol* (2023) doi:10.3389/fbioe.2023.1091157.

88. Pashneh-Tala, S., MacNeil, S. & Claeyssens, F. The Tissue-Engineered Vascular Graft—Past, Present, and Future. *Tissue Eng Part B Rev* (2016) doi:10.1089/ten.teb.2015.0100.

89. Heuschkel, M. A. *et al.* In Vitro Evaluation of Bovine Pericardium After a Soft Decellularization Approach for Use in Tissue Engineering. *Xenotransplantation* (2018) doi:10.1111/xen.12464.

90. Wu, K. Y., Dave, A., Daigle, P. & Tran, S. D. Advanced Biomaterials for Lacrimal Tissue Engineering: A Review. *Materials* (2024) doi:10.3390/ma17225425.

91. Sawicki, L. A. *et al.* Tunable Synthetic Extracellular Matrices to Investigate Breast Cancer Response to Biophysical and Biochemical Cues. *APL Bioeng* (2019) doi:10.1063/1.5064596.

92. Wang, W. Y., Davidson, C. D., Lin, D. & Baker, B. M. Actomyosin Contractility-Dependent Matrix Stretch and Recoil Induces Rapid Cell Migration. *Nat Commun* (2019) doi:10.1038/s41467-019-09121-0.

93. Davidson, C. D., P. Jayco, D. K., Wang, W. Y., Shikanov, A. & Baker, B. M. Fiber Crimp Confers Matrix Mechanical Nonlinearity, Regulates Endothelial Cell Mechanosensing, and Promotes Microvascular Network Formation. *J Biomech Eng* (2020) doi:10.1115/1.4048191.

94. Mierke, C. T. Bidirectional Mechanical Response Between Cells and Their Microenvironment. *Front Phys* (2021) doi:10.3389/fphy.2021.749830.

95. Liu, J. *et al.* Hepatic Spheroid Formation on Carbohydrate-Functionalized Supramolecular Hydrogels. *Biomacromolecules* (2023) doi:10.1021/acs.biomac.2c01390.

96. Xiao, C. *et al.* Synergistic Effects of Matrix Biophysical Properties on Gastric Cancer Cell Behavior via Integrin-Mediated Cell-ECM Interactions. *Small* (2024) doi:10.1002/smll.202309907.

97. Slivac, I. *et al.* Bioactivity Comparison of Electrospun PCL Mats and Liver Extracellular Matrix as Scaffolds for HepG2 Cells. *Polymers (Basel)* (2021) doi:10.3390/polym13020279.

98. Sheng, K. *et al.* Reconstructing Monosynaptic Connectivity From<i>in Vivo</I>Spike Trains Using Deep Domain-Adaptive Matching. (2022) doi:10.1101/2022.10.03.510694.

99. Xing, H. *et al.* Preparation of an Acellular Spinal Cord Scaffold to Improve Its Biological Properties. *Mol Med Rep* (2019) doi:10.3892/mmr.2019.10364.

100. Gilpin, A. & Yang, Y. Decellularization Strategies for Regenerative Medicine: From Processing Techniques to Applications. *Biomed Res Int* **2017**, (2017).

101. Bourgine, P. E. *et al.* Engineered Extracellular Matrices as Biomaterials of Tunable Composition and Function. *Adv Funct Mater* **27**, (2017).

102. Baert, Y. & Goossens, E. Preparation of Scaffolds From Decellularized Testicular Matrix. (2017) doi:10.1007/7651_2017_29.

103. Jin, S. *et al.* A Biomimetic Hierarchical Nanointerface Orchestrates Macrophage Polarization and Mesenchymal Stem Cell Recruitment to Promote Endogenous Bone Regeneration. *ACS Nano* (2019) doi:10.1021/acsnano.9b00489.

104. Aamodt, J. M. & Grainger, D. W. Extracellular matrix-based biomaterial scaffolds and the host response. *Biomaterials* **86**, 68–82 (2016).

105. Barsch, F. *et al.* Semiautomated Quantification of the Fibrous Tissue Response to Complex Three-dimensional Filamentous Scaffolds Using Digital Image Analysis. *J Biomed Mater Res A* (2021) doi:10.1002/jbm.a.37293.

106. Carpenter, R. *et al.* Scaffold-Assisted Ectopic Transplantation of Internal Organs and Patient-Derived Tumors. *ACS Biomater Sci Eng* (2019) doi:10.1021/acsbiomaterials.9b00978.

107. Xuan, Y. *et al.* 3d-Printed Bredigite Scaffolds With Ordered Arrangement Structures Promote Bone Regeneration by Inducing Macrophage Polarization in Onlay Grafts. *J Nanobiotechnology* (2024) doi:10.1186/s12951-024-02362-2.

108. Calabrese, G. *et al.* Bone Augmentation After Ectopic Implantation of a Cell-Free Collagen-Hydroxyapatite Scaffold in the Mouse. *Sci Rep* (2016) doi:10.1038/srep36399.

109. Yan, Z. *et al.* Enhanced Immune Modulation and Bone Tissue Regeneration Through an Intelligent Magnetic Scaffold Targeting Macrophage Mitochondria. *Adv Healthc Mater* (2025) doi:10.1002/adhm.202500163.

110. Ikeda, T. *et al.* Fabrication and Characteristics of Chitosan Sponge as a Tissue Engineering Scaffold. *Biomed Res Int* (2014) doi:10.1155/2014/786892.

111. Inzana, J. A. *et al.* 3D Printing of Composite Calcium Phosphate and Collagen Scaffolds for Bone Regeneration. *Biomaterials* (2014) doi:10.1016/j.biomaterials.2014.01.064.

112. Verrier, S., Blaker, J. J., Maquet, V., Hench, L. L. & Boccaccını, A. R. PDLLA/Bioglass® Composites for Soft-Tissue and Hard-Tissue Engineering: An in Vitro Cell Biology Assessment. *Biomaterials* (2004) doi:10.1016/j.biomaterials.2003.09.081.

113. Souza Falcão, L. de *et al.* Starch as a Matrix for Incorporation and Release of Bioactive Compounds: Fundamentals and Applications. *Polymers (Basel)* (2022) doi:10.3390/polym14122361.

114. James, A. W. *et al.* A Review of the Clinical Side Effects of Bone Morphogenetic Protein-2. *Tissue Eng Part B Rev* **22**, 284–297 (2016).

115. Zara, J. N. *et al.* High Doses of Bone Morphogenetic Protein 2 Induce Structurally Abnormal Bone and Inflammation *In Vivo*. *Tissue Eng Part A* **17**, 1389–1399 (2011).

116. Houlihan, D. D. *et al.* Isolation of mouse mesenchymal stem cells on the basis of expression of Sca-1 and PDGFR-α. *Nat Protoc* **7**, 2103–2111 (2012).

117. Morikawa, S. *et al.* Prospective identification, isolation, and systemic transplantation of multipotent mesenchymal stem cells in murine bone marrow. *Journal of Experimental Medicine* **206**, 2483–2496 (2009).

118. Ferrari, D. & Kosher, R. A. Dlx5 Is a Positive Regulator of Chondrocyte Differentiation during Endochondral Ossification. *Dev Biol* **252**, 257–270 (2002).

119. Inada, M. *et al.* Critical roles for collagenase-3 (Mmp13) in development of growth plate cartilage and in endochondral ossification. *Proceedings of the National Academy of Sciences* **101**, 17192–17197 (2004).

120. Little, S. C. & Mullins, M. C. Bone morphogenetic protein heterodimers assemble heteromeric type I receptor complexes to pattern the dorsoventral axis. *Nat Cell Biol* **11**, 637–643 (2009).

121. Zhu, W. *et al.* Noggin regulation of bone morphogenetic protein (BMP) 2/7 heterodimer activity in vitro. *Bone* **39**, 61–71 (2006).

122. Mathavan, N. *et al.* 18F-fluoride as a prognostic indicator of bone regeneration. *Acta Biomater* **90**, 403–411 (2019).

123. Gentili, C. & Cancedda, R. Cartilage and Bone Extracellular Matrix. *Curr Pharm Des* **15**, 1334–1348 (2009).

124. Uludag, H., D'Augusta, D., Palmer, R., Timony, G. & Wozney, J. Characterization of rhBMP-2 pharmacokinetics implanted with biomaterial carriers in the rat ectopic model. *J Biomed Mater Res* **46**, 193–202 (1999).

125. Dong, X., Wang, Q., Wu, T. & Pan, H. Understanding Adsorption-Desorption Dynamics of BMP-2 on Hydroxyapatite (001) Surface. *Biophys J* **93**, 750–759 (2007).

126. Lackington, W. A. *et al.* Incorporation of hydroxyapatite into collagen scaffolds enhances the therapeutic efficacy of rhBMP-2 in a weight-bearing femoral defect model. *Mater Today Commun* **29**, 102933 (2021).

127. La, W. *et al.* The Efficacy of Bone Morphogenetic Protein-2 Depends on Its Mode of Delivery. *Artif Organs* **34**, 1150–1153 (2010).

128. Jeon, O. *et al.* Long-term delivery enhances in vivo osteogenic efficacy of bone morphogenetic protein-2 compared to short-term delivery. *Biochem Biophys Res Commun* **369**, 774–780 (2008).

129. Miao, C. *et al.* BMP2/7 heterodimer enhances osteogenic differentiation of rat BMSCs via ERK signaling compared with respective homodimers. *J Cell Biochem* **120**, 8754–8763 (2019).

130. Parvizi, J. & Kim, G. K. Bone Grafting. in *High Yield Orthopaedics* 64–65 (Elsevier, 2010). doi:10.1016/B978-1-4160-0236-9.00042-0.

131. Koons, G. L., Diba, M. & Mikos, A. G. Materials design for bone-tissue engineering. *Nat Rev Mater* **5**, 584–603 (2020).

132. Langer, R. & Vacanti, J. P. Tissue Engineering. *Science (1979)* **260**, 920–926 (1993).

133. O'Brien, F. J. Biomaterials & scaffolds for tissue engineering. *Materials Today* **14**, 88–95 (2011).

134. Pittenger, M. F. *et al.* Multilineage Potential of Adult Human Mesenchymal Stem Cells. *Science (1979)* **284**, 143–147 (1999).

135. Freed, L. E. *et al. Biodegradable Polymer Scaffolds for Tissue Engineering*. http://www.nature.com/naturebiotechnology (1994).

136. Simonsen, J. L. *et al. Telomerase Expression Extends the Proliferative Life-Span and Maintains the Osteogenic Potential of Human Bone Marrow Stromal Cells*. http://biotech.nature.com (2002).

137. Chen, G., Deng, C. & Li, Y. P. TGF-β and BMP signaling in osteoblast differentiation and bone formation. *International Journal of Biological Sciences* Preprint at https://doi.org/10.7150/ijbs.2929 (2012).

138. Salazar, V. S., Gamer, L. W. & Rosen, V. BMP signalling in skeletal development, disease and repair. *Nat Rev Endocrinol* **12**, 203–221 (2016).

139. Martin, I., Wendt, D. & Heberer, M. The role of bioreactors in tissue engineering. *Trends in Biotechnology* vol. 22 80–86 Preprint at https://doi.org/10.1016/j.tibtech.2003.12.001 (2004).

140. Mao, A. S. & Mooney, D. J. Regenerative medicine: Current therapies and future directions. *Proc Natl Acad Sci U S A* **112**, 14452–14459 (2015).

141. Hussey, G. S., Dziki, J. L. & Badylak, S. F. Extracellular matrix-based materials for regenerative medicine. *Nat. Rev. Mater* **3**, 159–173.

142. Tang, G. *et al.* Recent Trends in the Development of Bone Regenerative Biomaterials. *Front Cell Dev Biol* **9**, 1–18 (2021).

143. Bonnans, C., Chou, J. & Werb, Z. Remodelling the extracellular matrix in development and disease. *Nat Rev Mol Cell Biol* **15**, 786–801 (2014).

144. Hussey, G. S., Dziki, J. L. & Badylak, S. F. Extracellular matrix-based materials for regenerative medicine. *Nat Rev Mater* **3**, 159–173 (2018).

145. Fattahi, R., Chamkhorami, F. M., Taghipour, N. & Keshel, S. H. The effect of extracellular matrix remodeling on material-based strategies for bone regeneration: Review article. *Tissue Cell* **76**, 101748 (2022).

146. Mouw, J. K., Ou, G. & Weaver, V. M. Extracellular matrix assembly: A multiscale deconstruction. *Nat Rev Mol Cell Biol* **15**, 771–785 (2014).

147. Assunção, M. *et al.* Cell-Derived Extracellular Matrix for Tissue Engineering and Regenerative Medicine. *Front Bioeng Biotechnol* **8**, 1–10 (2020).

148. Hinderer, S., Layland, S. L. & Schenke-Layland, K. ECM and ECM-like materials - Biomaterials for applications in regenerative medicine and cancer therapy. *Adv Drug Deliv Rev* **97**, 260–269 (2016).

149. Filippi, M., Born, G., Chaaban, M. & Scherberich, A. Natural Polymeric Scaffolds in Bone Regeneration. *Front Bioeng Biotechnol* **8**, (2020).

150. Hu, K. & Olsen, B. R. The roles of vascular endothelial growth factor in bone repair and regeneration. *Bone* **91**, 30–38 (2016).

151. Duda, G. N. *et al.* The decisive early phase of bone regeneration. *Nat Rev Rheumatol* **19**, 78–95 (2023).

152. Behr, B., Tang, C., Germann, G., Longaker, M. T. & Quarto, N. Locally applied vascular endothelial growth factor A increases the osteogenic healing capacity of human adipose-derived stem cells by promoting osteogenic and endothelial differentiation. *Stem Cells* **29**, 286–296 (2011).

153. Burger, M. G. *et al.* Robust coupling of angiogenesis and osteogenesis by VEGF-decorated matrices for bone regeneration. *Acta Biomater* **149**, 111–125 (2022).

154. Otto, F. *et al.* Cbfa1, a candidate gene for cleidocranial dysplasia syndrome, is essential for osteoblast differentiation and bone development. *Cell* **89**, 765–771 (1997).

155. Komori, T. Runx2, an inducer of osteoblast and chondrocyte differentiation. *Histochemistry and Cell Biology* vol. 149 313–323 Preprint at https://doi.org/10.1007/s00418-018-1640-6 (2018).

156. Tuckermann, J. & Adams, R. H. The endothelium–bone axis in development, homeostasis and bone and joint disease. *Nat Rev Rheumatol* **17**, 608–620 (2021).

157. Chen, Z. *et al.* Osteoimmunomodulation for the development of advanced bone biomaterials. *Materials Today* **19**, 304–321 (2016).

158. Xie, Y. *et al.* Osteoimmunomodulatory effects of biomaterial modification strategies on macrophage polarization and bone regeneration. *Regen Biomater* **7**, 233–245 (2020).

159. Ramakrishnaiah Siddappa, Ruud Licht, Clemens van Blitterswijk, J. de B. Donor variation and loss of multipotency during in vitro expansion of human mesenchymal stem cells for bone tissue engineering. *Journal of Orthopaedic Research* **25**, (2007).

160. Golchin, A., Shams, F. & Karami, F. Advancing Mesenchymal Stem Cell Therapy with CRISPR/Cas9 for Clinical Trial Studies. in *Cell Biology and Translational Medicine,* vol. 8 89–100 (2019).

161. Hazrati, A., Malekpour, K., Soudi, S. & Hashemi, S. M. CRISPR/Cas9-engineered mesenchymal stromal/stem cells and their extracellular vesicles: A new approach to overcoming cell therapy limitations. *Biomedicine & Pharmacotherapy* **156**, 113943 (2022).

162. Pigeot, S. *et al.* Manufacturing of Human Tissues as off-the-Shelf Grafts Programmed to Induce Regeneration. *Advanced Materials* **33**, (2021).

163. Grigoryan, A. *et al.* Engineering of human mini-bones for the standardized modeling of healthy hematopoiesis, leukemia and solid tumor metastasis. *bioRxiv* 2021.09.11.459806 (2021).

164. Gao, C., Peng, S., Feng, P. & Shuai, C. Bone biomaterials and interactions with stem cells. *Bone Res* **5**, 1–33 (2017).

165. Ran, F. A. *et al.* Genome engineering using the CRISPR-Cas9 system. *Nat Protoc* **8**, 2281–2308 (2013).

166. Bock, C. *et al.* High-content CRISPR screening. *Nature Reviews Methods Primers* **2**, (2022).

167. Khodabukus, A. *et al.* Translating musculoskeletal bioengineering into tissue regeneration therapies. *Sci Transl Med* **14**, (2022).

168. Wu, A.-M. *et al.* Global, regional, and national burden of bone fractures in 204 countries and territories, 1990–2019: a systematic analysis from the Global Burden of Disease Study 2019. *Lancet Healthy Longev* **2**, e580–e592 (2021).

169. Kronenberg, H. M. Developmental regulation of the growth plate. *Nature* Preprint at https://doi.org/10.1038/nature01657 (2003).

170. Henkel, J. *et al.* Bone Regeneration Based on Tissue Engineering Conceptions — A 21st Century Perspective. *Bone Res* **1**, 216–248 (2013).

171. Scotti, C. *et al.* Engineering of a functional bone organ through endochondral ossification. *Proc Natl Acad Sci U S A* **110**, 3997–4002 (2013).

172. Bernhard, J. *et al.* Tissue-engineered hypertrophic chondrocyte grafts enhanced long bone repair. *Biomaterials* **139**, 202–212 (2017).

173. Bernhard, J. C. *et al.* Effects of Endochondral and Intramembranous Ossification Pathways on Bone Tissue Formation and Vascularization in Human Tissue-Engineered Grafts. *Cells* **11**, 3070 (2022).

174. Piñeiro-Ramil, M. *et al.* Usefulness of Mesenchymal Cell Lines for Bone and Cartilage Regeneration Research. *Int J Mol Sci* **20**, 6286 (2019).

175. Zeiter, S. *et al.* Evaluation of Preclinical Models for the Testing of Bone Tissue-Engineered Constructs. *Tissue Eng Part C Methods* **26**, 107–117 (2020).

176. Dawson, J. I. & Oreffo, R. O. C. Bridging the regeneration gap: Stem cells, biomaterials and clinical translation in bone tissue engineering. *Arch Biochem Biophys* **473**, 124–131 (2008).

177. Petrus-Reurer, S. *et al.* Immunological considerations and challenges for regenerative cellular therapies. *Commun Biol* **4**, 798 (2021).

178. Soltanmohammadi, F., Mahmoudi Gharehbaba, A., Alizadeh, E. & Javadzadeh, Y. Innovative approaches to tissue engineering: Utilizing decellularized extracellular matrix hydrogels for mesenchymal stem cell transport. *Int J Biol Macromol* **290**, 138893 (2025).

179. Adigbli, G. Humanization of Immunodeficient Animals for the Modeling of Transplantation, Graft Versus Host Disease, and Regenerative Medicine. *Transplantation* **104**, 2290–2306.

180. Fahy, N. *et al.* Chondrogenically Primed Human Mesenchymal Stem Cells Persist and Undergo Early Stages of Endochondral Ossification in an Immunocompetent Xenogeneic Model. *Front Immunol* **12**, (2021).

181. Cunniffe, G. M. *et al.* Chondrogenically primed mesenchymal stem cell-seeded alginate hydrogels promote early bone formation in critically-sized defects. *Eur Polym J* **72**, 464–472 (2015).

182. Nilsson Hall, G. *et al.* Developmentally Engineered Callus Organoid Bioassemblies Exhibit Predictive In Vivo Long Bone Healing. *Advanced Science* **7**, 1902295 (2020).

183. Zhang, D. *et al.* Research Progress of Macrophages in Bone Regeneration. *J Tissue Eng Regen Med* **2023**, 1–13 (2023).

184. Gou, M., Wang, H., Xie, H. & Song, H. Macrophages in guided bone regeneration: potential roles and future directions. *Front Immunol* **15**, (2024).

185. Zhu, Y. *et al.* Regulation of macrophage polarization through surface topography design to facilitate implant-to-bone osteointegration. *Sci Adv* **7**, (2021).

186. Crapo, P. M., Gilbert, T. W. & Badylak, S. F. An overview of tissue and whole organ decellularization processes. *Biomaterials* vol. 32 3233–3243 Preprint at https://doi.org/10.1016/j.biomaterials.2011.01.057 (2011).

187. Longoni, A. *et al.* Endochondral Bone Regeneration by Non-autologous Mesenchymal Stem Cells. *Front Bioeng Biotechnol* **8**, 1–14 (2020).

188. Maeda, A. *et al.* The Innate Cellular Immune Response in Xenotransplantation. *Front Immunol* **13**, 858604 (2022).

189. Kiernan, C. H. *et al.* Allogeneic chondrogenically differentiated human bone marrow stromal cells do not induce dendritic cell maturation. *J Tissue Eng Regen Med* **12**, 1530–1540 (2018).

190. Kiernan, C. H. *et al.* Allogeneic chondrogenically differentiated human mesenchymal stromal cells do not induce immunogenic responses from T lymphocytes in vitro. *Cytotherapy* **18**, 957–969 (2016).

191. Pereira, R. C., Martinelli, D., Cancedda, R., Gentili, C. & Poggi, A. Human Articular Chondrocytes Regulate Immune Response by Affecting Directly T Cell Proliferation and Indirectly Inhibiting Monocyte Differentiation to Professional Antigen-Presenting Cells. *Front Immunol* **7**, 415 (2016).

192. Bolander, J. *et al.* Healing of a Large Long-Bone Defect through Serum-Free In Vitro Priming of Human Periosteum-Derived Cells. *Stem Cell Reports* **8**, 758–772 (2017).

193. Zhu, G., Wang, G. & Li, J. J. Advances in implant surface modifications to improve osseointegration. *Materials Advances* vol. 2 6901–6927 Preprint at https://doi.org/10.1039/d1ma00675d (2021).

194. Golebiowska, A. A., Intravaia, J. T., Sathe, V. M., Kumbar, S. G. & Nukavarapu, S. P. Decellularized extracellular matrix biomaterials for regenerative therapies: Advances, challenges and clinical prospects. *Bioact Mater* **32**, 98–123 (2024).

195. Jang, J. W. *et al.* Review: Scaffold Characteristics, Fabrication Methods, and Biomaterials for the Bone Tissue Engineering. *International Journal of Precision Engineering and Manufacturing* vol. 24 511–529 Preprint at https://doi.org/10.1007/s12541-022-00755-7 (2023).

196. Murphy, S. V. & Atala, A. 3D bioprinting of tissues and organs. *Nature Biotechnology* vol. 32 773–785 Preprint at https://doi.org/10.1038/nbt.2958 (2014).

197. Murphy, M. P. *et al.* Articular cartilage regeneration by activated skeletal stem cells. *Nat Med* **26**, (2020).

198. Noor, N. *et al.* 3D Printing of Personalized Thick and Perfusable Cardiac Patches and Hearts. *Advanced Science* **6**, (2019).

199. Kim, B. S. *et al.* 3D cell printing of in vitro stabilized skin model and in vivo pre-vascularized skin patch using tissue-specific extracellular matrix bioink: A step towards advanced skin tissue engineering. *Biomaterials* **168**, 38–53 (2018).

200. Hinton, T. J. *et al.* Three-dimensional printing of complex biological structures by freeform reversible embedding of suspended hydrogels. *Sci Adv* **1**, (2015).

201. Dubbin, K., Tabet, A. & Heilshorn, S. C. Quantitative criteria to benchmark new and existing bio-inks for cell compatibility. *Biofabrication* **9**, 044102 (2017).

202. Chen, M. H. *et al.* Methods To Assess Shear-Thinning Hydrogels for Application As Injectable Biomaterials. *ACS Biomater Sci Eng* **3**, 3146–3160 (2017).

203. Levato, R. *et al.* From Shape to Function: The Next Step in Bioprinting. *Advanced Materials* **32**, (2020).

204. Chimene, D., Kaunas, R. & Gaharwar, A. K. Hydrogel Bioink Reinforcement for Additive Manufacturing: A Focused Review of Emerging Strategies. *Advanced Materials* **32**, (2020).

205. Lee, S. *et al.* Human-Recombinant-Elastin-Based Bioinks for 3D Bioprinting of Vascularized Soft Tissues. *Advanced Materials* **32**, (2020).

206. De Santis, M. M. & Wagner, D. E. Collagen IV: a critical new starting point for engineering upper airways. *European Respiratory Journal* **55**, 2001130 (2020).

207. Hamilton, N. J. I. *et al.* Bioengineered airway epithelial grafts with mucociliary function based on collagen IV- and laminin-containing extracellular matrix scaffolds. *European Respiratory Journal* **55**, 1901200 (2020).

208. Gao, T. *et al.* Optimization of gelatin–alginate composite bioink printability using rheological parameters: a systematic approach. *Biofabrication* **10**, 034106 (2018).

209. Crowley, C. *et al.* Surface modification of a POSS-nanocomposite material to enhance cellular integration of a synthetic bioscaffold. *Biomaterials* **83**, 283–293 (2016).

210. Kim, M. K. *et al.* Decellularized extracellular matrix-based bio-ink with enhanced 3D printability and mechanical properties. *Biofabrication* **12**, 025003 (2020).

211. Yu, C. *et al.* Scanningless and continuous 3D bioprinting of human tissues with decellularized extracellular matrix. *Biomaterials* **194**, 1–13 (2019).

212. Pati, F. *et al.* Printing three-dimensional tissue analogues with decellularized extracellular matrix bioink. *Nat Commun* **5**, 3935 (2014).

213. Lee, H. *et al.* Development of Liver Decellularized Extracellular Matrix Bioink for Three-Dimensional Cell Printing-Based Liver Tissue Engineering. *Biomacromolecules* **18**, 1229–1237 (2017).

214. Kim, B. S., Kim, H., Gao, G., Jang, J. & Cho, D.-W. Decellularized extracellular matrix: a step towards the next generation source for bioink manufacturing. *Biofabrication* **9**, 034104 (2017).

215. Pouliot, R. A. *et al.* Development and characterization of a naturally derived lung extracellular matrix hydrogel. *J Biomed Mater Res A* **104**, 1922–1935 (2016).

216. de Hilster, R. H. J. *et al.* Human lung extracellular matrix hydrogels resemble the stiffness and viscoelasticity of native lung tissue. *American Journal of*

Physiology-Lung Cellular and Molecular Physiology **318**, L698–L704 (2020).

217. Athirasala, A. *et al.* A dentin-derived hydrogel bioink for 3D bioprinting of cell laden scaffolds for regenerative dentistry. *Biofabrication* **10**, 024101 (2018).

218. Wagner, D. E. *et al.* Design and Synthesis of an Artificial Pulmonary Pleura for High Throughput Studies in Acellular Human Lungs. *Cell Mol Bioeng* **7**, 184–195 (2014).

219. Rezende, R. A., Bártolo, P. J., Mendes, A. & Filho, R. M. Rheological behavior of alginate solutions for biomanufacturing. *J Appl Polym Sci* **113**, 3866–3871 (2009).

220. Giobbe, G. G. *et al.* Extracellular matrix hydrogel derived from decellularized tissues enables endodermal organoid culture. *Nat Commun* **10**, 5658 (2019).

221. Ribatti, D. *et al.* Chorioallantoic membrane capillary bed: A useful target for studying angiogenesis and anti-angiogenesis in vivo. *Anat Rec* **264**, 317–324 (2001).

222. Fleischer, S., Tavakol, D. N. & Vunjak-Novakovic, G. From Arteries to Capillaries: Approaches to Engineering Human Vasculature. *Adv Funct Mater* **30**, (2020).

223. Kolesky, D. B. *et al.* 3D Bioprinting of Vascularized, Heterogeneous Cell-Laden Tissue Constructs. *Advanced Materials* **26**, 3124–3130 (2014).

224. Utracki, L. A. & Wilkie, C. A. *Polymer Blends Handbook*. vol. 1 (Kluwer academic publishers Dordrecht, 2002).

225. Rous, P. Tumor implantations in the developing embryo. Experiments with a transmissible sarcoma of the fowl. *J. Amer. med. Ass.* **56**, 741–742 (1911).

226. Lin, L., Spoor, M. S., Gerth, A. J., Brody, S. L. & Peng, S. L. Modulation of Th1 Activation and Inflammation by the NF-κB Repressor Foxj1. *Science (1979)* **303**, 1017–1020 (2004).

227. Ganong, W. F. Review of medical physiology. *Dynamics of blood and lymph flow* **30**, 525–541 (1995).

228. Anderson, J. M., Rodriguez, A. & Chang, D. T. Foreign body reaction to biomaterials. *Semin Immunol* **20**, 86–100 (2008).

229. Wagner, D. E. *et al.* Three-dimensional scaffolds of acellular human and porcine lungs for high throughput studies of lung disease and regeneration. *Biomaterials* **35**, 2664–2679 (2014).

230. Greaney, A. M. *et al.* Platform Effects on Regeneration by Pulmonary Basal Cells as Evaluated by Single-Cell RNA Sequencing. *Cell Rep* **30**, 4250-4265.e6 (2020).

231. Brown, B. N., Ratner, B. D., Goodman, S. B., Amar, S. & Badylak, S. F. Macrophage polarization: An opportunity for improved outcomes in biomaterials and regenerative medicine. *Biomaterials* **33**, 3792–3802 (2012).

232. Brown, B. N. *et al.* Macrophage phenotype as a predictor of constructive remodeling following the implantation of biologically derived surgical mesh materials. *Acta Biomater* **8**, 978–987 (2012).

233. BOYDEN, E. A. A Critique of the International Nomenclature on Bronchopulmonary Segments. *Dis Chest* **23**, 266–269 (1953).

234. Petrou, C. L. *et al.* Clickable decellularized extracellular matrix as a new tool for building hybrid-hydrogels to model chronic fibrotic diseases *in vitro*. *J Mater Chem B* **8**, 6814–6826 (2020).